2014

Approaches to Reduce Selection of Genomic Variants in Human Pluripotent Stem Cell Culture

Marion Riggs
Virginia Commonwealth University

APPROACHES TO REDUCE SELECTION OF GENOMIC VARIANTS IN HUMAN PLURIPOTENT STEM CELL CULTURE

A dissertation submitted in partial fulfillment of the requirements for the degree of Doctor of Philosophy at Virginia Commonwealth University.

by

Marion Joseph Riggs
University of South Florida, B.S. 2003.
University of South Florida, M.S. 2005.

Director: Raj R. Rao
Associate Professor
Department of Chemical and Life Science Engineering
Department of Human and Molecular Genetics

Virginia Commonwealth University
Richmond, Virginia
May, 2014

Acknowledgements

I would like to express my deepest appreciation to my family for all their support throughout my training to be a research scientist. My daughter Elyce and mom, Mary Davis, for their patience. In loving memory, I express my fondest appreciation for the support given by Tina, who stood by me through the toughest challenges. My PI, Dr. Raj Rao, for his instrumental support and to my committee mentors, Dr. Fong, Dr. Lemmon, Dr. Tombes, and Dr. Valerie, for their invaluable guidance. Finally, to my program director Dr. Eggleston for all his moral support that made final progression through the program possible.

.

Table of Contents

List of Tables

List of Figures

List of Abbreviations

ABR	Active BCR-related Gene
aCGH	Array Comparative Hybridization
AP	Alkaline Phosphatase
APRT	Adenine Phosphoribosyltransferase
ARHGDIA	Aplysia Ras- Related Homolog Guanine Dissociated Inhibitor Alpha
ART	Assisted Reproductive Technology
BCL-XL	B-cell CLL/lymphoma 2- Like 1
bFGF	Basic Fibroblast Growth Factor (FGF2)
BG01 (Arg)	BG01 Line Constitutively Overexpressing ARHGDIA Gene
BG01 (GFP)	BG01 Line Constitutively Expressing Green Fluorescent Protein
BMP4	Bone Morphogenic Protein 4
CIN	Chromosomal Instability
CMV	Cytomegalovirus
C-myc	Myc Proto-Oncogene Protein
CNV	Copy Number Variation
CT	Collagenase/Trypsin passage
EB	Embryoid Body
EC	Embryonic Carcinoma
ECM	Extracellular Matrix

EpiSCs	Epiblast Stem Cells (post- implantation)
ES	Embryonic Stem
ESC	Embryonic Stem Cells
FBS	Fetal Bovine Serum
FDR	False Discovery Rate
FGF4	Fibroblast Growth Factor 4
FISH	Fluorescent In Situ Hybridization
G- band	Geimsa Band
GAP	GTPase activating proteins
GATA6	GATA Binding Protein 6
GDP	Guanine Di-phosphate
GEF	Guanine Exchange Factors
GFP	Green Fluorescent Protein
GSK3β	Glycogen Synthase Kinase 3 Beta, CHIR99021
GTP	Guanine Tri-phosphate
H9 (Arg)	H9 Line Constitutively Overexpressing ARHGDIA Gene
H9 (GFP)	H9 Line Constitutively Expressing Green Fluorescent Protein
HDAC	Histone Deacetylase
hDF	Human Dermal Fibroblast
hEC	Human Embryonic Stem Cells
hPDF	Human Pluripotent Derived Fibroblasts

HPRT	Hypoxanthine Phosphoribosyltransferase
hPSCs	Human Pluripotent Stem Sells
HR	Homologous Recombination
ICC	Immunocytochemistry
ICM	Inner Cell Mass
iMEF	Inactivated Mouse Embryonic Fibroblast (Mitomycin-treated)
iPSC	Induced Pluripotent Stem Cells
IQGAP1	IQ motif containing GTPase activating protein 1
IRES	Internal Ribosomal Entry Site
IVF	In Vitro Fertilization
KLF2	Kruppel-like factor 2
KLF4	Kruppel-like factor 4
KSR	Knock-out Serum Replacement
LIF	Leukemia Inhibitory Factor
LIFrβ	LIF Receptor Beta
MEKi	MEK Inhibitor, PD0325901
mEpiSCs	Mouse Epiblast Stem Cells (post- implantation)
MIN	Microsatellite Instability
MLC	Myosin Light Chain
mPSCs	Mouse Pluripotent Stem Sells
MTOC	Microtubule Organizing Center

NANOG	Nanog homeobox
OCT4	POU class 5 homeobox 1
ORF	Open Reading Frame
PAK1	p21- activated Kinase
PCR	Polymerase Chain Reaction
PGC	Primordial Germ Cells
PGS	Pre-implantation Genetic Screening
pMLC	Phosphorylated Myosin Light Chain
PSC	Pluripotent Stem Sells
QPCR	Quantitative Real Time Polymerase Chain Reaction
RAC1	Ras-Related C3 Botulinum Toxin Substrate 1
RHOA	Ras Homolog Family Member A
ROCK	Rho Associated Coil Coiled Protein Kinase
SCC	Spermatogonial Stem Cells
SCID	Severe Combined Immunodeficiency
SCNT	Somatic Cell Nuclear Transfer
SKY	Spectral Karyotyping
SNP	Single Nucleotide Polymorphism
SOX2	SRY (sex determining region Y)-box 2
SSEA1	Stage Specific Embryonic Antigen 1
SSEA3	Stage Specific Embryonic Antigen 3

SSEA4	Stage Specific Embryonic Antigen 4
STAT3	Signal Transducer and Activator of Transcription 3
tGFP	Turbo Green Fluorescent Protein
TZV	Thiazovivin
WB	Western Blot
WT	Wild Type
β	Beta

Abstract

APPROACHES TO REDUCE SELECTION OF GENOMIC VARIANTS IN HUMAN PLURIPOTENT STEM CELL CULTURE

By Marion Joseph Riggs, Ph.D.

A dissertation submitted in partial fulfillment of the requirements for the degree of Doctor of Philosophy at Virginia Commonwealth University.

Virginia Commonwealth University, 2014.

Director: Raj R. Rao
Associate Professor
Department of Chemical and Life Science Engineering
Department of Human and Molecular Genetics

Optimizing culture conditions that reduce genomic instability in human pluripotent stem cells (hPSCs) is an unmet challenge in the field. Results from our lab and numerous research groups demonstrate that hPSCs are prone to genomic aberrations and single-cell passaging increases the rate of genomic alterations. However, single-cell based passaging maintains advantages for scale-up and standardizing differentiation protocols. In this study, we investigated the problem of genomic instability in hPSC cultures with the goal towards identifying and characterizing candidate genes that could contribute to generation and survival of abnormal hPSCs. Based on microarray analysis, we identify ARHGDIA, located on 17q25, as a candidate gene conferring selective advantage to trisomy 17 hPSCs. Using lentiviral approaches to overexpress ARHGDIA in hPSCs, [hPSC (Arg)], we

functionally validate that in enzymatically passaged co-cultures, hPSC (Arg) lines exhibit competitive advantage against wild type hPSCs, [hPSC (WT)]. Additionally, hPSC (Arg) lines exhibit increased single-cell survival at low density plating. In co-cultures with hPSC (WT), ROCKi exposure attenuated the competitive advantage of hPSC (Arg) subpopulations. For the first time, this work demonstrates that increased expression of a gene on 17q25 confers selective advantage to hPSCs. In parallel studies, using medium devoid of bFGF containing LIF plus two inhibitors, MEK inhibitor (PD0325901) and p38 inhibitor (SB203580), we demonstrate that hPSCs are LIF responsive and can be stably maintained in naive pluripotent culture conditions. Based on their clonal viability, we propose that naive hPSCs are a more genetically stable population than primed hPSCs, when passaged as single- cells. These studies will aid the long-term goal of hPSC scale-up while promoting stable propagation of genomically normal hPSCs.

CHAPTER 1

Introduction and Review of the Literature

1.1 Human Pluripotent Stem Cells: Origins and Characterization

Human pluripotent stem cells (hPSCs) have two defining qualities, limitless self-renewal; and, the capacity to differentiate into each of the three embryonic germ layers: ectoderm, endoderm, and mesoderm [1]. These unique properties of these hPSCs and their expansion potential, has generated significant excitement in the scientific community and media for their potential to be used as an off-the-shelf cell source for tissue replacement strategies, human tissue models for toxicity testing and drug discovery, disease- in- the- dish modeling, and studying early human development [2-4]. Human PSCs are classified according to their origin and method of derivation [5]. Different origins for diploid pluripotent stem cells (PSCs) include: (a) embryonic stem cells (ESCs) from the inner cell mass of blastocysts or epiblast [6], (b) Germline cells including primordial germ cells (PGCs) [7], embryonic carcinoma cells (ECs) from teratocarcinomas [8], and spermatogonial stem cells (SCCs) [5], (c) somatic cells that are reprogrammed to a pluripotent state, called induced pluripotent stem cells (iPSCs) [9], and (d) enucleated oocytes with transfer of a full complement of donor DNA via a process termed somatic cell nuclear transfer (SCNT) [10].

While starting materials for hPSC derivation is highly varied from embryonic to adult tissue, a common set of cell surface and intracellular markers characteristic of pluripotency is widely accepted to indicate self-renewal capacity and differentiation potential [6, 9, 11]. An extensive set of assays for gene and protein expression are routinely used to validate self-renewal. Self-renewal can be tested at each passage; however, validating tri-lineage developmental potential requires several weeks or more [12]. The pluripotent state is strongly defined by a core set of transcription factors that include OCT4, NANOG, and SOX2. These transcription factors are so

tightly coupled with the pluripotent state that in somatic cells, forced expression of a set of four transcription factors, including OCT4 and SOX2, is sufficient to reprogram somatic cells back to the pluripotent state [9]. IPSCs have opened new horizons for studying the genetic basis of disease in stem cell derived human tissue models from Mendelian based genetic disorders to complex disorders like schizophrenia [13]. For the remainder of this review, we will restrict hPSCs to mean either hESCs or iPSCs.

The first step in screening for hPSCs is morphological analysis which demonstrate that undifferentiated hPSCs form tightly packed colonies with cobblestone morphology. Alkaline phosphatase (AP) activity is a quick assay that can be conducted without any specialized equipment, with positive activity indicative of an undifferentiated state [14, 15]. Extra-cellular markers, SSEA3, SSEA4, Tra-1-60, Tra-1-81 can be readily used for flow-cytometry analysis or sorting; and routinely, immunocytochemistry (ICC) is used for both intracellular and extracellular protein identification. Commonly, quantitative real-time polymerase chain reaction (QPCR) is used to demonstrate expression of the essential pluripotent stem cell transcription factors, OCT4, SOX2, and NANOG. While these assays are limited to showing self-renewal, differentiation potential for hPSCs can be demonstrated by either *in vitro* or *in vivo* differentiation protocols, embryoid body (EB) formation in suspension cultures or teratoma forming assay in mice, respectively [6, 12]. EB formation is most commonly performed using the hanging drop method over a three week period [12, 15]. Teratoma forming assay takes 6-8 weeks requiring hPSCs to be injected into severe- combined immunodeficiency (SCID) mice in the kidney capsule or the tail [6, 16].

Interestingly, while mouse embryonic stem cells (mESCs) and hESCs share many of the same molecular features, there are clear differences. For example, mESCs express cell surface marker SSEA1 but not SSEA-3/4; whereas, hPSCs do not express SSEA1 but express SSEA-3/4 [17]. Initially, these differences were attributed to species divergence [18]; however, a growing body of work is demonstrating that PSCs are compartmentalized by a primed vs naïve pluripotent stem cell state, human and mouse ESCs, respectively, are indicative of two different *in vivo* counterparts [19-33]. The "naïve" state is similar to cells from the pre- implantation epiblast, while the "primed" state is characteristic of post- implantation epiblast stem cells (EpiSCs) [5, 24]. HESCs and mEpiSCs have been shown via key developmental markers to be strikingly similar [31].

1.2 Naïve vs. Primed Human Pluripotent Stem Cell States

An emerging view is the existence of a transient ground state of pluripotency in epiblast cells the form in the founder tissue of the embryo proper that during this developmental period acquires the capacity to form all lineages and is distinct in potential from blastomeres and ICM [24, 27, 28, 31, 34]. The egg and blastocyst only give rise to two cell types, trophoblast and ICM, with the ICM then forming the hypoblast and epiblast. Thusly, Nichols and Smith argue the pre-implantation epiblast is not a reduction in potency from totipotent cells but uniquely acquire an unrestricted ground state of pluripotency, without developmental bias, that can form all embryonic lineages [24]. Of significant question and active area of research is whether ESCs in culture are true analogs of an *in vivo* developmental stage or are culture epiphenomena [25].

Perpetual expression of pluripotency and the non-native cell culture environment invokes continual pressure for genomic and epigenetic adaptations in hPSCs [27]. However recent research is clarifying our view of pluripotency as comprised of different metastable states [35]. Notably, researchers have come to appreciate two different pluripotent stem cells states, "naïve" and "primed" PSCs as they pertain to cell culture and their associated developmental analogs [25]. The differences between mPSCs and hPSCs are now attributed to their occupation in these two different states, as opposed to species divergence [31]. Mouse PSCs are naïve pluripotent stem cells akin to the pre-implantation epibast; whereas hPSCs are in a primed state consistent with post-implantation epiblast of mice, mouse epiblast stem cells (mEpiSCs) [36]. Naïve pluripotency and the "ground state" are highly similar; however, the ground state in mice has been shown to have the additional characteristic of growth factor independence, and to simply rely on the inhibition of differentiation cues [23, 29]. In mice, culture conditions for mPSCs have been established to recapitulate the ground state of pluripotency and most similarly mirror the *in vivo* ESCs of the pre- implantation epiblast [29]. Progress has been made on developing culture conditions to support naïve hPSC culture; however, identifying the signaling for capturing the ground state in hPSCs remains a significant scientific hurdle [20, 31, 37].

The establishment of mEpiSCs has enabled researchers with a comparison model for hPSCs; and significant similarities strongly support the view that hPSCs exist in the primed pluripotent state [38, 39]. A striking cell culture similarity is the reliance of both mEpiSCs and hPSCs on basic fibroblast growth factor (bFGF) to promote self-renewal; while, mPSCs are leukemia inhibitory factor (LIF) responsive for stem cell maintenance [27, 31, 40, 41]. Therefore, bFGF is associated with maintaining primed pluripotency and LIF for supporting

naïve pluripotency. LIF is a member of the interleukin-6 cytokine family with a transmembrane glycoprotein, GP130, which heterodimerizes with LIF receptor β (LIFrβ) to activate downstream transcription factor, STAT3, to promote self- renewal in mPSCs [42]. It is of considerable significance to develop culture conditions for the derivation and propagation of naïve hPSC lines and further towards that goal, establishment of the ground state for hPSCs. The difference between naïve and primed PSCs has significant biological and technical implications for their full realization in basic research and clinical applications. While hPSCs have been most exciting since their initial derivation in 1998, several technical facets in comparison to mPSCs have impeded their use in biomedical research.

The scale- up of hPSCs is a challenge compared to mPSCs, since mPSCs have a much higher population doubling time than hPSCs [43]. This is because mPSCs have faster cell cycle times [44] and high clonal survival at plating [45]. Where hPSCs can be expanded at 10- fold per week, mPSCs can be expanded at 1000- fold per week [43]. A longer G1 phase was determined in mEpiSCs compared to mPSCs, suggesting that establishing naïve culture conditions may result in reduced cell cycle times for primed hPSCs, as well [46]. HPSCs are heterogeneous in their expression of pluripotent genes with consequent variation in self-renewal likelihood [47, 48]. As well, hPSCs demonstrate differentiation bias with variable propensity for different lineages, this may indicate prior specificity that is attributed to their post-implantation epiblast-like primed state [25, 49]. Whereas, naïve stem cells and in particular, ground state stem cells are believed to have greater homogeneity and unrestricted lineage potential [27]. Ground state establishment in hiPSC lines has significant practical implications for overcoming limitations in their differentiation potential [50]. In contrast to mPSCs, hPSCs are not amenable to homologous

recombination (HR), and this has significantly hindered genetic engineering of hPSCs to model disease and development, as well as gene correction in iPSCs [30, 31]. Buecker and colleagues have reported the development of naïve- state like hiPSCs by 5 reprogramming factors and LIF-based culture conditions that enabled HR of the hPSCs. While these hPSCs self-renewed, they lost their differentiation capacity, suggesting further work is needed to develop true naïve hPSCs; however, this is a promising sign that HR amenable hPSCs is possible in the naïve state [51]. MPSCs can be simply maintained on gelatin, whereas hPSCs require feeder cells or elaborate protein-based substrates. Recently, in medium containing soluble fibronectin and ROCK inhibitor, Y-27632, single- cell hPSCs were successfully cultured on gelatin [52]. While adding ROCKi and fibronectin to medium doesn't necessarily reduce culture complexity or costs, it is tantalizing to consider that culturing hPSCs in the ground state will reduce hPSC culture complexity and costs by enabling expansion on gelatin alone.

Key differences in intracellular signaling between naïve and primed pluripotency have been determined; however, the expression of the core transcription factor circuitry of OCT4, SOX2, NANOG is conserved. Through iPSC research, it is appreciated that the expression of key transcription factors, including OCT4 and SOX2 are masters of pluripotency capable of reprogramming a somatic cell back to a pluripotent state [9, 27]. OCT4 and SOX2 are both essential regulators of self-renewal and are independently post-implantation lethal in null mice. OCT4 is essential for both hypoblast and epiblast formation [24]. OCT4 heterodimerizes with SOX2 and together they bind their own promoters for autoregulation and a recursive self-reinforcing circuit, and together bind other pluripotency and development associated genes, for

co-regulation [27, 42]. Along with promoting self-renewal, in mPSCs, OCT4 and SOX2 initiate the differentiation process by driving the expression of the FGF4 signaling [27].

A role for NANOG in *de novo* establishment of the ground state is emerging. Unlike OCT4, NANOG is only expressed in the epiblast [24, 53]. Forced expression of NANOG obviates LIF requirement [54]; however NANOG- null mESCs continue to self-renew, even though the embryos are post-implantation lethal [55]. NANOG co-localizes with OCT4 and SOX2 at transcriptional binding sites [42, 56]. In the ground state, NANOG may act by "buffering" FGF4-ERK signaling [27]. Bi-allelic expression of NANOG is a marker for the ground state of pluripotency in contrast to naïve pluripotency [22]. FGF4-ERK regulates allelic expression of NANOG, while inhibiting FGF-ERK leads to bi-allelic expression of NANOG and the poor development of ICM in heterozygous NANOG expressing mice [22]. Together, these findings support a critical role for NANOG in epiblast formation and ground state pluripotency. During iPSC generation, NANOG's essential developmental role in establishing pluripotent stem cells is recapitulated [26]. In murine embryos, FGF4-ERK inhibition abrogates hypoblast development, as measured by GATA6, and promotes all cells to form NANOG expressing epiblast cells [23]. In mPSC lines, differentiation is initiated by auto-inductive FGF4 signaling on downstream effector ERK1/2; therefore, inhibiting FGF4-ERK signaling prevents differentiation *in vivo* and *in vitro* [29]. This suggests that pluripotency is inherently stable and self- maintaining if the effects of extrinsic stimuli are neutralized, and that inhibition of FGF4 is critical to capturing the ground state and the most developmentally authentic embryonic stem cells [28].

Finally, in 2008, after decades of research, mPSC cell culture converged to a stable point with the establishment of culture conditions that maintained mPSCs in the ground state of pluripotency. While a good review on the evolution of mPSC culture has been published by Blair and colleagues as well as a comparative study on mPSC culture protocols [57, 58], we will briefly summarize the critical advancements mPSC culture and their significance, for the purpose of understanding the current state and establishing a roadmap for hPSC culture. Like hESCs, mESCs were first grown on iMEFs [59], with further studies indicating that iMEFs secrete LIF and that extrinsic stimulation of STAT3 by LIF supplemented medium was sufficient to replace the iMEF feeder cell layer with simple gelatin coating [60]. Inhibitor of differentiation (ID) proteins present in serum were determined replaceable by BMP-4 and N2B27 containing medium; thereby, establishing a chemically- defined culture system, without the unknown components of serum and a feeder layer [61, 62]. As in mPSCs, establishing defined hPSC culture conditions has been an important goal and is an ongoing research effort of many labs [63, 64]. Remarkably, it was determined that only two inhibitors are needed to culture mPSCs in the ground state. These two inhibitors are a highly specific MEK inhibitor (PD0325901) and GSK3β inhibitor (CHIR99021) [23, 28, 29, 65]. In the presence of these two inhibitors, LIF is not necessary for mPSC self- renewal; however, LIF also promotes mPSC growth and viability, thus the preferred ground state cocktail has been established as LIF + MEKi + GSK3i (LIF + 2i). The MEKi inhibits the FGF4-ERK signaling cascade and GSK3i works through WNT signaling and stabilization of intracellular β-catenin, [27, 66].

The ground state is a significant advance for being able to generalize the rodent system among genetic strains, to the rat-species, increase phenotypic homogeneity of fully unrestricted

pluripotent cells, and generate the most authentic embryonic stem cells. Since the initial derivation of mESCs, much of the research has involved a single genetic strain, 129; since, other mouse strains were recalcitrant to mESC line establishment [67, 68]. Using ground state culture conditions, LIF + 2i (GSK3), mPSC lines were derived from non-permissive mouse genetic strains, NOD, C57Bl6, CBA, and FVB ES, as well as, the first germline competent rat ES cells were derived [31, 69, 70]. Generalization of conditions for derivation of rodent pluripotent stem cell lines is strongly supportive that a ground state of pluripotency exists and has been achieved in murine culture; furthermore, that through inhibition of the FGF4-ERK axis, this ground state is a perpetual and intrinsically sustained fate choice for mPSCs [27]. Recent work has made advances in establishing culture conditions to support naïve hPSCs; but, the signaling network for the hPSC ground state is unknown and furthermore may have significant species- specific differences [40].

Rodents exhibit the phenomena of diapause, in which, blastocysts in suckling mothers hatch to form the epiblast and hypoblast but the blastocysts fails to progress to implantation until estrogen is restored [71]. During diapause the epiblast cells remain in the naïve state and are LIF/STAT3/GP130 dependent [72]. During early embryogenesis, gene targeting on the LIF signaling proteins did not influence self-renewal, but GP130- null mice cannot maintain pluripotency during diapause [42]. Thus, the role of LIF may be developmentally restricted to this potential for diapause. Diapause in rodents and this LIF responsive state has been shown to facilitate the derivation of naïve mPSC lines [73]. So far, in mammals without diapause, true ESCs have not been established [40]. This may suggest difficulty in establishing naïve and/or ground state hPSCs, especially if the human epiblast cells are unresponsive to LIF/STAT3 [24].

However, if epiblast and embryonic stem cell pluripotency are founded on a common ground state, then this is expected to be conserved between mammalian species [27]. Nichols and colleagues found when human IVF embryos are cultured in FGF-ERK inhibitors or in MEKi + GSK3βi, the epiblast maintains NANOG expression. This would not be expected in a primed embryonic stem cell state, suggesting a naïve pluripotent epiblast and ground state exists during human embryogenesis [31]. Recently, diapause was induced in sheep, even though sheep do not normally exhibit diapause, suggesting that diapause may be an evolutionary conserved phenomena in mammals with only some animals expressing diapause, such as mice [74, 75].

Strategies to generate naïve hPSCs include direct derivation from pre-implantation embryos, reprogramming somatic cells to naïve pluripotency, and novel culture conditions that can revert primed hPSCs to naïve hPSCs and support continued naïve hPSC propagation [31]. Each of these approaches has been successful in mice. In reprogramming of mPSCs, naïve vs primed state pluripotency is cytokine dependent on LIF or bFGF, respectively, suggesting that culture conditions are sufficient to determine pluripotency state [31]. Progress has been made by several groups in reprogramming naïve hPSCs with a combination of transcription factors, LIF, inhibitors, and histone deacetylase (HDAC) inhibitors. However, none of the current approaches have fully established naïve hPSCs [30]. Recently, Gafni and colleagues used a complex medium formulation containing LIF and bFGF plus inhibitors, MEKi, GSK3B, p38i, and JNKi to culture hPSCs that exhibited some of the characteristics of naïve pluripotent stem cells [20]. Ware and colleagues used the MEKi and GSK3βi, common to the ground state in mPSCs, but in the presence of bFGF. In order to reverse the hPSCs from the primed to the naïve state, the cells were “reverse toggled” using the HDAC inhibitors butyrate and suberoylanilide hydroxamic acid

[37]. In each of these two studies using only culture medium, the hPSCs exhibited an X pre-inactivated state and formed well- differentiated teratomas. Interestingly, the simplest formula published on naïve hPSC conversion, suggests simply using LIF plus MEKi PD0325901 and p38i (SB203580) [45], wherein p38i was determined by a high throughput chemical screening. While Xu and colleagues state the successful conversion of hPSCs to mouse- like hPSCs in this LIF + 2i (p38) medium, there isn't any presentation of data on the self- renewal or differentiation of these naïve converted hPSCs [45].

A significant cell culture distinction between naïve and primed PSCs is their difference in clonality, where in one week mPSCs can be expanded 1000 fold and comparatively hPSCs only 10 fold [43]. Recently, a molecular pathway explaining the pluripotent state dependency for dissociation-induced apoptosis between mPSCs and hPSCs was demonstrated [76]. Ohgushi and colleagues show RHO signaling activation upon loss of E-cadherin based cell-cell contact is different between naïve and primed PSCs. Upon loss of E-cadherin-dependent intercellular contact, primed PSCs are characterized by a high amount of active RHOA and low amount of active RAC1. Thus, primed PSCs activate ROCK-induced blebbing and cell death upon dissociation. Conversely, naïve PSCs are characterized by low active RHOA and high active RAC1 and do not exhibit the same pathway induced cell death. They propose an upstream epiblast state linked regulator that is an effector of both RHOA and RAC1 activation upon loss of E-cadherin based cell- cell contact [76]. Xu and colleagues also show RHO signaling in hPSCs is regulated by E- cadherin based cell- cell contact; and that upon single- cell dissociation, mPSCs have stable E-cadherin expression- attributed to decreased intracellular turnover- and exhibit minimal RHOA activation, thereby explaining the robust clonality of naïve PSCs [45]. A

morphological distinction between mPSCs and hPSCs are the small, compact, and dome- shaped colonies of naïve PSCs compared to flatter and more spread out colonies of primed PSCs [37]. Table 1 summarizes molecular differences between ground state PSCs, naïve PSCs, and primed PSCs relevant to this report.

Table 1 Metastable pluripotent stem cell states profile

Marker	**Ground State**	**Naïve**	**Primed**
Cytokine	Independent	LIF, BMP4	bFGF, Activin A
Inhibitors	MEKi, GSK3β	Serum (ID)	ROCKi
Clonal	Yes	Yes	No
Morphology	Compact, Multilayer, Cobblestone	Compact, Multilayer, Cobblestone	Spread out, Flattened, Cobblestone
Transcription Factors	KLF4 (high), KLF2 (high), NANOG, OCT4, SOX2	KLF4 (high), KLF2 (high), NANOG, OCT4, SOX2	KLF4 (low), KLF2 (low), NANOG, OCT4, SOX2
Cell Surface	SSEA1, AP	SSEA1, AP	SSEA3/4, AP
ECM Adhesion	E-cadherin	E-cadherin	β-integrin 1 E-cadherin
Substrate	Gelatin	Gelatin	BD Matrigel™
Epigenetic	Both X- active (female) Biallelic NANOG expression	Both X- active (female) Monoallelic NANOG expression	One X- inactive (female) Monoallelic NANOG expression

Ground state, naïve, and primed pluripotency exhibit differential expression of cell surface markers, transcription factors, epigenetic modifications, and have different cytokine growth factor requirements. Abbreviations: ID- inhibitor of differentiation proteins, AP- Alkaline Phosphatase.

1.3 Culture of Human Pluripotent Stem Cells

Current inefficiencies in successful implantation during assisted reproductive technologies (ART) necessitates the generation of excess *in vitro* fertilization (IVF) embryos [77]. hESC lines that are part of the NIH stem cell registry are derived from the inner cell mass (ICM) of donated IVF embryos under informed consent and are no longer intended for reproductive purposes [78]. Pluripotency, *in vivo,* is acquired during ICM formation and is a transient in the epiblast cells of the embryo proper [27]. However, hESC lines maintain pluripotency indefinitely and have successfully been cultured for months to years [79-81]. Maintaining the pluripotent state during long-term propagation puts strong selective pressure for culture adaptation that includes changes in genomic DNA, mitochondrial DNA, epigenetic modifications, and protein networks [82-86].

Nearly a decade of scientific investigation identifying genomic alterations during hPSC culture has established the recurrent genomic aberrations during culture and has culminated in a comprehensive library of numerical, structural, and copy number variations [87-90]. In spite of the substantial progress in identifying genomic alterations, little is known about the impact of mechanisms known to cause mutation in somatic cells; and, even less is known about the genotype to phenotype relationship that accounts for selection of genomic variants. To date, the causative genes and signaling network responsible for selection of common genomic alterations has not been determined and remains elusive [87]. Confounding the issue is a report that hPSCs can express phenotypic features of neoplastic progression in absence of large scale chromosomal changes but in simply upon small-scale copy number variations (CNVs) [91]. Culture adaptation is an integration of two separate processes, causative mechanisms that result in a genomic

alteration and culture selection of genomic variant cells with phenotypic advantage [92]. A hallmark of culture adaptation is increased self-renewal but reduced differentiation capacity [93-96]. Since extended culture is a parameter for culture adaptation, it is difficult to parse the basis for reduced differentiation capacity, as resulting from changes in DNA or adaptive gene networks to the culture environment. Theoretical considerations are particularly interesting on this phenomena, as attractor state theory may suggest that continual selection will increase the "basin of attraction" of the pluripotent state; and therefore, increase the energy barrier to differentiation, as opposed to a reduced capacity for differentiation [29, 97]. Strikingly, it has been reported that differentiation can select for some genomic alterations [88]. Potentially, a significant cause for concern as we move towards using cells for therapies, but also interesting developmentally and in disease pathology [98-101]**.** With chromosomal abnormalities being a hallmark of cancer, it is of clinical importance that we maintain karyotypically normal hPSCs (Figure 1) [92, 94, 95, 102].

In recent years, a preponderance of data is painting a picture of the intrinsic chromosomal instability (CIN) of cells during early embryonic development and of hPSCs *in vitro* [103-106]. Reducing the mutation rate of hPSCs is an important strategy for stably propagating genomically normal culture populations [107]. However, it is well appreciated by academia and industry that *in vitro* conditions are sub-optimal and induce significant pressure for selection of genomic alterations that increase clonality, proliferation, self-renewal, and anti- apoptosis [84, 87, 88, 92, 108]. For scale-up of sufficient cell numbers to be used in clinical applications, hPSC viability remains a pressing concern [64, 109]. Human pluripotent stem cells are known for high rates of apoptosis that can be influenced by culture conditions and passaging protocols [43]. Unlike

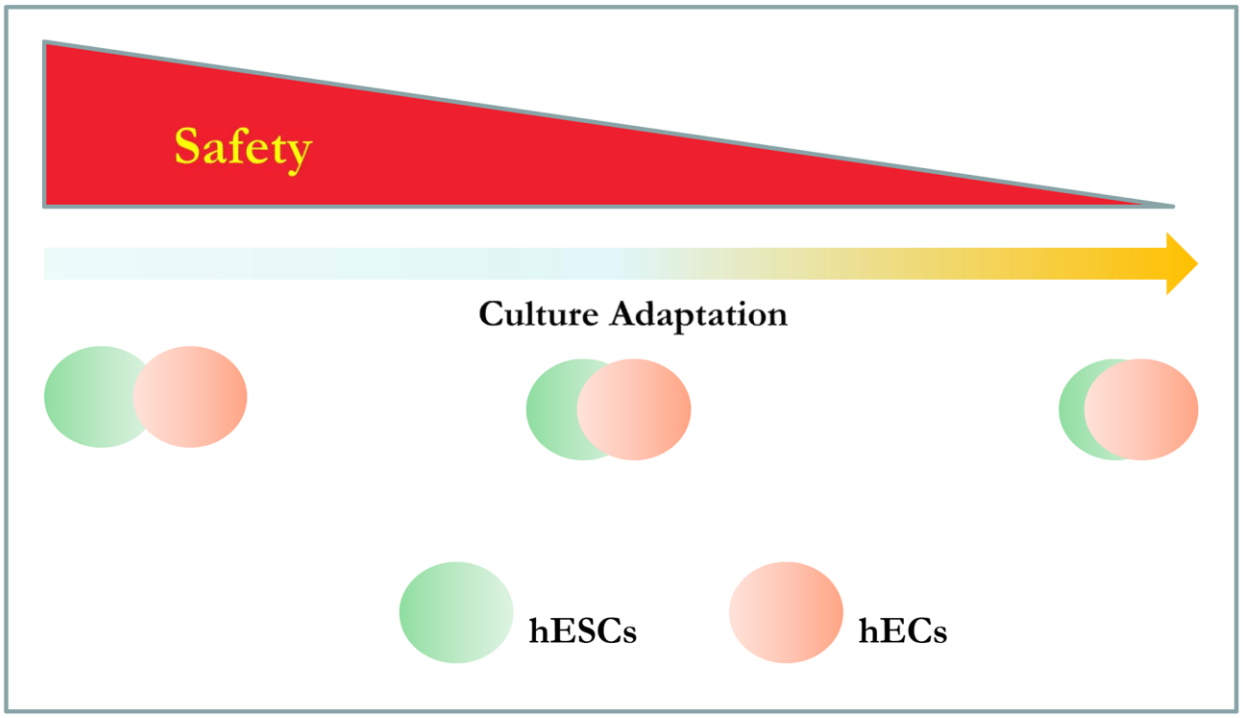

Figure 1. Genomic abnormalities in hESCs are similar to those seen in hECs. Trisomy 12 and 17 are commonly observed in hESCs and these genomic alterations are characteristic to germ cell tumors and hECs and pose clinical concern for cellular therapies. Abbreviations: hESC- human embryonic stem cells, hEC- human embryonic carcinoma cells.

mPSCs, hPSCs are prone to cell death upon loss of cell- cell contact that occurs during enzymatic dissociation of colonies into single- cells [45, 76]. The disruption of e-cadherin junctions induces actin- based cytoskeletal changes through RHOA activation of the kinase,ROCK. ROCK phosphorylates myosin light chain (MLC) to induce blebbing associated cell- death through hyperactive actin- myosin contraction [110]. ROCK inhibitors, such as Y27632, are commonly used to reduce cytoplasmic blebbing and improve hPSC survival at passaging, cryopreservation, and thawing [109, 111]. Manual passaging maintains e-cadherin based cell- cell contact improving cell viability at plating, while manually maintained cultures [76, 112], also, exhibit a lower prevalence of genomic alterations during prolonged propagation [82]. However, manual passaging is not amenable to scale- up [3]. HPSCs plated as single- cells exhibit poor survival and increased genomic instability during serial passage; however, in principle, single- cell plating is the most promising approach for scale-up and standardizing optimized differentiation protocols [45, 64, 113]. The increased genomic instability of hPSC single- cell cultures is consistent with the hypothesis of selection on survival and clonality [87].

Adherent culture conditions for hPSCs are complex and the essential components are conserved for hiPSCs and hESCs. The general requirements of hPSC culture are basal medium, medium supplements such as amino acids, serum or serum replacement factors for viability and proliferation, feeder cell- layer or feeder-free substrates to support attachment, growth factors to support stem cell self-renewal, and optional small molecules to support viability and inhibit differentiation. Similar to the evolution of mPSC culture, optimizing hPSC culture conditions remains a significant research challenge; however, several milestones in hPSC culture have been achieved. The modest goal of industry is to reach scale- up of hPSCs in fully defined conditions

that reduce variability and increase standardization of protocols. Clinical applications will warrant xeno- free conditions and genomically normal cell products [2, 3, 80]. Two significant advances in hPSC culture has been the development of knock-out serum replacement (KSR) and Matrigel™ [111, 114]. KSR is a proprietary, commercially available defined formulation that replaces fetal bovine serum (FBS) and has been critical step to developing fully defined culture conditions. Matrigel™ is a non-defined xenogeneic substrate that eliminates the need for a supportive inactivated mouse embryonic fibroblast feeder layer (iMEF) when used in conjunction with iMEF conditioned medium or a specialty medium such as, Essential 8™ [115]. However, Matrigel™ does not meet the goal of establishing fully defined humanized conditions. Abraham and colleagues have developed a non- xenogeneic feeder- free substrate by decellularizing human foreskin fibroblasts and have extensively its usefulness in developing 'humanized' conditions for hPSC culture [116]. Recently, Primorigen Biosciences launched a defined and xeno- free substrate, Vitronectin XF™, but similar to Matrigel™, this substrate does not support clonal passaging, and thusly is amenable to manual passaging or as dissociated small clumps in split ratios between 1:6 and 1:12. BioLamina commercially provides a xeno- free and defined substrate, LN- 521™, which is a laminin isoform, expressed in the ICM that supports single- cell plating at split ratios up to 1:30. However, laminins are hetero-trimeric proteins that are costly to produce and difficult to purify [113]. The cost of LN-521™ at $1,374 per 1mg compared to $80 for 1mg of Vitronectin XF™ makes routine use of LN- 521™ cost- prohibitive and a non- pragmatic substrate- based solution for culture viability, for the foreseeable future. Recently a chemically defined and xeno- free LN-521/E- cadherin matrix was reported to support clonal hPSC culture [64]. Interestingly this matrix was successfully used to clonally derive a hESC line, for the first time, from biopsy of a single blastomere from an 8-cell embryo.

Significantly, the addition of e-cadherin to LN- 521™ is critical to the single- cell clonal survival, as LN- 521™ alone has been determined to improve single- cell plating by increasing the migration of hESCs to promote cell- cell contact [64]. Development of culture conditions that support propagation of naïve hPSCs may provide novel cost- effective solutions that improve survival, increase proliferation rates, and reduce protein matrix dependency.

Research on suspension and three dimensional culture systems that more accurately mimic *in vivo* biology is very active [63]. It has been hypothesized that 3 dimensional culture will improve stable propagation of genomically normal hPSCs by presenting a more natural environment that reduces artificial selection. While this is a reasonable assumption, to date, there isn't any data or published study on the beneficial impact of 3-D culture in reducing the presence of genomic aberrations during continued propagation. Current approaches to study cell- culture influences on genomic instability are problematic. Efficient assays for such analysis are non-existent [113] and experimental designs entailing long term culture is prohibitive. However, defined genetically engineered lines with competitive advantage may enable investigating selection dynamics in various culture conditions on an amenable time- scale for statistical analysis. High throughput single- cell assays on genomic instability will be a significant advance for comparing mutation pressure across varying conditions [117, 118].

1.4 Genomic Instability During Early Embryonic Development

Chromosomal mosaicism is highly prevalent during early embryonic development. Embryos are classified as: (a) diploid- where all cells of the embryo are euploid, (b) aneuploid- all cells are define by the same genomic aberration, (c) diploid- aneuploid- where some cells are euploid and

other cells are of the same or multiple aneuploidies, or (d) aneuploid mosaic- where all cells exhibit aneuploidy [104]. Chaotic embryos refer to aneuploid mosaics with greater than three distinct aneuplodies [119, 120]. In 1978, the world witnessed the first birth of a baby conceived in the laboratory using *in vitro* fertilization (IVF) [121]. Pre-implantation genetic screening (PGS) is a process where 1-2 cells are taken from a blastomere of a morula stage IVF embryo to test for the genetic make-up [122]. Advances in molecular and cytogenetic approaches are enabling researchers to profile the human genome during early development at unprecedented resolution and specificity [123, 124]. Cytogenetics, traditionally performed via conventional g-band karyotyping, spectral-karyotyping, or fluorescent *in situ* hybridization (FISH) has been further empowered by advances in single- cell genomic technologies. With cellular precision we can interrogate the human genome using high through put technologies, such as array comparative genomic hybridization (aCGH), single nucleotide polymorphism (SNP) arrays, and deep sequencing from amplified DNA from a single- cell [125, 126]. The application of single-cell approaches has become increasingly apparent as chromosomal mosaicism is highly prevalent during cleavage stage embryos [127, 128].

Compared to other mammalian species human embryos have an order of magnitude higher prevalence of aneuploidy [129]. Sixty-five percent of spontaneous miscarriages have chromosomal abnormalities [104] and only 30% of conceptions result in live-birth. This suggests that CIN is a significant barrier to successful reproduction and that data from IVF embryos is also mirrored in pregnancies [130]. Errors from meiosis have two distinct features compared to mitotic-based errors: (a) uninform throughout embryo [131] and (b) maybe more resistant to self-correction at the peri-implantation stage [124, 132]. For our purposes of elucidating genomic

instability in hPSC culture, we emphasize mitotic-based mechanisms. PSCs have a characteristic cell cycle profile distinct from somatic cells. A shortened G1 phase of the cell cycle and absence of interphase and mitotic cell cycle checkpoints may explain the high rate of CIN during early development [44, 133-135]. For the first 3 days, until compaction, the post-zygotic embryo relies on maternal mRNA for cellular instruction, upon which it activates its own genome [104]. Vanneste and colleagues report that at day 3, 91% of cleavage stage embryos had at least one aneuploid cell [105] and only 49% contain any normal diploid blastomeres [136]. Blastocyst stage embryos carry a high degree of chromosomal abnormalities; however, the proportion of abnormalities decreases from the cleavage to the blastocyst stages, indicating negative selection by the time of peri-implantation [130]. In a study of 1,290 embryos using aCGH, 56% of blastocysts were classified as chromosomally abnormal, including meiotic and mitotic originations. Of this 56%, ~30% of the blastocysts were aneuploid mosaic and diploid- aneuploid mosaic, indicative of mitotic instability during early cell divisions. Of the diploid-aneuploid mosaics only 9% are greater than 33% euploid. With this low percentage of euploid cells in diploid-aneuploid mosaic it is unlikely these embryos are peri-implantation viable Figure 2 [104].

Dekel-Naftali and colleagues report the following percentages of chromosomally normal IVF embryos during 0-13 days of culture. On day three, 31.1% of embryos were classified as normal and by day 6 the percentage increased to 45.0. The trend continued on day 7 to 57.1%; and, on days 8-13 the average percent normal was 52.6% [130]. The data from both studies suggests aneuploidy is selected against throughout early development. The types of genomic alterations observed in mosaics are similar to those seen in children born with developmental disorders and

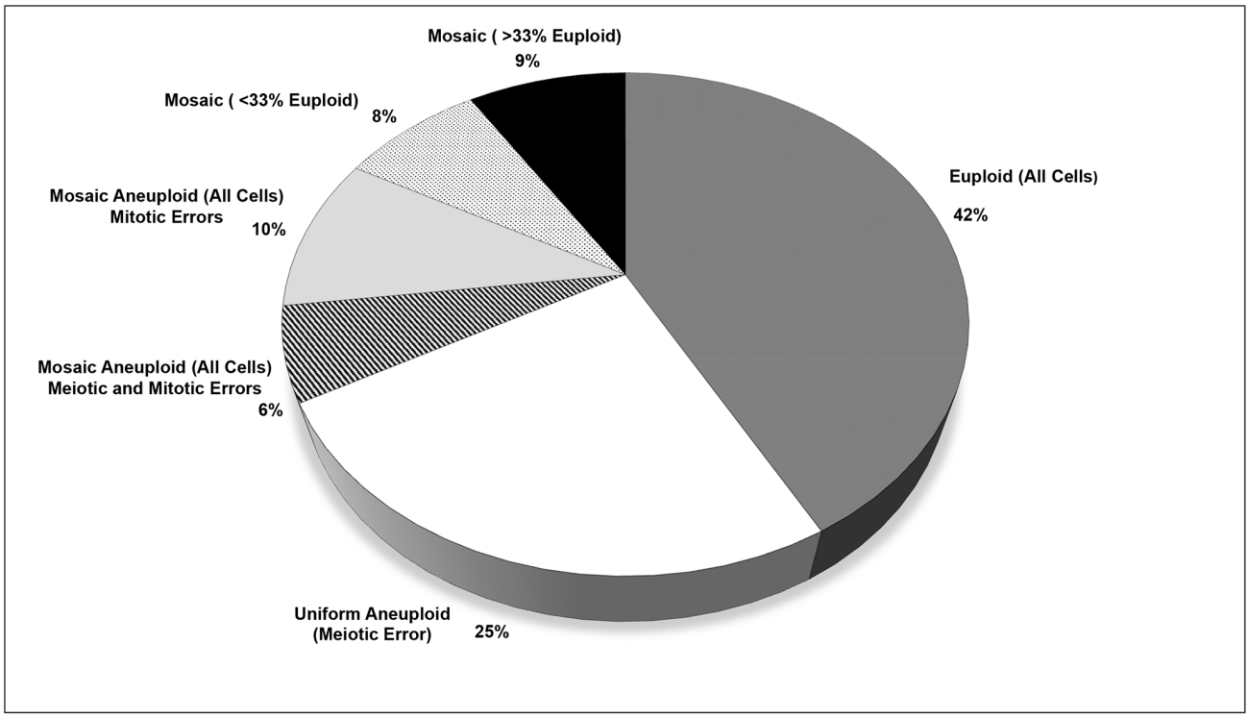

Figure 2 Chromosomal mosaicism in early embryonic development. Only 42% of pre-implantation genetic screening embryos are euploid for all cells. Aneuploidy from mitotic errors are very prominent in early development in up to 33% of embryos. The fraction of viable aneuploid embryos is likely very low since only 9 percent have greater than 33% euploid cells. Figure is adapted from *Aneuploidy in the human blastocyst* [104].

those seen in cancer, suggesting a clinical significance to understanding the CIN of embryonic stem cells [105]. Numerical and structural abnormalities are common. In cleavage- stage embryos, Mertzanidou and colleagues found that 70% contained large-scale structural chromosomal alterations [123]. Two large independent studies differed on the frequency of monosomy compared to trisomy, but the tendency is to report a higher prevalence of monosomy in aneuploid pre-implantation embryos [124, 137]. Post-zygotic mitotic errors are commonly caused by anaphase lagging and can also result from mitotic nondisjunction [130]. Micronuclei formed from extruded lagging chromosomes and are appreciably observed at cleavage stage embryos, validating the prominence of this mechanisms in contributing to genomic instability in totipotent and pluripotent cells [124]. Common to two studies, the most frequently observed aneuplodies of IVF embryos are reported as chromosomes 22, 16, 15, and 21, [104, 124] respectively; however, recurrent aneuploidies has not been observed at the pre-implantation stage [130].

Self-correction has been attributed to reducing the number of aneuploid embryos at the blastocyst-stage and peri-implantation relative to cleavage embryo [122, 131]. Of the abnormal embryos tested on day 3 by PGS, it was found that 35.5% became normal by the time of final testing at developmental arrest [130]. Munne and colleagues report self-correction in aneuploid embryos monitored at day 3, day 6, and day 12 post-implantation [138]. In 4 mosaic embryos with an average of 12.5% normal cells on day 6, 47.8% were normal by day 12; thereby, supporting the important role for post-blastocyst stage normalization in embryonic development [138]. Fragouli and colleagues report a decrease in abnormalities per embryo from 3.3 at the cleavage stage to 1.1 in blastocyst cells [124]. The same mechanisms for genomic instability may account for self-correction, anaphase-lag, nondisjunction, or chromosome demolition [138]. It is likely that in

diploid- aneuploid mosaic embryos, diploid cells during cleavage divide better than aneuploid cells leading to disomic enrichment by day 5 [131]. Apoptosis and decreased viability of aneuploid cells is another means for selection of disomic cells. In the blastocyst, apoptotic pathways are activated and some aneuploid blastomeres undergo apoptosis [139]. Interestingly, reprogramming somatic cells has demonstrated genomic mosaicism originating from adult cells, however their embryonic origin is unknown [140, 141]. As well, healthy mitotic and post-mitotic neurons have been shown to commonly exhibit aneuploidy [142-144] and genomic alterations during embryonic brain development is increasingly speculated to cause adult neurological diseases, such as schizophrenia [100, 101, 145].

Narwani and collagues derived 12 hESC lines from PGS- identified aneuploid blastocysts containing trisomies 14, 15, or 18 and monosomies 14, 16, 18, or 21. Interestingly, all the aneuploid- derived hESC lines were euploid; except, for one exception, the CSES14 line contained a partial translocation of chromosome 17 to chromosome 7 with karyotype 46XX, t(7;17). The authors show through polymorphic maker expression that euploidy was not established through mitotic- based self-correction [146]. They propose in vitro selection favored euploid proliferation [147] and conclude that aneuploid mosaic blastocysts can be used to establish normal euploid hESC lines.

1.5 Genomic Instability of Human Pluripotent Stem Cells During Culture

Culture adaptation is the integration of two separate processes, mechanisms resulting in genomic alterations and selection of genomic variant cells. Recent publications have underscored the presence of chromosomal mosaicism in normal and abnormal hPSC lines [148] . Using FISH,

Dekel-Naftali and colleagues demonstrated across 5 hPSC lines, hESC and iPSC, that normal cultures exhibit low- grade mosaic aneuploidy. Probing hESCs for chromosomes 12, 13, 16, 17, 18, 21, X, and Y, it was determined that hESCs had a statistically significant increase in aneuploidy compared with amniotic fluid cell controls. Both iPSCs and hESCs exhibited increased aneuploidy percentages over time in culture. Per chromosome, gains and losses appeared stochastic; however, monosomy was found more often than trisomy, a characteristic not often reflected in recurrent hPSC genomic alterations. The average aneuploidy rate per chromosome was found to be 1.3% (+/- .6), suggesting an expectation of 29.9% of cells in any given culture to contain an aneuploidy [148].

Peterson and colleagues propose that mosaic aneuploidy is a normal characteristic of hPSCs that may help explain the phenotypic heterogeneity of hPSC lines. Their extensive analysis on 6 hESC lines and 1 iPSC lines at early passage (<p50) demonstrate a significant presence of aneuploidy and preference for monosomy compare to trisomy, with common exhibition of hypoploidy. By conventional g-band scoring, the monosomies could be misconstrued as artifact; however, the high presence of monosomies was confirmed by FISH. Their results showed that within a given culture of hPSCs, between 18-35% of cells may be aneuploid. This percentage of aneuploidy is consistent with observations by Dekel-Naftali and colleagues who found 1.3% per chromosome were aneuploid. The presence of aneuploid mosaicism was independent of laboratory, culture conditions, and passage number with chromosomal gains and losses observed to be stochastic and non- clonal. They suggest chromosomal mosaicism may be a vital part of the pluripotent state to "endow hPSC lines with fitness" for self-renewal and to respond to environmental cues for differentiation [103].

In 2012, Biancotti and colleagues, investigated 419 aneuploid PGS embryos to look at patterns of monosomy and trisomy *in vitro* and found a total of 341 monosomies and 361 trisomies. Notably, a bias towards monosomy relative to trisomy as a whole or per chromosome was not observed. However, some chromosomes were determined prone to numerical alterations. Of the 12 chromosomes interrogated by FISH, chromosomes 8, 17, and 20 had the least frequency of numerical alterations [106]. Chromosome 8 contains C-myc, a known oncogene significant in reprogramming [9], and chromosome 17 and 20 are among the most frequently observed abnormalities in culture [88]. Selection bias for trisomy was observed. hESC lines were established from blastomeres exhibited trisomy for 13, 16, 17, 20, and 21; however, only one hESC line from a monosomy blastomere for X could be generated, suggesting that monosomy is deleterious for cell survival and development. Interestingly, trisomy 17 or 20 in blastomeres increased the likelihood of hESC line establishment, indicating significant selective advantage for these chromosomes. Viability difference between trisomy and monosomy is attributed to gene expression and it is likely that 50% loss of gene expression is more deleterious than a 1.5 fold dosage increase [106].

Over the past decade, since the first report on the presence of chromosomal abnormalities in hPSC culture, a significant amount of data has accumulated cataloguing recurrent abnormalities and their relative frequency. Initial studies using g-band karyotyping have progressed in technical capacity to high resolution SNP arrays, including two recent publications that analyzed a total of 322 hPSC lines using Illumina 1M Quad SNP array technology [87, 88]. The most frequently chromosomal abnormalities are chromosomes 1, 12, 17, 20, and X, with trisomy 17 being the most frequent aberration in our bibliographic review of 22 publications (Figure 3), and

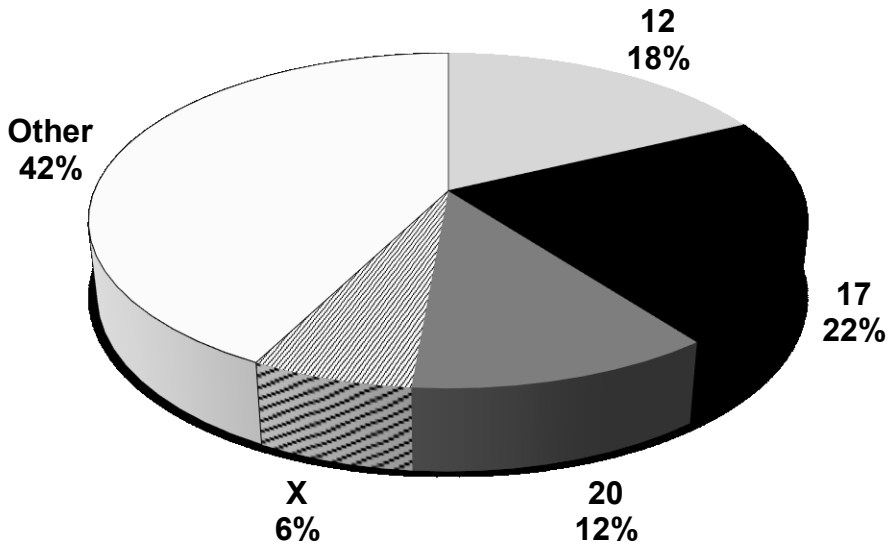

Figure 3 Distribution of Recurrent Chromosomes Alterations in hPSCs. 22 publications were surveyed for numerical and structural chromosomal gains. Trisomy 17 is the most commonly observed chromosomal alteration. "Other" is all chromosomes not specifically listed.

in the International Stem Cell Initiative's consortium study of 136 ethnically diverse hPSC lines [87]. Along with chromosome 17 alterations, Laurent and colleagues report a high frequency of copy number increases for chromosomes 12, 20, and X across 186 lines [88]. SNP arrays detect post-selection clonal genomic alterations conferring phenotypic advantage; however, little is known regarding the genes on these amplified loci and their phenotypic association. Small scale duplications on chromosome 12 encompassing NANOG and/or the pseudogene NANOGP1 have been observed, but so far, no functional relevance for selective advantage has been demonstrated for either. Interestingly, a minimal amplicon for chromosome 20 at 20q11.21 has been widely observed encompassing the gene BCL-XL. Recent reports have demonstrated a clear phenotypic advantage for increased expression of BCL-XL in hPSCs and a driver mutator phenotype in hPSCs has been suggested for this well- known oncogene [149-151]. Chromosome 17 is largely characterized by numerical alterations but a minimal amplicon on 17q25 has been reported [87, 88, 92]. Currently, no reports have demonstrated a functional relevance for any gene to help explain trisomy 17.

1.6 Mechanisms and Assays for Quantitating Genomic Instability in hPSC Cultures.

CIN and microsatellite instability (MIN) are largely reported as mutually exclusive events [152]. Independently using the HPRT and APRT loci, researchers have been able to demonstrate that ESCs have reduced base pair mutation compared to somatic cells [153]; and, hESCs are associated with very robust DNA repair machinery [154-157]. Aneuploid- mosaicism is prominent in IVF blastocysts, and hPSCs are prone to numerical and structural genomic alterations [88, 103, 104, 130, 148]. Critical cell cycle checkpoints associated with protecting against CIN are absent in hPSCs, such as the mitotic spindle assembly checkpoint and the

decatenation checkpoint [134, 135]. Therefore, we decided to focus our efforts on quantitating CIN in hPSC cultures. Culture conditions that influence CIN are largely unknown, but more importantly assays to measure CIN in hPSC cultures are poorly developed and inefficient [113]. An efficient assay for quantitating CIN in hPSC cultures would meet the following criteria: (a) high throughput, (b) devoid of any selection process, and (c) significantly capture the biology underlying genomic alterations. To avoid selection dynamics, single- cell approaches are requisite. High throughput assays have significant advantage in sensitivity and performing statistical analysis. An ideal biomarker is one serving as a primary driver of CIN, by reducing these events, the extended propagation of euploid populations should be improved.

Gisselsson proposes direct and indirect measures for assessing rate of CIN [158]. Direct measures screen genomic content to ascertain mutation rate. Technical challenges can limit resolution and specificity of genomic- based approaches, however advances in single- cell genomics is enabling this approach to unparalleled detail [159]. Non-clonal G-banding, FISH, and spectral karyotyping (SKY) can quantitate the amount of CIN at any given passage [160]. Each of these approaches are labor- intensive and require significant specialized training. Indirect measures for CIN look at biomarkers associated with chromosomal alterations, such as supernumerary centrosomes, micronuclei, anaphase bridges, and nuclear budding [158, 161]. A leading cause of CIN is malsegregation of chromosomes during mitosis [162]; however, nuclear budding during S- phase can expel excess DNA from the nucleus [163]. Micronuclei can form from either of these mechanisms [164, 165]. Anaphase bridges form from telomere associated break- fusion- bridge cycles [166]. Centrosomes coordinate the spindle apparatus of the microtubule organizing center (MTOC) and are responsible for the faithful segregation of sister

chromatids into two daughter cells. Supernumerary centrosomes are a significant cause of chromosome missegregation during mitosis and are an established mechanism for inducing CIN through multipolar mitosis **(**Figure 4) [167]. Our lab took two approaches to quantitating the CIN at any given passage in culture. We looked directly at non- clonal genomic alterations in two lines at early and late passage. Secondly, we took an indirect approach by quantitating the number of supernumerary centrosomes.

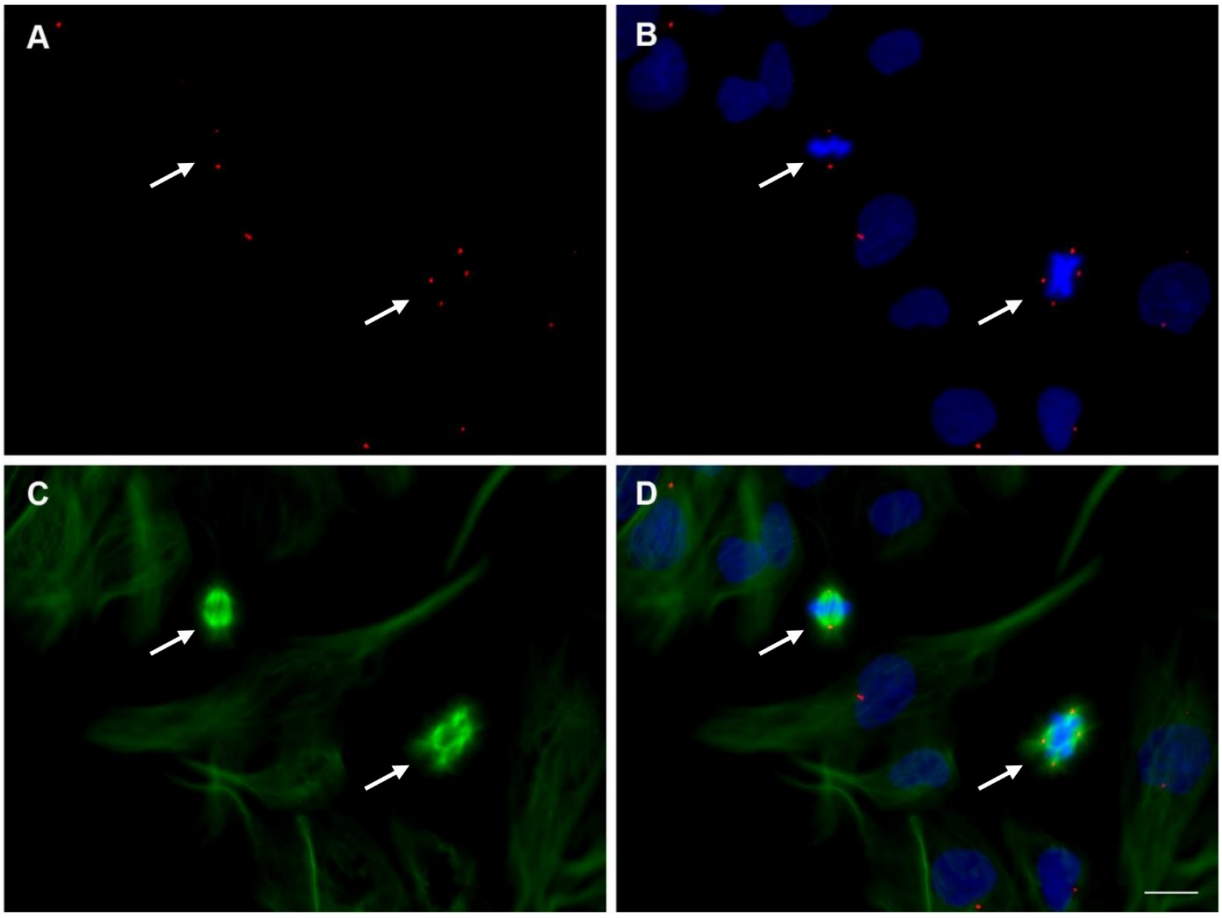

Figure 4 Multipolar mitosis in hPSCs with supernumerary centrosomes. The BG01 hPSC line was stained for centrosomes against pericentrin (red) (A), DAPI for nuclei (blue) (B), and β-tubulin for spindle assembly (green) (C). Normal bipolar mitosis consisting of 2 centrosomes (left arrow) and abnormal tetrapolar mitosis with 4 centrosomes (right arrow) (D). Scale bar= 50μm.

1.7 Research Summary

After considering the above mentioned studies which clearly demonstrate the importance of reducing genomic instability in culture, we investigated centrosome instability and a candidate gene, ARHGDIA, hypothesized to confer selective advantage in single- cell culture. Our work focuses on single- cell culture for its potential benefit in scale- up and standardizing differentiation protocols. We found that single- cell culture can adversely influence centrosome behavior during the initial culture transition by an unidentified mechanism. Further towards our goal of studying culture adaptation, we overexpress this candidate gene to develop a genetically defined biologically relevant selection model and demonstrate the application of our selection system to hPSC cultures passaged as single- cells and exposed to ROCKi, Y27632. Building upon the literature, we tested newly reported naive state hPSC culture conditions and demonstrate LIF- responsiveness with successful long- term self- renewal and differentiation capability. We propose that naive hPSCs may be a more genetically stable population by its clonal advantage. This work is unique in demonstrating phenotypic advantage of a gene located on chromosome 17 that may help explain the widespread observation of trisomy 17 in many labs.

CHAPTER 2

The Role of ARHGDIA in Increasing Single- Cell Survival of Human Pluripotent Stem Cells

ABSTRACT

Human pluripotent stem cells (hPSCs) have generated a lot of interest in the scientific community based on their potential applications in regenerative medicine. However, numerous research groups have continued to report a propensity for genomic alterations during hPSC culture that poses concerns for basic research and clinical applications. Work from our laboratory and others has demonstrated that amplification of chromosomal regions is correlated with increased gene expression. To date, the phenotypic association of common genomic alterations remains unclear and is a cause for concern during clinical use. In this study, we focus on a common genomic aberration and a list of candidate genes with increased gene expression to hypothesize a gene that may confer selective advantage when overexpressed. Our transduced candidate gene overexpressing hPSC line exhibited culture dominance in co-cultures of modified overexpression lines with non-overexpression lines. Furthermore, during low density seeding, we demonstrate increased clonality of our overexpression line against matched controls. A striking observation is that we could reduce this selective advantage by varying the hPSC culture conditions with the addition of ROCKi. This work is unique in (a) demonstrating a novel gene that confers selective advantage to hPSCs when overexpressed and may help explain a common trisomy dominance, (b) providing a selection model for studying culture conditions that reduce the appearance of genomically altered hPSCs, and (c) aiding in elucidation of a mechanism that may act as a molecular switch during culture adaptation.

INTRODUCTION

Human pluripotent stem cells (hPSCs) are defined by their ability to self-renew, undergo tri-lineage differentiation, and maintain a normal karyotype [6]. However, earlier results from our laboratory and others demonstrates a propensity for hPSCs to acquire abnormal genomic signatures upon prolonged propagation [82, 87, 88]. Moreover, the presence of genomic alterations can be increased by specific hPSC passaging methodologies [87, 168]. Two general approaches to passaging hPSCs involves enzymatic dissociation into single- cells or manual dissociation into small clumps. Small clumps of hPSCs maintain e-cadherin based cell-cell contact which is critical to hPSC survival [76], while trypsinization of hPSCs results in cleavage of the extracellular domain of e-cadherin, which undergoes time-dependent turnover [45]. Significant debate in the stem cell community exists on whether hPSCs should be passaged as single cells or as small clumps. Ideally, hPSCs would be passaged as single-cells for the following advantages: (a) increased numbers for scale-up, (b) standardization of directed-differentiation protocols, and (c) clonal genetic manipulation [3, 43, 45]. While manual dissection of hPSC colonies allows for selection of morphologically superior colonies, this technique is time intensive and low throughput. Upon differentiation, lineage specificity is influenced by the size of the initial cluster or number of cells [169, 170]. Uniformity from single-cell seeding and accurate cell counts are thus important steps for reproducibly controlling size of aggregate formation and standardizing directed differentiation protocols [171, 172]. Unfortunately, increased genomic instability during single- cell passaging is a primary concern for this approach and poor single-cell viability at seeding remains a significant barrier to large-

scale production [87, 110]. In order to increase hPSC single cell survival at passaging, many researchers have incorporated small molecules in the culture medium.

Inhibition of the RHOA-ROCK- pMLC pathway has been demonstrated to increase hPSC single- cell survival [109]. Apoptosis from single-cell dissociation has been demonstrated to be highly specific through the phosphorylation of MLC, by the kinase ROCK, inducing blebbing associated cytoplasmic membrane rupture [110]. However, use of ROCK inhibitor (ROCKi) in culture medium is of considerable debate, as reducing apoptosis could lead to increased survival of genomically abnormal hPSCs, since apoptosis is a proposed mechanism for purging cultures of cells with genomic damage [173, 174]. Since hPSCs exhibit high rates of apoptosis and poor single- cell viability, strong selective pressure may exist for genomic alterations that increase clonal survival and are anti-apoptotic [92]. The strong selection for specific genomic species of hPSCs is evident by the common observance of particular genomic alterations, such as 12, 17, 20, and X. This is highly suggestive that in culture adaptation, comprised of both mutation and selection, selection is a particularly strong force in the emergence of genomic variants [82]. Therefore, by improving culture conditions, we may be able to reduce the selective pressure for genomic variants with phenotypic advantage.

Since hPSCs may be intrinsically characterized by a high degree of CIN, focusing on reducing selection may be the ideal strategy in preserving the genetic integrity of hPSC cultures [130, 175]. To date, the phenotype behind common and specific genomic alterations has been unclear, and more specifically the functionally relevant genes located on these genomic loci responsible for culture selection has remained elusive [87]. We have taken the approach of

passaging hPSCs as single cells in order to: (a) reproducibly generate genomic abnormalities for further study, (b) better understand single- cell passaging's influence on genomic instability, and (c) to determine conditions that may reduce genomic instability during single-cell passaging. The long-term goal of this work is to improve scale-up of genomically normal hPSCs. Improving single-cell culture of hPSCs while reducing genomic instability is of significant importance as the regenerative medicine industry seeks to fill the need of supplying billions of cells for a single regenerative medicine application [176]. Approaches for improving cultures inoculated with single- cells target reducing: (a) cell death during single- cell plating, (b) spontaneous differentiation during initial seeding, and (c) the presence of recurrent genomic alterations. We hypothesize that increasing cell- viability will reduce selection of genomic variants and promote the continued propagation of genomically normal hPSCs. This work is unique in demonstrating (a) a novel gene that confers selective advantage to hPSCs when overexpressed and may help explain a common trisomy dominance, (b) provide a selection model for studying culture conditions that reduce the appearance of genomically altered hPSCs,

METHODS

Human Pluripotent Stem Cell Culture

HPSCs were maintained on mitomycin C–inactivated mouse embryonic feeder (MEF) layers in DMEM/F-12, 20% knockout serum replacement, 2 mM L-glutamine, 1% nonessential amino acids, 50 U/mL penicillin, 50 microgram per mL streptomycin (all from Gibco/Invitrogen), 0.1 mM beta mercaptoethanol (Sigma), and 4 ng/mL bFGF (Sigma). Cells were enzymatically passaged via sequential dissociation using 1mg/ml type IV collagenase (Gibco) and 0.05% trypsin–ethylene-diamine tetra-acetic acid (trypsin-EDTA, Invitrogen) or manually passaged by fire-pulled pasteur pipette. hPSCs were replated on fresh feeder layers or BD Matrigel™. Cells grown in BD Matrigel™ were coated at the lot specific recommended dilution in 35mm plates. Medium was conditioned on iMEFS at 5 x 10^6 cells per T-75 flask for 24 hours up to day 10 from seeding.

Microarray Gene Expression Analysis

Statistical analysis was performed in the R environment. 6 HGU- 133A Affymetrix microarrays comprising two classes, BG01v's (aneuploid) and H9's (euploid), were normalized by cyclic loess and signal intensities summarized by GCRMA. Presence (P), marginal (M), and absence (A) calls were determined using the MAS 5.0 detection algorithm. A gene was considered for hypothesis testing, if it was considered present in either sample class. A gene was considered present in either the normal or abnormal set if it was called present in at least two of the three replicates. p-values were adjusted via Benjamini and Hochberg correction. Statistically significant genes were determined at a FDR less than 0.05. Fold changes were calculated in reference to the euploid sample arrays, such that positive fold change values reflect an increase

in expression in the aneuploid class and negative fold changes an increase in the relative expression of the normal class.

Chromosomal Distribution and Fold Change Calculation

Each probe set was annotated with chromosomal location via R using the *hgu133a.db* library. A normalized ratio for each chromosome was plotted on a histogram, with the values calculated by dividing the number of significant genes (either increased or decreased) by the number of known probe sets for each respective chromosome. Probe sets considered present among the normal class were considered for chromosomal fold change analysis. For each chromosome, the mean across replicates was found for each gene, then the 0.2 trimmed mean expression level of all genes for that chromosome was calculated, separately, for the normal and abnormal samples. The fold change of abnormal to normal samples was then calculated, such that positive fold change values reflect an increase in expression in the aneuploid class and negative fold changes an increase in the relative expression of the normal class.

Ontology Analysis

Genes were compiled from the following four sources: Gene Ontology, Cancer Genome Project, PluriNet [177], and Genomic Instability Set [178]. The Gene Ontology database was queried for each ontology of interest by the GO ID using the GO ID/Term search. The entire list of gene ontologies including children consists of 280 unique ontologies, translated in R from the GO ID using the *go.db* library. From the Cancer Genome Project, all the genes of the "complete working list" from the cancer gene consensus were included. Genes that were listed with an associated cancer or syndrome were annotated under phenotype as cancer or cancer

predisposition in our final gene list. Genes from the Genomic Instability set were listed as genomic instability and their associated function were included. Genes from the PluriNet were added and were annotated under phenotype as self-renewal. Ontologies were abbreviated and the phenotype translated to cancer, cancer disposition, self-renewal, and genomic instability. Significantly increased genes located on one of the trisomic chromosomes were then annotated with ontology and phenotype.

Preparation of hPSCs for Karyotype Analysis

Human PSC cultured in T-25 flasks were subjected to cytogenetic karyotype analysis. Cells were cultured to sub confluency with a growth medium change 24 hours before harvesting. 120 ng/mL of colcemid was added for 3 hours and 15 minutes at 37ºC. Cells were rinsed with HBSS–(Ca/Mg) and dissociated with 0.05% trypsin. Dislodged cells were centrifuged at 1000rpm for 8 minutes. The cell pellet was gently resuspended in 0.075 M KCl solution and fixed in a solution containing 3:1 of methyl alcohol and glacial acetic acid at -20ºC for 30 minutes followed by twice-repeated rinsing in fixative at 1000 rpm for 8 minutes. Cells were stored in fixative at -20ºC until analysis. Metaphases were spread on microscope slides, and chromosomes were classified according to the International System for Human Cytogenetic Nomenclature (ISCN) using the standard G banding technique. For non-clonal analysis, >50 metaphases were examined. For clonal g-banding, 20 metaphases for each sample were examined.

Generation of ARHGDIA overexpression lines

For lentiviral generation, Glycerol stock of Precision LentiORF ARHGDIA w/ Stop Codon (Open Biosystems) was stored at -80ºC. 10 µl of ARHGDIA glycerol stock was used to inoculate 3-5 mls of LB Medium with ampicillin and agitated for 16 hours at 300 rpm at 37ºC. 1 ml was further diluted in 250 ml, shaken at 300 rpm and incubated another 24 h at 37ºC. The plasmid was extracted using the Qiagen Maxi Prep kit by following the manufacturer's directions, and plasmid concentration quantitated using the BioMate3 UV-VIS Spectrophotometer (Thermo Scientific, Waltham, MA). Lentivirus was generated using HEK293 cells on a 10 cm cell culture plate. 80% confluent HEK293 cultures were transfected with 10 µg of the ARHGDIA plasmid, 7.5 µg of the packaging plasmid (psPAX2) (Addgene, MA), and 2.5 µg of the envelope plasmid (pMD.2) (Addgene, MA) using Roche transfection reagent, XtremeGENE 9. After 48 h exposure, the viral supernatant was collected, 0.45 µm filtered, and stored at 4ºC for less than 24 hours. The viral supernatant was concentrated using the Lenti-X concentrator (Clontech, CA) by following the manufacturer's protocol. The concentrated virus was resuspended in 500 µl of DMEM/F12 medium and aliquotted for storage at -80ºC . One 50 µl aliquot was added to a 35mm petri dish containing hPSCs cultured on Matrigel™ or iMEFs along with the addition of 6 µg per ml of polybrene (Santa Cruz Biotechnology, CA). 24 hours later, virus containing medium was exchanged with the hPSC growth medium. Subsequently, the hPSCs monitored for GFP- positive expression by the Nikon Eclipse TE 2000-S inverted microscope (Nikon, Melville, NY). GFP- positive colonies were marked by objective- marker lens, manually selected, and propagated until use in experimentation.

In vitro differentiation of hPSCs and histopathology of hPSC-derived embryoid bodies.

To generate embryoid bodies (EBs), hPSCs were dissociated using 0.05% Trypsin and resuspended in growth medium without bFGF. EB formation was facilitated using suspension culture by a hanging drop method, where cells at a density of 5,000 cells per 20 μl drop were suspended from a Petri dish lid in 50-100 droplets with the addition of 10 μM ROCKi in the culture medium. After 3 days, the surviving EBs were transferred onto agar plates at in 20 ml of EB medium (hPSC growth medium without bFGF) to facilitate further differentiation with medium changes every 2 days for a total differentiation duration of 15-20 days. EBs were prepared for morphological analysis by fixation in 4.0% PFA in 1.5 mL microfuge tubes at 50-100 EBs per tube. EBs were rinsed with PBS to remove PFA, resuspended in 200 μL melted 4% low melting point agarose (Sigma Aldrich) at 42^{o}C, and incubated for 2 h to allow settling. Final pelleting and agarose solidification were performed with brief room temperature centrifugation at 500g. Agarose embedded samples were removed as single plugs and processed by dehydration with increasing ethanol concentration to 100% followed by xylene and paraffination in a Leica TP1020 tissue processor. Hematoxylin and Eosin (H and E) staining was performed on microscope slide mounted 5 mm sections in a Leica Autostainer XL workstation (Leica Microsystems, Richmond, IL). Images were acquired using an Olympus BX51 microscope (Olympus, Center Valley, PA) using the default imaging parameters.

Antibodies and Immunocytochemical Analysis

HPSCs cultured on Matrigel™ or iMEFs in four chambered glass slides or cover slips in 35mm dishes were fixed via paraformaldehyde (PFA, 4%) in PBS or 80% Methanol. Permeabilization for intracellular markers was achieved with 0.2% Triton X-100 in PBS. 3%

normal goat serum was used for blocking and to dilute antibodies. Fixed cells were incubated with primary antibodies: OCT4 (Santa Cruz Biotechnology, Santa Cruz, CA), SSEA4 (Millipore, Temecula, CA), Pericentrin (Abcam), Beta-tubulin (Developmental Studies Hybridoma Bank), ARHGDIA (Santa Cruz Biotechnology, Inc.). Goat anti-mouse IgG, anti- rabbit conjugated to Alexa 488 or Alexa 594 (Molecular Probes, Eugene, OR) were used as secondary antibodies. Centrosomes were visualized with percentrin and the spindle apparatus by β-tubulin. Cells were counterstained with DAPI (4'-6-diamidino-2-phenylindole). At 40x magnification, centrosomes were counted per mitotic cell and the polarity recorded. Fluorescent images were acquired using a Cool- Snap EZ camera (Photometrics, Tucson, AZ) mounted on a Nikon Eclipse TE 2000-S inverted microscope (Nikon, Melville, NY) with NIS Elements BR software.

RNA isolation, real time reverse transcription quantitative polymerase chain reaction and gene expression analysis

RNA was isolated from hPSCs using DNA/RNA All Prep (Qiagen) and quantified using BioMate3 UV-VIS Spectrophotometer (Thermo Scientific, Waltham, MA) or Nanodrop 2000. cDNA was synthesized from 1 mg of RNA using cDNA High Capacity reverse transcription kit (Applied Biosystems, Foster City, CA). Transcriptional expression on various genes listed in Table 6 were analyzed using quantitative real time RT-PCR (QPCR). QPCR was performed on a Bio-Rad CFX96 Touch Real-Time PCR Detection System. Comparative gene expression analysis (three replicates) was conducted using the ΔCT or ΔΔCT method depending on the analysis and samples. GAPDH was used for normalization in all analyses. Relative gene expression for hPSC experimental samples was assessed against hPSC controls and reported as fold change and the student's T- test used for statistical significance testing.

Alkaline Phosphatase Assay

Staining for alkaline phosphatase was performed as per manufacturer instructions (Vector Laboratories, Burlingame, CA). Briefly, the hPSCs were rinsed with deionized water to remove traces of growth medium. The final solution was prepared by adding in order 2 drops of each constituent to 200mM Tris HCl buffer, pH 8.5. The hPSCs were incubated in the final mixture for 45 min in the dark and images were acquired using a Nikon DS-Fi1 camera mounted on a Nikon TS100 Microscope (Nikon, Melville, NY).

Clonality Assay

For low-density survival assays, 1000 hPSC cells obtained after passing through a 40 μm filter were plated onto iMEFs in 35mm plates. To visualize hPSC colonies, cultures were stained for alkaline phosphatase on Day 7 after initial seeding. The number of colonies were counted using an inverted Nikon TS100 Microscope (Nikon, Melville, NY).

Competition Assay

HPSCs (Arg) and hPSC(WT) were maintained independently by manual passaging until use in specific experiments. Upon initial enzymatic passage, cells were obtained after passing through a 40 μm filter and seeded at a mixed ratio of an estimated 70% hPSC(WT) and 30% hPSC(WT) onto Matrigel™ or iMEFs. Cultures were serially passaged enzymatically and passed through 40 μm filter at each passage. The percent of ARHGDIA overexpressing cells at each passage was quantitated by flow cytometry, using the Accuri C6 instrumentation. The percentage

of GFP positive hPSCs was gated against similar plots of control hPSC (WT) cells under similar cell culture handling.

Western Blot

At time of cell harvest and protein lysis, adherent cells were kept on ice and rinsed twice with ice-cold PBS+/+ (containing 0.9 mMCaCl2, 0.52 mMMgCl2 and 0.16 mM MgSO4) solution. After aspiration of the PBS+/+ solution, cells were lysed using the lysis buffer (Part# GL36) with protease inhibitor from the G-lisa kit, Cat# BK124 (Cytoskeleton Inc., CO). Upon addition of the lysis buffer, the cells were scraped, then spun down for 1.5 min at 11.6K rpm, and snap frozen in liquid nitrogen followed by stored at -80^{o}C. 20 µl of the protein lysate was used to quantitate the protein concentration using the Precision Red Assay (Cytoskeleton, Inc.).

For Western analysis, each lane on the gel was loaded with 30 µg of protein sample. Beta-tubulin (DSHB, Iowa) was used as the loading control. Proteins were separated by SDS-PAGE and transferred onto nitrocellulose membranes (BioRad) for western blotting. The membranes were exposed to primary antibodies at 1:500 to 1:2,000 dilutions at 4^{o}C overnight. Specific protein bands were detected and quantified using infrared-emitting conjugated secondary antibodies—anti-mouse 680 Alexa (Molecular Probes, Eugene, OR) or anti-rabbit IRDYE 800 (Rockland Immunochemicals, Gilbertsville, PA). Blots were exposed to secondary antibodies for 2 hours. Odyssey Infrared Imaging System and Image Studio Lite version 3.1 from Li-Cor Biosciences (Lincoln, NE) was used for image capture and densitometric analysis. For densitometric analysis, protein signal intensities were calculated and normalized against the loading control protein using the signal intensity of the lane divided by the maximum intensity of β- tubulin as the normalization ratio.

RESULTS

Clonal and Non- clonal Genomic Alterations Under Single- cell Passaging

For genomic instability studies and karyotypic analysis, we cultured four hPSC (H9, H1, BG01(v), and iPSC) lines of different origin. Each line was routinely maintained on iMEFs and were continuously cultured for greater than 25 passages. Previous work from our laboratory generated the hyperdiploid line, BG01(v), with a complex karyotype containing trisomies on autosomes 12, 14, 17, and an extra copy of the sex chromosome, X (Insert Reference). Using similar methodologies, we enzymatically dissociated cultures into single- cells by sequential exposure to collagenase followed by trypsin, denoted as CT throughout the remainder of this document. Prior observations from our lab suggest that genomic abnormalities present after 25 consecutive enzymatic passages [82], so we initiated g-band karyotyping after this window of continuous CT passaging. Karyotyping the BG01(v) line validated the existence of previously reported genomic alterations on chromosomes 12, 14, 17, and X. Additionally, in the BG01(v) cultures, a significant number of low-grade mosaics were observed for particular chromosomes. Of the metaphase cells analyzed, trisomy 3 was present in 14%, trisomy 11 in 18%, trisomy 20 in 34%, and a derivative of chromosome 16 in 16% of the cells. The presence of distinct and highly complex genomic species is suggestive of a high rate of genomic instability in the BG01(v) line. Under continuous culture, the H9 line was karyotyped at two passages, passage 71 (CT-26) and passage 150 (CT-105). The H9 line was aneuploid at passages 71 and 150. At passage 71, 67% of the karyotyped H9 cell line were determined to be trisomy 17. At passage 150, g-band analysis on the H9 cell line identified trisomy 12 and trisomy 17, suggesting an accumulation of genomic alterations upon extended culture. The H9 associated trisomy 17 at passage 150,

contained a deletion of p11.2. Trisomy 17 mosaicism of the H9 line at CT-26 suggests capture of the initial culture dominance of this genomic species. It is likely that the trisomy 17 at passage 150 is the same one as the original trisomy 17 but had simply undergone a structural deletion. The iPSC line, at passage 45 (CT-31), was trisomy for 17 and harbored a gain of X. The H1 line was karyotyped at two enzymatic passage points, CT-29 and CT-58, passages 68 and 97, respectively. While the initial H1- CT-29 sample was euploid, at CT-58, we found a previously unreported structural gain on chromosome 15 at p11.2. The karyograms of hPSC genomic alterations under single-cell passage are presented in Figure 5 and the genomic profile of the hPSC lines is summarized in Table 2.

Non-clonal genomic alterations can indicate an increased rate of genomic instability by inclusion of aberrations that are non-beneficial and do not undergo positive selection [160, 179]. Non-clonal g-band analysis, on a minimum of 50 metaphase spreads, was performed on the H9 line at passage 71 and the BG01(v) line. The BG01(v) line demonstrates a high presence of random non-clonal genomic alterations, with 18 of 50 metaphase cells exhibiting a unique genomic alteration (Table 3). In stark contrast to the observations in the BG01(v) sample, random non-clonal aberrations in the H9 line at CT-26 were only observed in 3 of 52 metaphase cells. This suggests that emergence of the competitive genomic species with trisomy 17 was not paired with an increase in genomic instability, as measured by the presence of non-clonal aberrations.

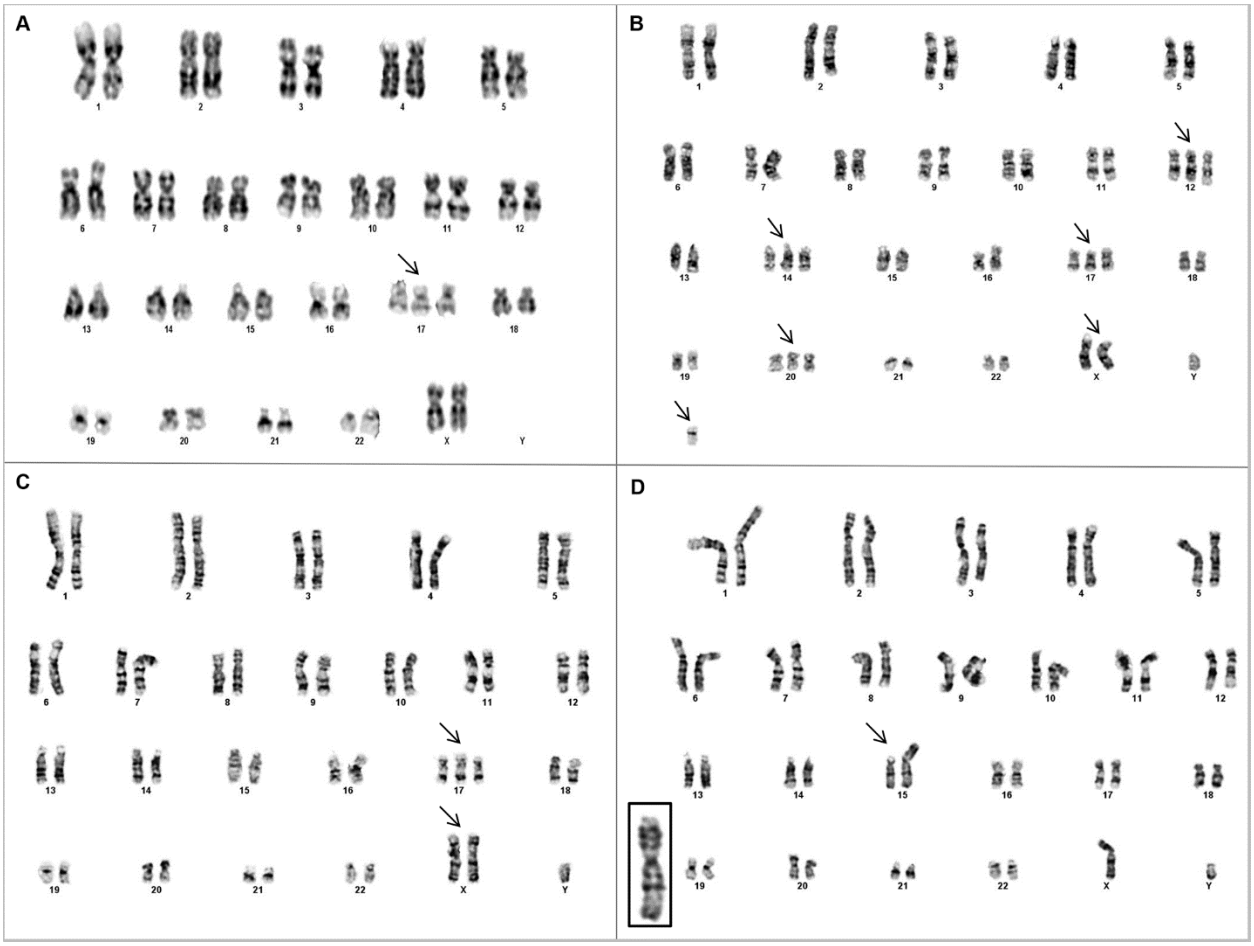

Figure 5. Karyogram of 4 hPSC lines serially passaged as single cells. H9 line at passage 71 exhibiting trisomy 17 (A). BG01(v) line exhibiting multiple trisomies on 12, 14, 17, 20, and X and a +der(16) (B). hiPSC exhibiting trisomy 17 and gain of X (C). H1 line with a segmental duplication on 15p11.2 (D).

Table 2 Clonal genomic abnormalities during serial single- cell culture

Cell Line	Passage #	CT #	Metaphase #	Karyotype (%)
H1	68	29	20	46, XY
H1	97	58	20	46, XY,add(15)(p11.2)
H9	71	26	52	47, XX, +17 (67)
H9	150	105	20	48, XX,+12,+del(17)(p11.2)
BG01(v)	69	NR	50	50, XXY (94); +3 (14); +11 (18); +12 (92); +14 (84); +17 (92); +20 (34); +der(16) (16)
iPSC	45	31	20	48, XXY,+17

HPSCs dissociated as single cells and cultured on iMEFs. The H1 and H9 lines were continuously passaged and karyotyped at two different passage points. H1 at passage 97 gained a segmental duplication of 15p11.2. H9 at early enzymatic passage, CT-26, was 67 percent mosaic for trisomy 17 and subsequently gained an additional chromosome 12. BG01(v) exhibits hyper-diploidy and culture mosaicism. The iPSC gained an X and chromosome 17. Non-clonal analysis was performed on BG01(v) and H9 passage 71 lines, with 50 and 52 metaphase spreads analyzed, respectively. The (%) is the percentage of cells in culture expressing the indicated genomic alteration. Abbreviations: add- addition, del- deletion, der- derivative, CT- collagenase/trypsin passage, NR- not recorded.

Table 3 Non- clonal karyotype analysis of hESCs exhibiting a unique genomic species

Cell Line	Metaphases	Mode	Range	Non-clonal (Range)
BG01(v)	50	50-51	44-58	18 of 50 (1-5)
H9p71 (CT-26)	52	47	37-48	3 of 52 (1)

The BG01(v) line demonstrates a high degree of genomic complexity with 18 of 50 metaphase cells exhibiting a unique genomic complement. In the H9 sample, only 3 of 52 cells had a unique genomic aberration. (Range) is the range on number of aberrations in the non- clonal cell. The modal karyotype is listed. The chromosome range includes hypoploid hESCs, which cytogeneticists most often attribute to a technical artifact; however, recently it was reported that hypoploid hESCs are viable [103].

Characterization of Centrosomal Amplification in hPSCs

Chromosomal instability (CIN) may be a hallmark of the PSC state. A high presence of aneuploid- mosaicism is well documented in the blastocyst and recent studies have established the prominence of CIN in hPSC culture [103, 104, 106, 124, 132, 175, 180]. Centrosomes are critical mitotic machineries that act like bipolar pulleys responsible for the faithful segregation of sister chromatids into two daughter cells during cell division. During S-phase of the cell cycle, the centrosome replicates to form two centrosome organelles that separate at mitosis and form each of the two microtubule organizing centers (MTOC) for bipolar division [181]. Supernumerary centrosomes have been shown to cause aneuploidy and are used as an indirect measure of the rate of CIN in cancer lines [158]. The presence of more than two centrosomes can lead to multipolar mitosis, which can induce chromosomal missegregation errors during cell division. However, the post-mitotic viability of multipolar cell division is likely low but in rare cases can drive clonal aneuploidy [167, 182]. Recently, it was reported that centrosomal amplification is characteristic to hPSCs and that increased passage number puts downward pressure for centrosome errors [175].

We sought to characterize centrosome behavior in hPSC across: (a) cell lines of different origin, (b) over passage number, (c) during initial enzymatic induced single- cell dissociation, and (d) aneuploidy vs euploidy. ICC was used to stain pericentrin for centrosome visualization and β-tubulin for microtubules of the spindle-assembly apparatus. First, we investigated the baseline supernumerary centrosome profile of various hPSCs: hEC, H1, H9, BG01, BG01(v), and hiPSC (Figure 6). The hEC line, 2102Ep, is an established pluripotent carcinoma line from germ cell tumors with a high degree of karyotypic abnormalities [183]. Thusly, the hECs served

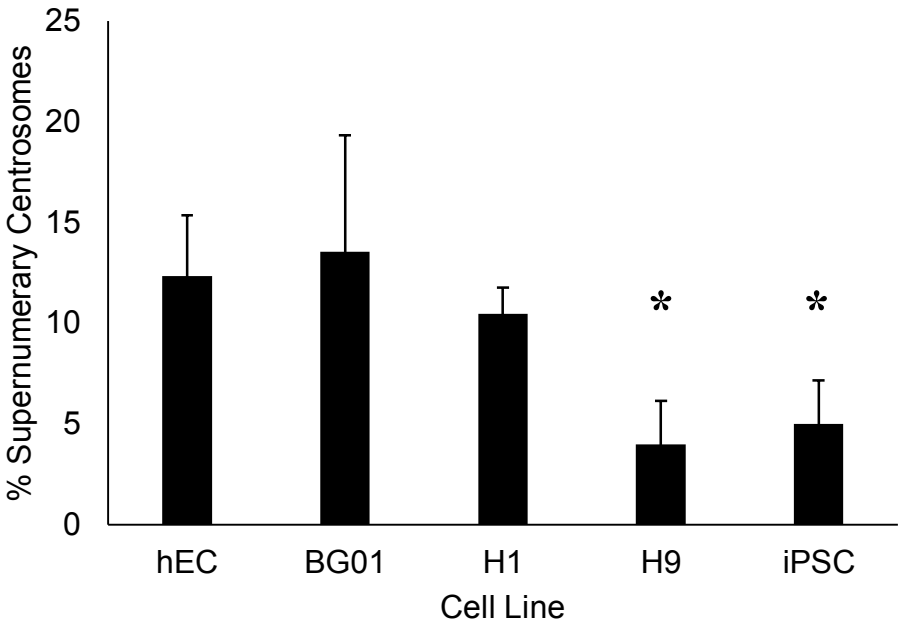

Figure 6. Human PSC lines exhibit variable expression of supernumerary centrosomes. BG01s have the highest percent of centrosomes errors. H9s and iPSCs have significantly lower centrosome errors than either BG01 or H1 line, (*) indicates $p < 0.05$.

as a reference line with known CIN. HECs were profiled in triplicate across three continuous passages, 55, 89, and 104, with an average centrosome error rate of 12.35% (+/- 3.03). For passages 55, 89, and 104, the supernumerary centrosome error percentages was 15.82% (+/- 1.76), 11.12% (+/- 1.61), and 10.13% (+/-1.38), respectively. Our results indicate that there is a certain degree of decreased centrosome errors in the hEC line under prolonged passage. The H1 and BG01 cell line exhibit a high percentage of supernumerary centrosomes. In the H1 cell line propagated by manual dissection, the supernumerary centrosome percentage was quantitated in triplicate at three different passages, spanning 70 continuous passages. The percentage of supernumerary centrosomes at passages 30, 72, and 100 are 10.66 (+/- 1.61), 9.10 (+/- 1.67), and 11.69 (+/- 5.46), respectively, with the average centrosome error across all three manual passages being 10.48 (+/- 1.3). The increased standard deviation in the H1 cell line at passage 100 is noteworthy, possibly indicating the precipice of centrosome error reduction; however, in general, we did not observe a decrease in centrosome amplification in the first 100 passages of the H1 line. Similarly, the BG01 supernumerary centrosome were quantitated in triplicate at two continuous manual passages, 39 and 64. The percentages of supernumerary centrosomes in BG01s were found to be 9.48 (+/- 1.26) and 17.65 (+/- 5.50), respectively with a mean of 13.56% (+/- 5.77). The BG01 line at passage 64 was found to contain the highest percentage of centrosome amplification in our baseline error analysis. Interestingly, among hESC lines, we found an exception to the high centrosome error rate in the H9 line. On three independently thawed H9 sublines, at manual passage numbers, 50, 51, and 65- each passage quantitated in triplicate- we determined an average centrosome error rate of 4% (+/- 2.14). The H9 had significantly decreased centrosomes errors compared to H1 and BG01 lines, with a p-value less than 0.05 for each line. We quantitated the centrosome amplification of an iPSC line and found a

significantly lower percentage of centrosome errors compared to both the BG01 and H1 lines with p-value < 0.05. The iPSC line at manual passages 11 and 36, each quantitated in triplicate, exhibited a mean centrosome error rate of 5.01% (+/- 2.16). Therefore, in this analysis we observed variable expression of supernumerary centrosomes across cell lines and consistent centrosome errors within cell lines. We did not observe centrosome error reduction within the first 100 passages.

Since enzymatic dissociation into single cells is positively correlated with an increase in genomic alterations and centrosome errors are a dominant mechanism causing CIN, we tested whether passaging hPSCs as single cells would increase the percentage of centrosome anomalies. Initially, hPSC lines were maintained using manual passaging protocols. The lines were then switched to enzymatic single-cell dissociation protocols and continuously passaged as single-cells. Since the iPSC and H9 lines had lower centrosome errors, these lines were used for the centrosome analysis. Interesting, in serial enzymatic culture of the iPSC line, we observed an accumulation of centrosome errors and a statistically significant increase in centrosome amplification. Centrosome errors increased from CT-1 to CT-3 to CT-5 and then decreased by CT-10 and remained similar throughout at passages CT-15, CT-25, and CT-30. The centrosome error percentage of the hiPSC manually passaged control cells, CT-0, is 5.01 (+/- 2.16). The peak centrosome error percentage at CT-5 is 18.02 (+/- 2.63), a 3.6 fold increase compared to CT-0 samples. At CT-10, the centrosome percent error decreased to 8.18 (+/- 2.17). CT-5 was significantly increased relative to CT-0, CT-1, and CT-10 for $p< 0.05$. Additionally, iPSC CT-1 and CT-3 samples were significantly increased relative to iPSC CT-0 samples, with a $p< 0.05$. Continued centrosome analysis on the enzymatically passaged iPSC line showed similar

centrosome error percentages for CT-15, CT-25, and CT-30 of approximately 9% (Figure 7). In the H9 line, compared to manual controls with a percent error of 4% (+/- 2.14), we observed a statistically significant spike at CT-1 with a percent error of 10.88% (+/- 1.75). Two passages later at H9 CT-3 the centrosome percent error had already reduced to 4.9% (+/- 0.56) (Figure 8). Together, the iPSC and H9 data are consistent that transition to enzymatic passaging destabilizes the mitotic machinery leading to increased centrosomal instability of cell lines propagated as single-cells.

Next we analyzed differences between karyotypically normal vs abnormal in multiple (H1, H9, and BG01) hPSC lines. The BG01(v) line demonstrated a striking difference from the euploid BG01 line. The BG01 line had a centrosome error percentage of 13.56% (+/- 5.77) that was significantly less in the line of same origin, BG01(v), with a centrosome error percentage of 3.24% (+/- 1.04) (Figure 9). H9 cells with an already low centrosome error rate of 4.0% (+/- 2.14) had an insignificant reduction at trisomy containing passages 125 and 150 with percentages of 2.64% (+/- 0.43) and 0.68% (+/- 0.96), respectively. The H1 line had acquired a structural duplication on chromosome 15p11.2 at passage 97 but displayed no reduction in centrosome errors by passage 105 with a mean of 15.66% (+/- 1.12). The karyotype analysis does not suggest that there is an association with genomic selection and centrosome stability. The reduction in the BG01(v) line could be accounted for by passage number difference between samples.

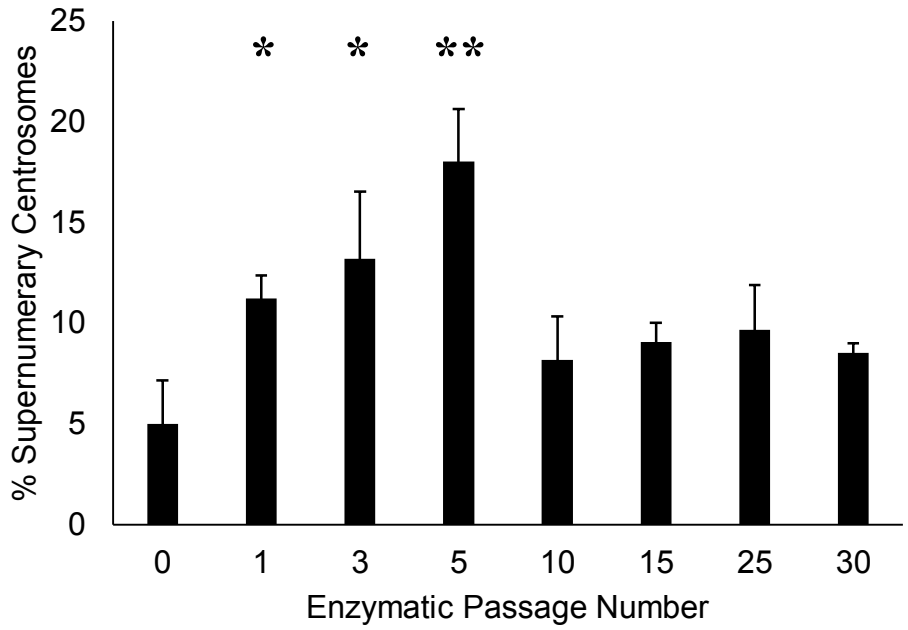

Figure 7. Transition to single- cell passaging increases centrosome errors in iPSCs. IPSCs were maintained by manually passage, CT-0, and then switch to single- cell dissociation (CT). At CT-0, CT-1, CT-3, CT-5, CT-10, CT-15, CT-25, and CT-30, the percentage of supernumerary centrosomes were quantitated. Human iPSCs at CT-5 had the highest percentage of centrosome errors. (*) indicates statistical significance to CT-0, $p < 0.05$. (**) indicates statistical significance to CT-0, CT-1, and CT-10, $p < 0.05$.

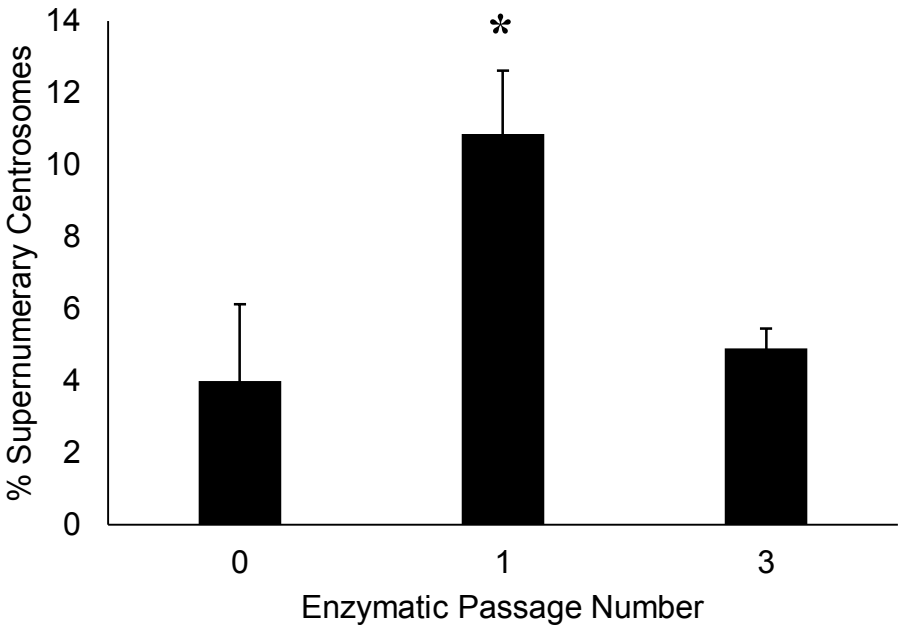

Figure 8. Transition to single- cell passaging increases centrosome errors in H9s. H9s were maintained by manually passage, CT-0, and then switch to single- cell dissociation (CT). At CT-0, CT-1, CT-3, the percentage of supernumerary centrosomes were quantitated. (*) H9s at CT-1 had a statistically significant spike relative to CT-0 and CT-3, $p< 0.05$.

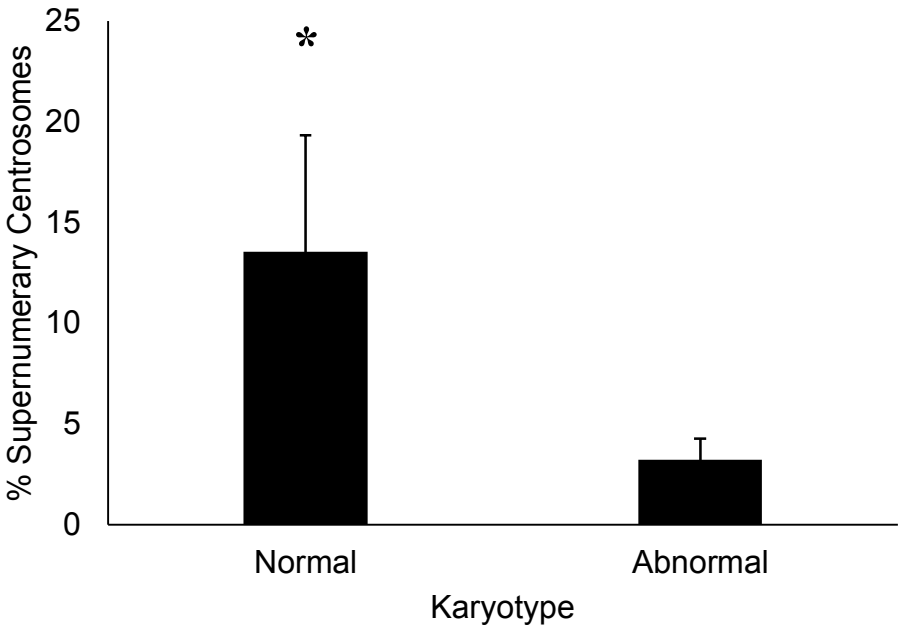

Figure 9. Supernumerary centrosome percentages of BG01 vs BG01(v) lines. Euploid early passage BG01s were compared to the aneuploid BG01(v) line. (*) BG01s have significantly more centrosome errors than BG01(v)s, $p < 0.05$.

Transcription Correlates With Genomic Copy Number

Culture dominance by variant hPSCs arise from phenotypic selection that likely has a genotypic association [92]. Therefore, we performed transcriptome analysis to identify transcriptional patterns and candidate genes conferring selective advantage. Three samples of abnormal hPSCs were compared to three samples of normal hPSCs in a genome-wide scan using Affymetrix HGU-133a microarrays. In order to discover biomarkers that might aid the understanding of genomic instability, differential gene analysis was performed. At a false discovery rate of 0.05, we found 450 probe sets corresponding to unique genes to be increased and 393 genes to be decreased. Prior to differential gene analysis, it was known that the BG01(v) samples contained trisomies on chromosomes 12, 14, 17, and X [82]. We investigated the existence of a transcriptional expression pattern reflecting these trisomies. It was discovered that a disproportionate number of significantly increased genes were located in a chromosome specific manner on chromosomes 12, 14, 17, and X. Specifically, the number of increased genes per chromosome were determined as 61, 40, 72, and 65, respectively . The normalized ratios of increased genes on the trisomic chromosomes is significant compared to the distribution of increased genes on the non-trisomic chromosomes with a p-value of 0.0046 (Figure 10)**.** One would expect that an extra chromosome would result in a constitutively expressed gene exhibiting an expression ratio of 3:2 by gene dosage alone. Thusly, on a chromosome specific basis, we looked at the average expression of all genes present in the normal samples. As predicted, we see positive fold changes of the mean chromosome expression in present genes between euploid and aneuploid hPSCs on 12, 17, 14, and X. Notably, chromosomes 17 and X have mean increases of 1.56 and 1.82, respectively. There is a general tendency for the mean

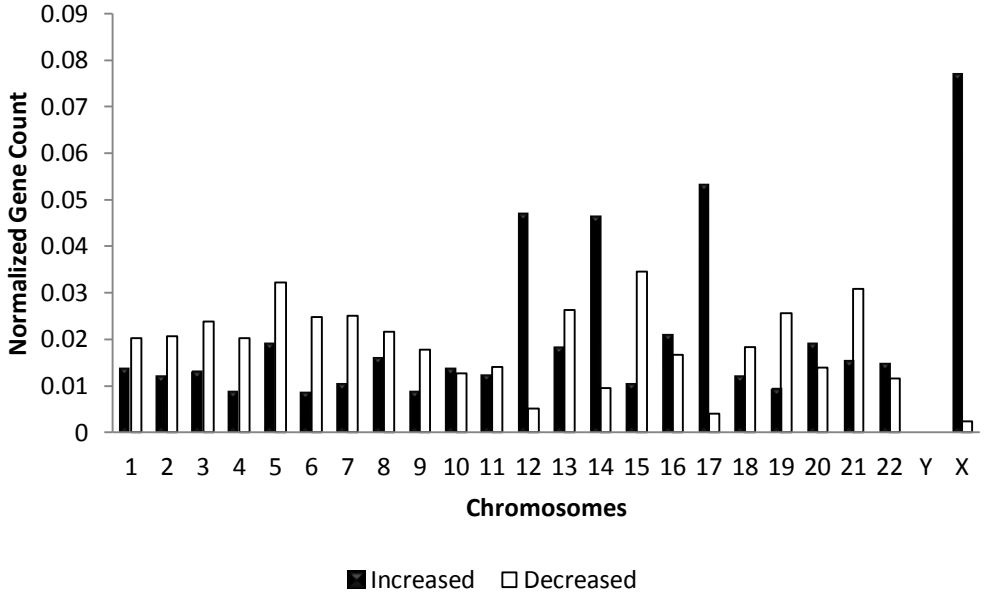

Figure 10. Trisomy enrichment of significantly increased genes. In differential gene expression analysis between normal and abnormal hESCs, 450 genes were found to be increased (black) and 393 decreased (white) between the cell lines. We normalized each chromosome's count by dividing by the number of array genes for the respective chromosome. Chromosomes 12, 14, 17, and X show a marked increase in the normalized ratio of genes that are differentially regulated and have an increased fold change. For normalized ratio between disomic and trisomic chromosomes, p-value = .0046.

expression of present genes on diploid chromosomes in normal hESCs to be negative relative to the mean expression of the respective chromosome in aneuploid hESCs. Many of the cases are of negligible value; however, chromosomes 3, 4, 15, and 19 each had their expression in abnormal hPSCs down-regulated at least 20%, with chromosome 15 exhibiting the highest decrease of 26% (Table 4).

We sought to further determine potential biomarkers. Utilizing four resources for *a priori* information, we collected a list of genes for annotation. From the Gene Ontology [184], biological processes and cellular components were chosen that could be causal in genomic instability or related to the abnormal hPSC phenotype. These processes included cell cycle, DNA replication, DNA repair, centrosome, centrosome cycle, centrosome organization, apoptosis, cell proliferation, cellular response to DNA damage, response to DNA damage. Werbowetski-Ogilvie and colleagues demonstrated through functional assays that abnormal hPSCs exhibit neoplastic progression, including increased self-renewal properties [91]. Therefore, we included in our list those genes from the PluriNet as a set of potentially biologically relevant genes that under altered regulation might confer adaptive advantage to abnormal hESCs through increased self- renewal [177]. Given the increased proliferation of abnormal hESCs that result in out-competing normal hESCs in culture and the reported similarities in normal and abnormal hESCs and cancer cells [92, 185], we also added the genes from the Cancer Genome Project [186]. Finally, we included genes reported to be involved in genomic instability [178]. 2031 genes were included in the analysis. We primarily focused on those genes that had a FDR less than 0.05 and were located on either chromosome 12, 14, or 17 (Table 5).

Table 4 Mean Chromosome Specific Transcript Expression of Present Genes

Chromosome	Normal	Abnormal	Fold Change	# Probe Sets
1	229.24	223.63	-1.03	1115
2	258.9	238.87	-1.08	728
3	179.77	149.66	-1.2	579
4	173.32	144.49	-1.2	381
5	249.16	244.07	-1.02	499
6	195.41	173.28	-1.13	629
7	196.65	181.39	-1.08	489
8	205.6	182.65	-1.13	389
9	166.3	146.32	-1.14	381
10	229.28	215.18	-1.07	423
11	266.95	231.15	-1.15	553
12	287.6	401.81	1.4	602
13	176.89	174.74	-1.01	203
14	229.57	333.79	1.45	374
15	205.81	163.87	-1.26	343
16	236.14	224.35	-1.05	427
17	266.14	416.29	1.56	602
18	188.63	167.99	-1.12	180
19	233.34	188.16	-1.24	590
20	220.23	201.3	-1.09	298
21	174.51	174.89	1	120
22	174.81	166.46	-1.05	247
Y	33.83	27.57	-1.23	14
X	202.56	369.47	1.82	394

For each chromosome the average of the signal intensities per chromosome for all present genes was calculated for normal and abnormal samples. The total number of probe sets per chromosome on the HGU-133A Affymetrix microarray was used to determine chromosome specific average. The fold change was calculated relative to normal samples, such that a positive fold change value implies the mean expression is higher in abnormal samples. Chromosomes 17 and X have fold changes greater than 1.5.

Table 5 Significantly Increased Genes Located on Trisomy Chromosomes in BG01(v) Line

Symbol	Cytoband	Ontology	Phenotype
KRAS	12p12.1	Ras mediated signal transduction	Cancer
SOCS2	12q	**Anti-apoptosis**	
DYRK2	12q15	**DNA damage response, induction of apoptosis**	
RFC5	12q24.2-q24.3	**DNA repair, DNA replication, checkpoint sensor**	Genomic Instability, Self-renewal
PSMD9	12q24.31-q24.32	**Mitotic cell cycle**	
POLE2	14q21-q22	**DNA repair**	
GPHN	14q23.3	establishment of synaptic specificity at neuromuscular junction	Cancer
ALKBH1	14q24.3	**DNA dealkylation**	
DYNC1H1	14q32.3-qter	**Mitotic spindle organization and biogenesis**	
USP22	17p11.2	**Positive regulation of mitotic cell cycle**	
RNMTL1	17p13.3	RNA processing	Self-renewal
PAFAH1B1	17p13.3	**Establishment of mitotic spindle orientation**	
RPA1	17p13.3	**DNA repair, checkpoint signaling**	Cancer predisposition, Genomic Instability, Self-renewal
NF1	17q11.2	**Positive regulation apoptosis, negative regulation of cell proliferation**	Cancer
TIAF1	17q11.2	**Anti-apoptosis**	
PSMD11	17q11.2	**Mitotic cell cycle**	Self-renewal
COL1A1	17q21.33	extracellular matrix	Cancer
RAD51C	17q22-q23	**DNA repair**, **HR**	Genomic Instability
SOX9	17q24.3-q25.1	**Apoptosis, Cell proliferation**	
SEP9	17q25	Cell cycle, GCPR signal transduction	Cancer
EXOC7	17q25.1	**Centriolar satellite**	
ARHGDIA	17q25.3	**Anti-apoptosis**	

Significant genes located on chromosomes 12, 14, or 17 with an FDR less than 0.05. A gene's ontology is bold if part of genomic instability [178] or an annotation of interest from Gene Ontology. Self- renewal genes are from the PluriNet gene set and phenotype cancer from the Cancer Genome Project. Abbreviations: HR- homologous recombination.

Candidate Gene Identification for Positive Selection of Trisomy 17

Chromosome 17 is one of the most common genomic abnormalities in hPSCs, occurring *in vitro* during hPSC culture and *in vivo* in hECs [95]. In our research, three hPSC lines (BG01(v), H9, iPSC) exhibited trisomy 17 during long-term propagation. Additionally, published reports suggest that 17q25 may be a minimal amplicon for genomically altered hESCs [92]. Interestingly, 17q25 is reported to be the only species conserved genomic amplification between *homo sapiens* and syntenic locus of *mus musculus* and *rhesus macaque* [187]. Therefore, we decided to focus specifically on the genes located on this region that were determined significantly expressed by microarray analysis. Of the three overexpressed genes on 17q25, SEPTIN 9, EXO7, and ARHGDIA, ARHGDIA caught our attention for its established role in the RHO-ROCK pathway [109, 110, 188]. ROCK inhibitor is used by many labs to reduce dissociation induced cell death upon loss of e-cadherin based cell-cell contact [45]. ARHGDIA, known as aplysia ras- related homolog guanine dissociated inhibitor- alpha, inhibits the activation of RHOA by preventing the GDP exchange for GTP [189]. ARHGDIA is an effector and chaperone for prenylated RHOA [190]. Since RHOA activation is necessary for ROCK activation, we hypothesized that overexpression of ARHGDIA would reduce activation of RHOA and therefore lead to increased single- cell survival conferring selective advantage to hPSCs (Figure 11). Given its genomic location on 17q25, ARHGDIA is of particular interest as a putative agent in trisomy 17 culture dominance. Notably, we found the protein ARHGDIA to be highly conserved across vertebrates (Figure 37).

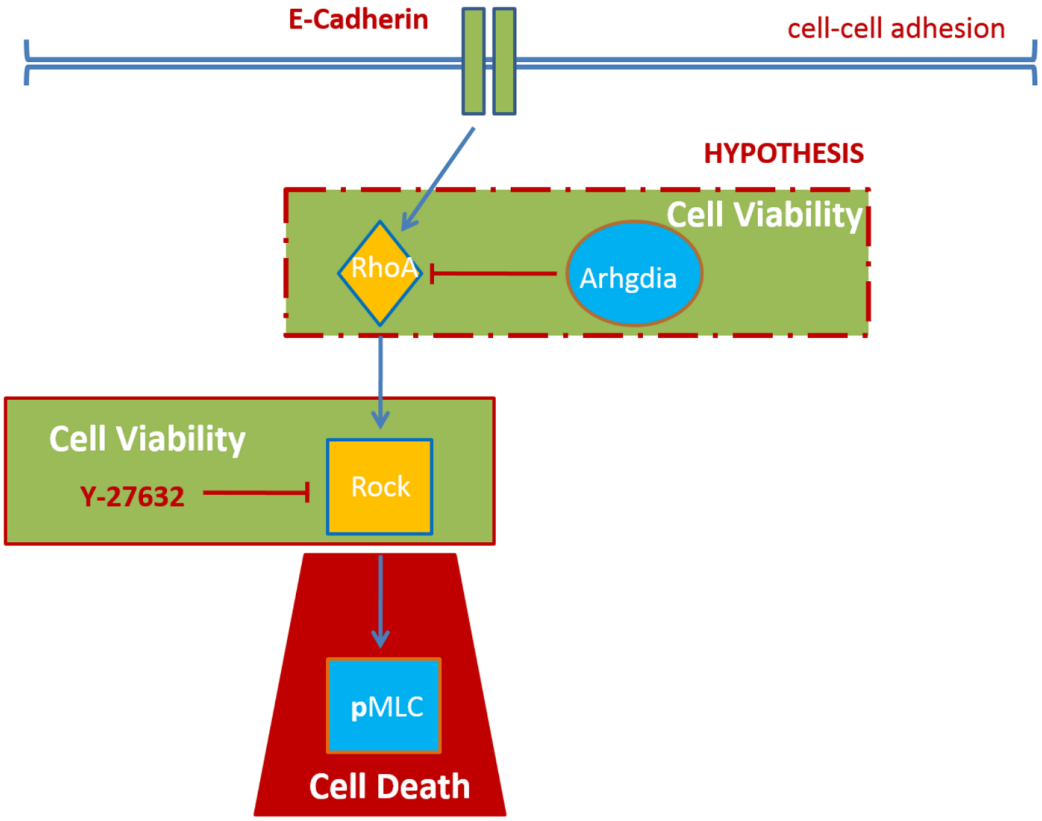

Figure 11. ARHGDIA inhibition of RHO signaling. Loss of cell-cell contact during single cell dissociation leads to cell death through activation of Rho signaling. Phosphorylation of myosin light chain by ROCK induces cytoplasmic membrane blebbing and rupture. ARHGDIA is a potent inhibitor of RHOA activation. ARHGDIA maintains the inactive RHOA-GDP bound state by preventing the switch to active RHOA-GTP. We hypothesize that overexpressing ARHGDIA will reduce RHOA activation, and therefore reduce ROCK associated, pMLC- dependent, apoptosis leading to increased viability of hPSCs. Abbreviations: pMLC- phosphorylated myosin light chain, ROCK- rho-associated coil coiled protein kinase.

Functional Analysis of ARHGDIA in Cell Culture

Having identified ARHGDIA as a candidate gene of interest in trisomy 17 hPSC lines, we hypothesized that increased expression of ARHGDIA in hPSCs would increase survival during single cell passaging and confer selective advantage to these populations. Additionally, with a hypothesized functional role, we further speculated that ARHGDIA could be an expression marker for trisomy 17. To date, genes located on altered genomic regions having a functional role in hPSC selective advantage have remained elusive. Since our genomic and transcriptional data supports an overexpression model, we focused our experimental approach on increased ARHGDIA expression. To test our selective advantage hypothesis, we established hPSC lines constitutively overexpressing ARHGDIA using lentivirus transduction approaches. An affordable and commercially available open reading frame (ORF) for ARHGDIA was obtained (Thermo Scientific), wherein the ARHGDIA ORF is cloned into their pLOC lentiviral expression vector. pLOC expression vectors are driven by the human cytomegalovirus (CMV) promoter and contain a green fluorescent protein (GFP) reporter, tGFP, that is expressed in the cell's nucleus and driven by an internal ribosomal entry site (IRES) (Figure 38). GFP expression is an essential technical feature of our experimental design enabling us to fluorescently identify cells expressing the ARHGDIA ORF. Via this pLOC based Precision LentiORF expression system, we stably transduced both H9 and BG01 hPSC lines. For both the H9 and BG01 hPSC lines, we established ARHGDIA overexpression lines, H9 (Arg) and BG01 (Arg). Similarly, to generate matched controls, we transduced H9 and BG01 hPSC lines, H9 (GFP) and BG01 (GFP) with lentivirus to established CMV promoter driven GFP only expressing cells. To enrich for GFP expressing cells in our transduced lines, all lines were propagated by manual dissection until time of experiment. Colonies expressing GFP were marked by an objective marker and

selected by manual cutting and plating. Serial positive selection on GFP was sufficient for experiment quality, high percentage, GFP expressing populations. For quality control, stringently, the percent of GFP expression was checked in each experimental culture. Of significant technical note, the transduced H9 and BG01 lines exhibited strikingly different promoter silencing behavior, as determined by GFP signal. The CMV promoter is prone to silencing in certain hPSCs . GFP silencing in the H9 line was very prominent for both transduced lines, H9 (Arg) and H9 (GFP), while for both transduced BG01 lines, BG01 (Arg) and BG01 (GFP), the GFP expression was relatively stable.

Arhgdia Overexpression in Transduced and Trisomy 17 containing lines

We first sought to validate overexpression of ARHGDIA in our genetically engineered lines. Overexpression of ARHGDIA was investigated by quantitative real-time PCR (QPCR), immunocytochemistry (ICC), and western blot (WB). For QPCR and WB analysis, samples were compared to matched GFP only and wild-type (WT) controls. For ICC, in the H9 (Arg) line differences in ARHGDIA signal intensity were compared among GFP positive and GFP negative reporter gene expressors. By ICC, all cells were positive for ARHGDIA and exhibited diffuse cytoplasmic localization. Within the H9 (Arg) colony, GFP positive cells had increased ARHGDIA positive antibody staining in the flourescent red emission channel, relative to GFP negative cells; thereby, validating that our primary antibody and ARHGDIA expression system was performing as expected **(**Figure 12). Next, by QPCR and WB, we compared the H9 and BG01 hPSC lines: H9 (Arg) relative to the H9 (GFP) and H9 (WT) lines and BG01 (Arg) relative to the BG01 (GFP) and BG01 (WT) lines. Our QPCR analysis demonstrated that

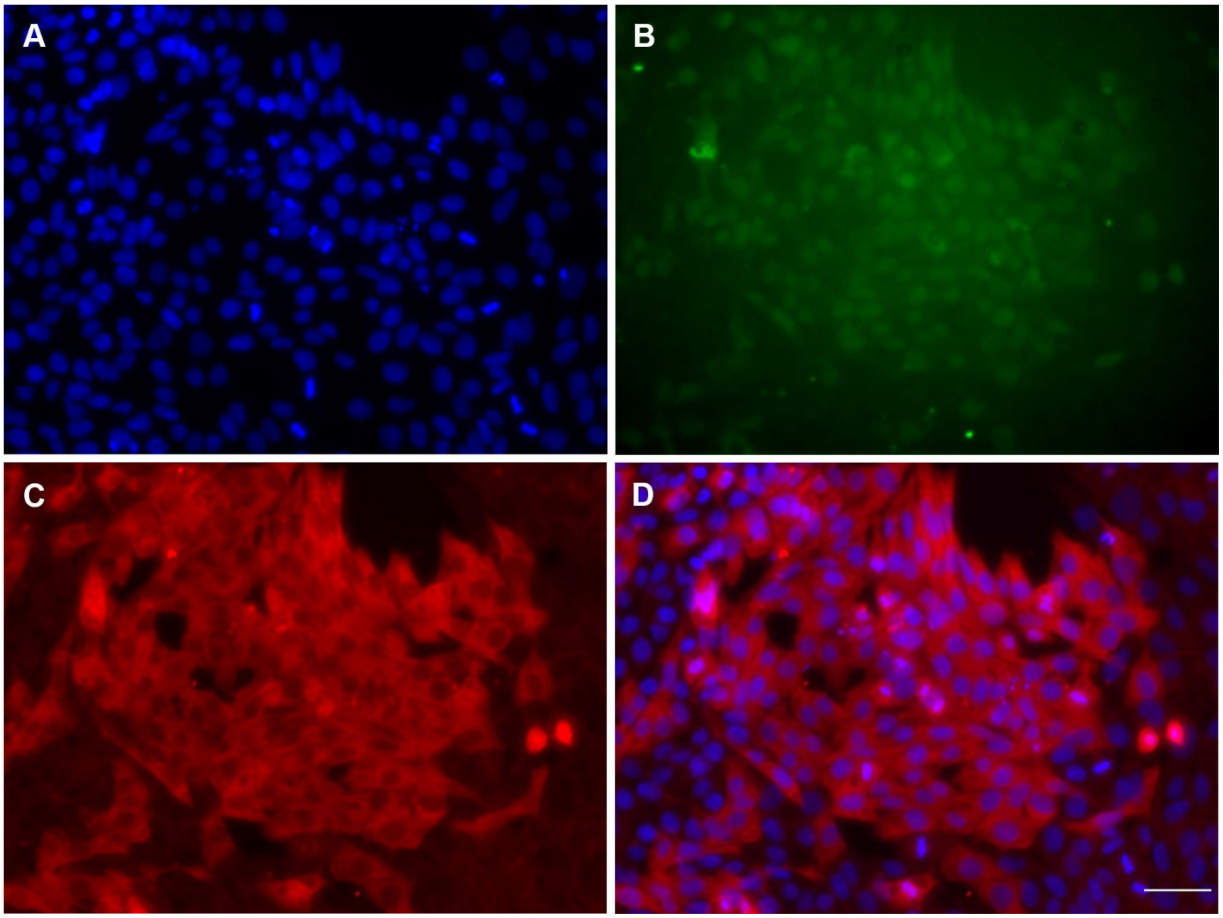

Figure 12. ARHGDIA cytoplasmic location and overexpression in transduced hPSC line. H9 stem cell line was transduced with lentivirus co-expressing the gene ARHGDIA (red) and GFP (green) driven by the CMV promoter. Cells expressing GFP (B), relative to DAPI (blue) only (A), have increased ARHGDIA protein expression (C, D). ARHGDIA is cytoplasmic localized. Scale bar= 50 μm.

ARHGDIA was overexpressed in the H9 (Arg) and BG01 (Arg) lines relative to respective GFP and WT controls. We determined the transcriptional fold change of H9 (Arg) compared to H9 relative to the BG01 (GFP) and BG01 (WT) lines. Our QPCR analysis demonstrated that ARHGDIA was overexpressed in the H9 (Arg) and BG01 (Arg) lines relative to respective GFP and WT controls. We determined the transcriptional fold change of H9 (Arg) compared to H9 (GFP) and H9 (WT) to be 5.57 and 5.63, respectively. We determined the transcriptional fold change of BG01 (Arg) compared to BG01 (GFP) and BG01 (WT) to be 3.83 and 3.05, respectively (Figure 13). Performing WB analysis, the bands in the lanes for H9 (Arg) and BG01 (Arg) were clearly stronger than the corresponding GFP and WT control lanes. Using densitometry, we quantitated the signal of each band and determined the fold change of H9 (Arg) relative to H9 (GFP) and H9 (WT), also likewise for the BG01 (Arg) relative to BG01 (GFP) and BG01 (WT). In the densitometric analysis, we normalized the values of the target protein signal intensity against the β-tubulin control signal intensity. We calculated the fold change of H9 (Arg) relative to H9 (GFP) and H9 (WT) to be 10.52 and 6.76, respectively. We calculated the fold change of BG01 (Arg) relative to BG01 (GFP) and BG01 (WT) to be 3.74 and 7.50, respectively (Figure 14).

By microscopic visualization, GFP expression in the H9 (Arg) line was brighter than GFP expression in the BG01 (Arg) cells. Additionally, on an absolute scale used in the Accuri C6 flow cytometer, the GFP fluorescence detection values measured on the H9 (Arg) line were higher than that of the BG01 (Arg); indicating that H9 (Arg) had higher ARHGDIA ORF expression than BG01 (Arg). This is consistent, with both QPCR and WB data, demonstrating

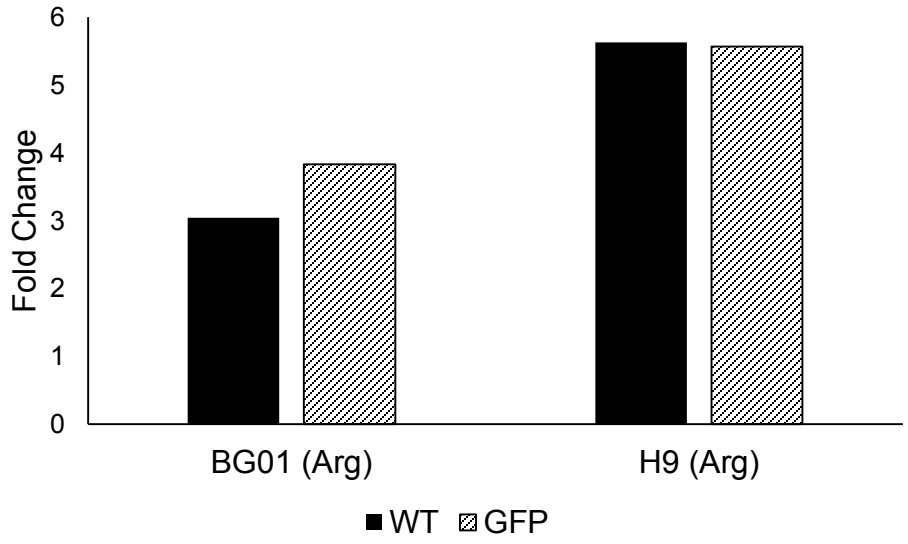

Figure 13. ARHGDIA is overexpressed in BG01 (Arg) and H9 (Arg) lines. Using real-time PCR, the BG01 (Arg) and H9 (Arg) lines overexpress ARHGDIA transcripts relative to their respective set of controls, BG01 (GFP), BG01 (WT), H9 (GFP), and H9 (WT). For each cell line n= 3.

A

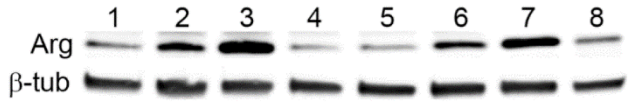

B

Cell Line	Arhgdia Normalized Ratio
1. H9 (WT)	1
2. H9 (v)	2.12
3. H9 (Arg)	10.52
4. H9 (GFP)	1
5. BG01 (WT)	1
6. BG01 (v)	2.68
7. BG01 (Arg)	3.74
8. BG01 (GFP)	1

Figure 14. ARHGDIA protein expression in transduced and variant hPSC lines. Western blot analysis on ARHGDIA protein expression in H9s and BG01s (A). The numbered lanes of the western blot (A) correspond to the numbered rows in the densitometric analysis (B). The signal intensities were normalized against maximum β-tubulin expression. Fold change values for H9 (Arg) and BG01 (Arg) are relative to H9 (GFP) and BG01 (GFP) and fold change values for H9(v) and BG01(v) are relative to H9 (WT) and BG01 (WT). β-tubulin= 5 kDa and ARHGDIA= 26 kDa. Abbreviations: Arg- ARHGDIA, β -tub- β -tubulin, WT- wild type, v- genomic variant, GFP- green fluorescent protein.

that relative to controls, ARHGDIA fold change was higher in the H9 (Arg) line; and, that total ARHGDIA expression was greatest in the H9 (Arg) line compared to all other samples. The H9 (Arg) relative to H9 (WT) fold change is similar between QPCR and WB data. Likewise, the BG01 (Arg) relative to BG01 (GFP) fold change is similar between QPCR and WB data. However the fold change values between QPCR and WB densitometry is different in magnitude for H9 (Arg) relative to H9 (GFP) and BG01 (Arg) relative to BG01 (WT) and can be possibly explained by technical variation in the WB experimentation, since mRNA expression of ARHGDIA is highly consistent across our euploid controls. Taken together, along with technical considerations in the densitometric normalization and protein loading variation, the QPCR and WB data are qualitatively consistent and quantitatively similar for ARHGDIA overexpression in our transduced lines validating our experimental system.

With a hypothesized functional role, we sought to determine whether increased ARHGDIA expression may serve as a transcription and protein marker for trisomy 17. To date, functionally relevant genes conferring selective advantage for trisomy 12, 17, and gain of X have not been determined. Our microarray data and the literature indicate a strong correlation between genomic copy number and transcript levels. In a recent study on 104 hPSCs lines, Mayshar and colleagues demonstrate that gene expression data can predict genomic alterations with ~10Mb resolution and very high accuracy [89]. Our results are promising but mixed for increased transcriptional expression of ARHGDIA in trisomy 17 lines. In the trisomy 17 iPSC(v) line, we observed 3.0 fold increase in ARHGDIA transcription (Figure 15). However, in the trisomy 17 BG01(v) and H9(v) lines, we did not observe increased ARHGDIA expression. Euploid hPSC samples exhibited consistent quantitative expression of ARHGDIA, similar in manner to a

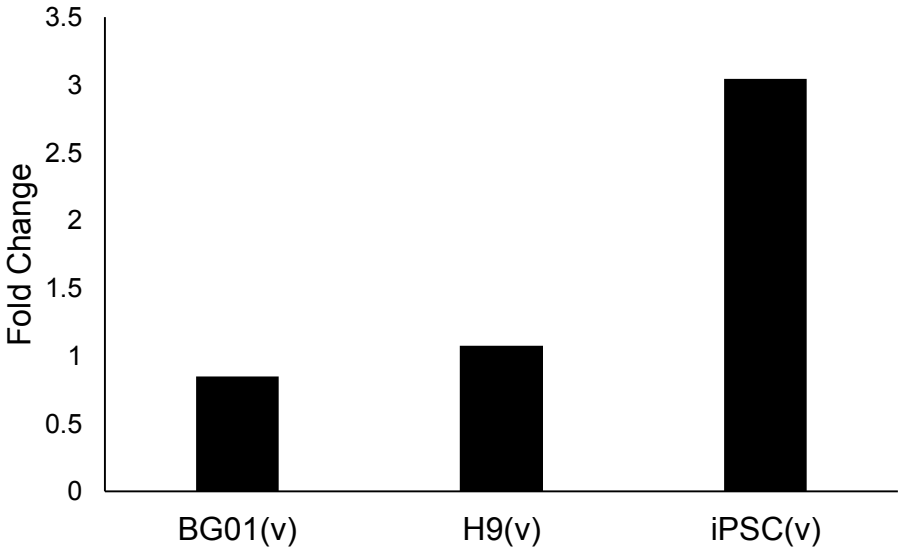

Figure 15. ARHGDIA gene expression in trisomy 17 lines. Trisomy 17 hPSC lines carry an extra genomic copy of ARHGDIA located on 17q25. By gene dosage, we expect to observe at least a 1.5 fold increase in trisomy 17 lines. In the iPSC(v) line we observe a 3.0 fold change increase for ARHGDIA. For each cell line n=3.

housekeeping gene; therefore, observing increased mRNA expression in the iPSC(v) line is noteworthy. Interestingly, we observed an increase in ARHGDIA expression in the BG01(v) and H9(v) WB samples, relative to the respective BG01 and H9 euploid samples (Figure 14). Since, it is notcommon to see relative to the respective BG01 and H9 euploid samples (Figure 14)., indicating that further experimentation is needed to demonstrate usefulness of ARHGDIA as a biomarker.

ARHGDIA Transduced Cell Lines Maintain Pluripotency

In order to confirm that ARHGDIA overexpression did not adversely influence self-renewal and differentiation, we fully characterized the H9 (Arg) line for pluripotency. For the BG01 (Arg) line, we conducted QPCR and ICC analyses on transcription factors and cell surface markers to validate the pluripotent cell state. Similarly, for the H9 (GFP) and BG01 (GFP) control lines, we conducted QPCR and ICC analyses on transcription factors and cell surface markers to validate pluripotency.

HPSCs exhibit a typical colony morphology that is more strongly bounded on iMEFs compared to feeder-free conditions. Cells propagated on Matrigel™ and other feeder-free conditions are more prone to form hESC fibroblast-like cells (hFs) than those hPSCs propagated on iMEFs. HFs are single- cells that migrate to the colony periphery forming a niche and are a sign of differentiation [191]. The iMEF layer density is thought to contribute an opposing force that increases constraint of the hPSC colony. E-cadherin is expressed in hPSCs and facilitates cell- cell contact through homotypic bonding to maintain colony morphology [192]. All transduced lines, ARHGDIA and GFP controls, exhibited standard colony morphology on iMEFs and Matrigel™. However, the colonies of H9 (Arg) cells manually passaged and maintained on iMEFs exhibited striking behavior that was significant and consistent compared to controls. HPSC colonies are often a flat monolayer that penetrate through the iMEF layer, pushes the iMEFs outward, and forms a raised ridge at the hPSC and iMEF contiguous boundary, with the hPSCs being concave to the iMEFs. In contrast, the H9 (Arg) colonies were highly mounded, very dense, and convex to the iMEF layer **(**Figure 16)**.** The random white-edge cobblestone morphology was significantly present and bright within the H9 (Arg) colony. The BG01 (Arg)

colonies did not exhibit a difference in monolayer cell formation from control lines BG01 (GFP) and BG01 (WT). Thus, overexpression of ARHGDIA was associated with cell line specific morphological alterations that were present in H9 (Arg) but not BG01 (Arg) cells.

Differentiating hPSCs lose expression of the AP activity; therefore, AP staining is a quick, reliable, and sensitive method to screen for hPSCs in culture [14]. The H9 (Arg) lines were AP positive at greater than 20 passages post- transduction (data not shown). Similarly, the H9 (GFP) lines were AP positive at greater than 10 passages, post- transduction (data not shown). While AP staining has been reported to be a sensitive marker, more specific pluripotent markers for cell-surface and transcription factors are routinely used to stringently validate pluripotency. The transcription factors OCT4, SOX2, and NANOG are essential to pluripotency and highly specific cell surface markers have been identified, such as SSEA4. Down regulation of hPSC markers during initial stages of differentiation is poorly understood; however our long term propagation of H9 (Arg) and BG01 (Arg) cultures indicate stable maintenance of pluripotency. At greater than 30 passages, post-transduction, the H9 (Arg) lines exhibited positive protein expression for OCT4 and SSEA4 by ICC. Similarly for the BG01 (Arg) lines, at greater than 30 passages, post- transduction, positive protein expression for OCT4 and SSEA4 was observed by ICC (Figure 17 and Figure 18). Using QPCR analysis, we quantitatively assessed gene expression for the pluripotent transcription factors OCT4 and NANOG. For H9 (Arg), QPCR was performed at greater than 25 passages, post-transduction. At each passage, the H9 (Arg) was transcriptionally positive for OCT4 and NANOG. Prior to RNA isolation, for each sample, we performed a quality control check on H9 (Arg) expression purity. By flow cytometry, we validated the percentage of cells in the H9 (Arg) sample overexpressing ARHGDIA by

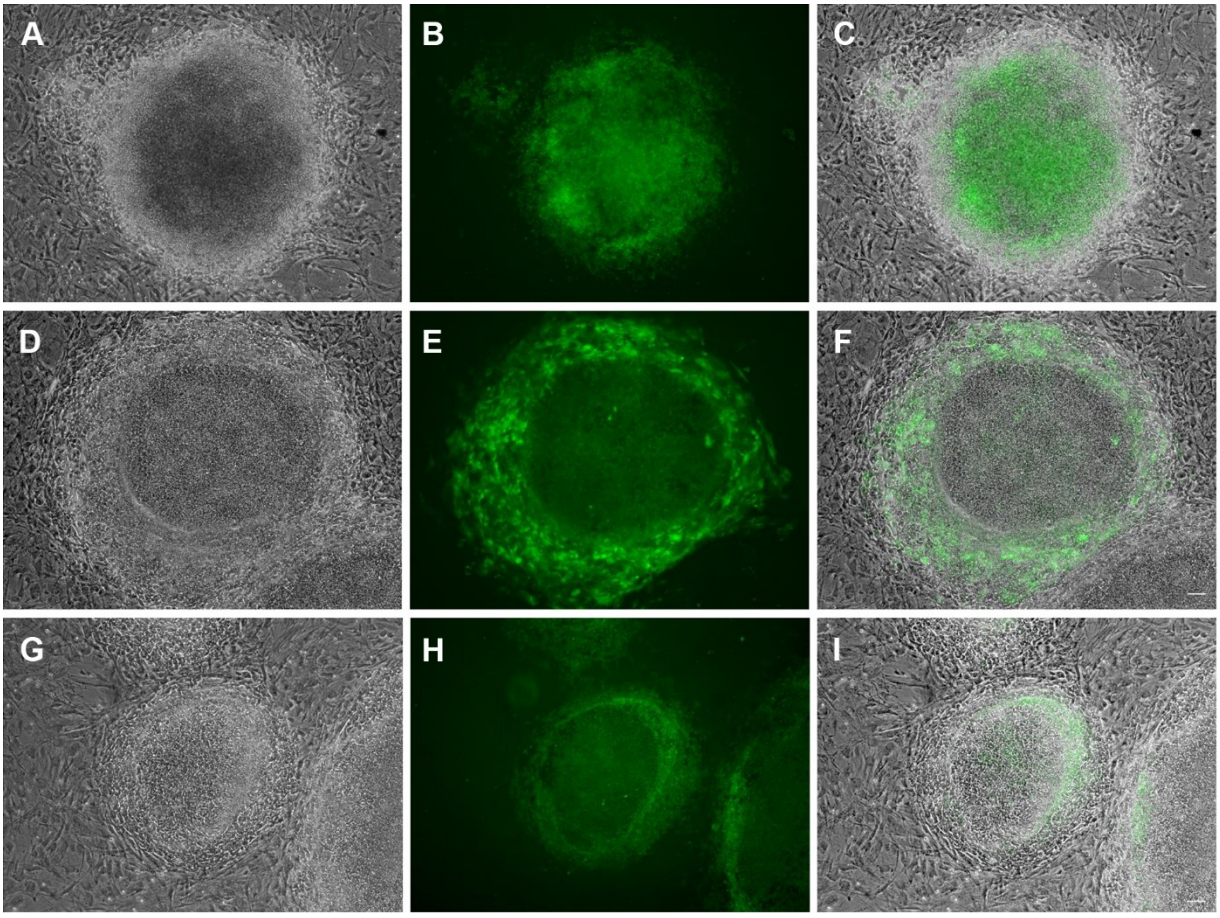

Figure 16. H9 (Arg) colonies exhibits increased cell- cell contact and mounded morphology. Each line exhibits standard pluripotent stem cell colony formation. H9 (Arg) (A-C) has marked increased multi- cell layer morphology as demonstrated by the increased density in phase contrast image (A) and fluorescent image (B) and overlay (C). H9 (GFP) (D-F) exhibits standard monolayer colony morphology concave to surrounding iMEF layer. BG01 (Arg) (G-I) exhibits standard monolayer colony morphology concave to surrounding iMEF layer. Scale bar= 100μm.

performed a quality control check on H9 (Arg) expression purity. By flow cytometry, we validated the percentage of cells in the H9 (Arg) sample overexpressing ARHGDIA by measuring the percentage of cells that were GFP- positive. Similarly, the BG01 (Arg) line at greater than 10 passages, post-transduction, was positive for OCT4 and NANOG mRNA. The H9 (GFP) and BG01 (GFP) lines positively expressed OCT4 and NANOG transcripts. When comparing H9 (Arg) and BG01 (Arg) lines for OCT4 and NANOG against human dermal fibroblasts, there were fold changes of one order of magnitude for OCT4 and 2 orders of magnitude for NANOG. Across hPSC lines, the fold changes patterns against the fibroblasts were similar (Figure 19). Within hPSC lines, the relative expression of OCT4 and NANOG for transduced lines is consistent with self- renewal. H9 (Arg) line exhibited an increase in fold change for OCT4 relative to H9 (WT) and H9 (GFP). In the other lines, there was a slight but acceptable decrease in OCT4 and NANOG expression relative to H9 (WT) and BG01 (WT) samples (Figure 20), decrease that may be attributed to culture time. The wild type samples were often freshly thawed cultures, where the transduced lines were subjected to long- term continuous passaging. The OCT4 and NANOG expression of H9 (Arg) and BG01 (Arg) relative to GFP, WT, and hDF controls confirms self- renewal of these lines.

Pluripotency is defined by self-renewal and differentiation potential into ectoderm, endoderm, and mesoderm. Having validated self-renewal, we sought to determine whether the H9 (Arg) line could differentiate into each of the three embryonic germ layers. We used the hanging drop method for EB formation, in which cells were dissociated as single cells, plated at 5000 cells per drop, and subsequently cultured in suspension in non- adherent agar plates. Interestingly, EB formation from single-cells was aided by the use of 10 μM ROCKi. Initial

attempts without ROCKi did not form cell aggregates. H9 (Arg) with ROCKi formed tight aggregates that were fixed at 20 days and subsequently sectioned and analyzed by histopathology for germ layer specific expression. We observed presence of all three primitive germ layers, indicating that the cells retained their differentiation capabilities (Figure 21). Taken together, this data suggest that ARHGDIA overexpression does not influence self-renewal and the stem cells remain pluripotent with tri-lineage potential.

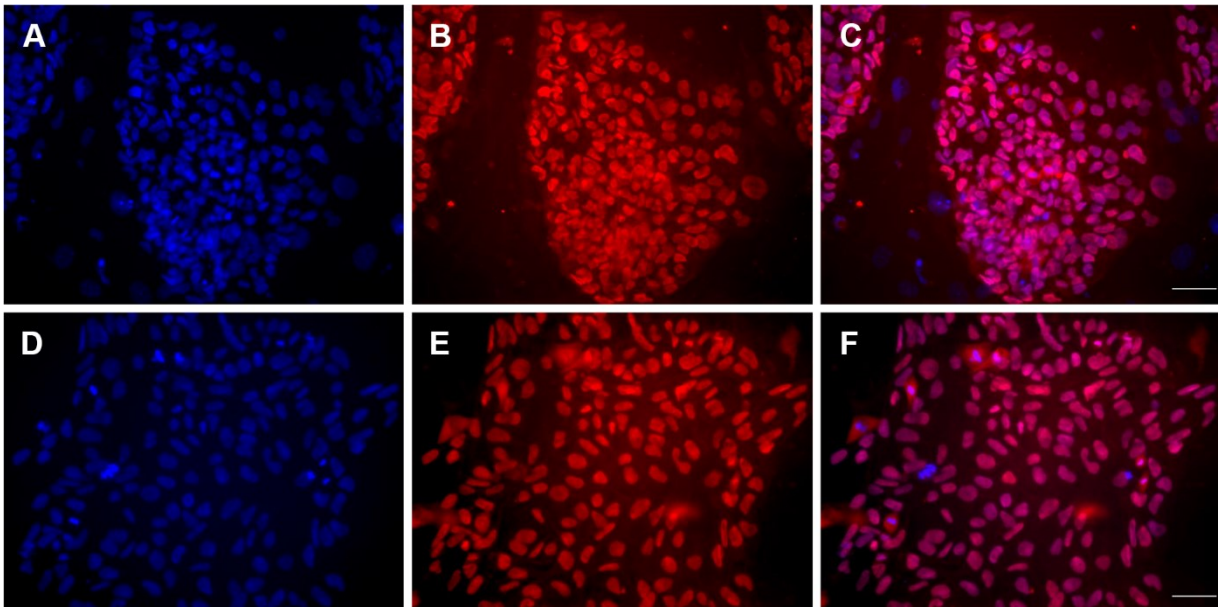

Figure 17. H9 (Arg) and BG01 (Arg) cells self- renew and express OCT4. Positive nuclear expression of the OCT4 transcription factor in H9 (Arg) lines (A-C) and BG01 (Arg) lines (D-F). H9 (Arg) and BG01 (Arg) lines were propagated greater than 20 and 10 passages, respectively. DAPI- blue (A, D), OCT4- red (B, E), and DAPI/OCT4 nucleus overlay (C, F). Scale bar= 50 μm.

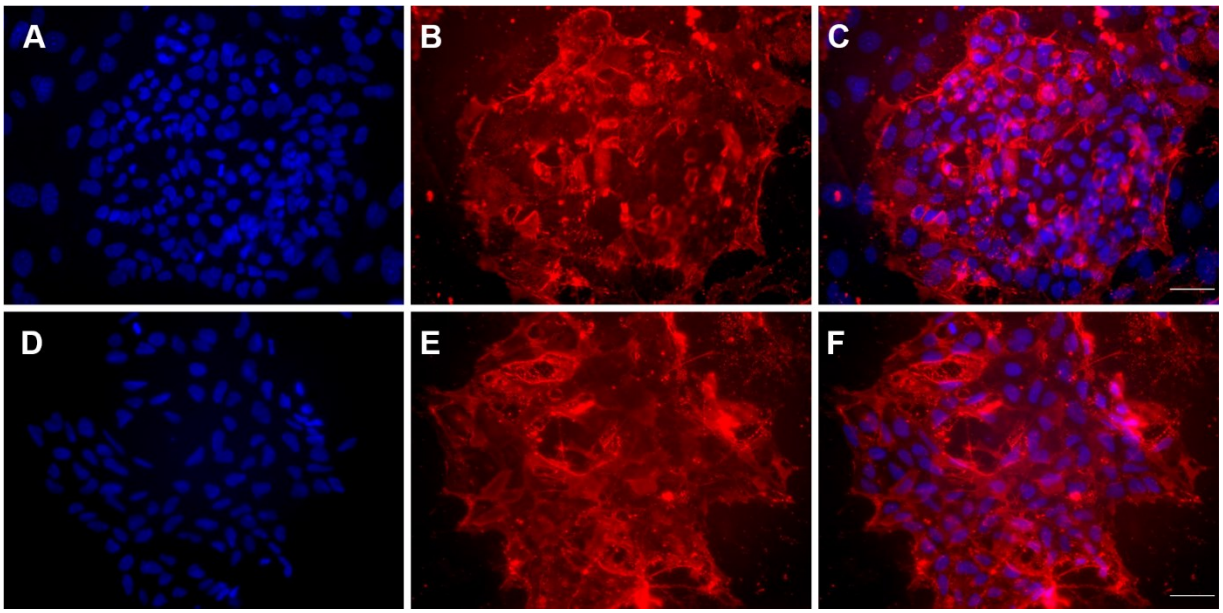

Figure 18. H9 (Arg) and BG01 (Arg) cells self- renew and express SSEA4. Positive expression of the cell surface marker, SSEA4, in H9-arg+ lines (A-C) and BG01-arg+ lines (D-F). The H9 (Arg) and BG01 (Arg) lines were propagated greater than 20 and 10 passages, respectively. DAPI-blue (A, D), SSEA4- red (B, E), and DAPI/SSEA4 overlay (C, F). Scale bar= 50 μm.

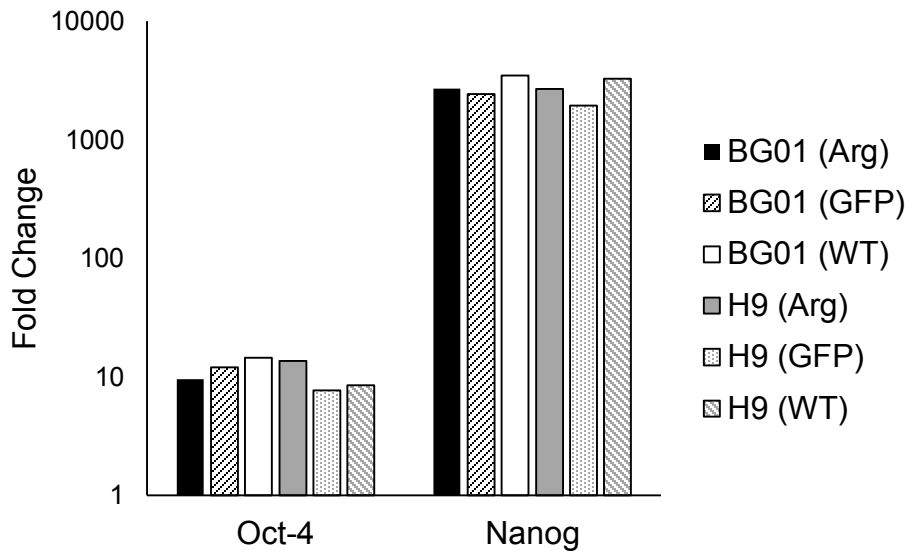

Figure 19. H9 (Arg) and BG01 (Arg) lines exhibit high expression of pluripotent transcription factors relative to human dermal fibroblasts. The experimental and control lines for H9s and BG01s were validated for pluripotent marker expression relative to human dermal fibroblast. The fold change values are determined via the ΔC_T method using GAPDH as the reference gene. Abbreviations: Arg- ARHGDIA, GFP- green flourescent protein, WT- wild type. For each cell line n=3.

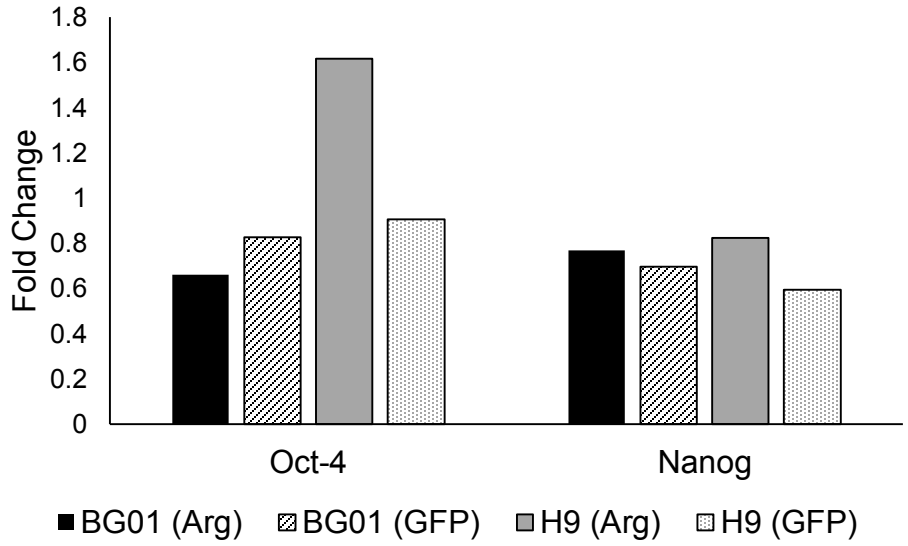

Figure 20. H9 (Arg) and BG01 (Arg) express pluripotent transcription factors. The experimental (Arg) and control lines (GFP) for H9s and BG01s were validated for pluripotent marker expression against WT lines. The fold change values are determined via the ΔC_T method using GAPDH as the reference gene. Fold change was calculated relative to hDFs. Abbreviations: Arg- ARHGDIA, GFP- green flourescent protein, WT- wild type. For each cell line n=3.

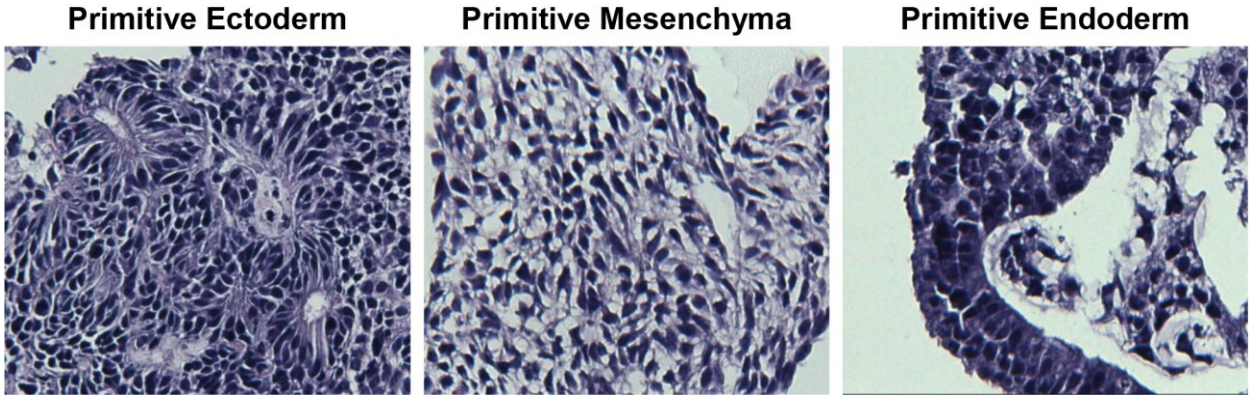

Figure 21. Histopathological evidence of germ- layer specification in embryoid bodies generated from H9 (Arg) lines. Hematoxylin and eosin-stained histologic sections of EBs from H9 (Arg) lines. The tri-lineage differentiation is indicative of pluripotency. Magnification is 20x.

ARHGDIA Confers Selective Advantage and Increases Clonality

For the H9 (Arg) line, we used two assays to test our hypothesis that ARHGDIA overexpression will improve hPSCs cultured as single-cells. The first, a competition based assay, consisted of co-cultures of cells overexpressing ARHGDIA vs. non-overexpressing cells. The second assay tested clonality of single- cells seeded at low density. Prior to the selection experiments and clonality assay, the H9 (Arg) lines were maintained by manual passage. Using an objective marker for identification, GFP- positive colonies were manually cut by fire- pulled Pasteur pipette and plated as small clumps. This provided a natural opportunity for co-cultures of H9 (Arg) that were GFP- positive and H9 (Arg) that were GFP- negative, H9 (Arg(+)) and H9 (Arg(-)), respectively. In this co-culture experimental design, all cells had been treated similarly, including lentiviral exposure and equivalent passage number. The only difference between the GFP- positive vs. GFP- negative subpopulations is differential ARHGDIA expression as validated by prior ICC, QPCR, and WB analysis. To determine the influence ARHGDIA overexpression has on selective advantage, competition co-culture experiments were performed on two independent H9 (Arg) sublines from the same transduction, H9 (Arg) s.1 and H9 (Arg) s.3. For each subline, the competition- based assay was initiated as a mixture of H9 (Arg(+)) and H9 (Arg(-)) co-cultures, discriminated by GFP reported expression, that were switched from manual passaging to enzymatic passaging. Co-cultures were continuously passaged on iMEFs, subjected to 40 μm filtering, and plated as single-cells.

At each passage, the percentage of GFP- positive cells was measured by flow cytometry with controls in place for autoflourescence and gating for live cells only. Both H9 (Arg) s.1 and H9 (Arg) s.3 sublines exhibited strong competitive advantage when passaged as single-cells. For the H9 (Arg) s.1 co-culture, there was a total of 53.2% H9 (Arg (+)) cells for the initial enzymatic

harvest prior to plating, CT-0. For the H9 (Arg) s.3 co-culture, there was a total of 42.0% H9 (Arg (+)) cells for the initial enzymatic harvest prior to plating, CT-0. After serial, single-cell passaging, the total H9 (Arg(+)) percentages for the H9 (Arg) s.1 and H9 (Arg) s.3 lines reached 90.6% and 93.5%, respectively (Figure 22 and Figure 23). The distribution of H9 (Arg (+)) cells is bimodal and thusly can be divided into H9 (Arg (high)) and H9 (Arg(low)), as measured by the strength of GFP signal intensity. For each subline, H9 (Arg) s.1 and H9 (Arg) s.3, the H9 (Arg(high)) increased relative to the H9 (Arg(low)), suggesting that magnitude of ARHGDIA expression positively correlated with increased selective advantage. For the H9 (Arg) s.1 subline, the initial percentage of H9 (Arg (high)) was 27.8%, equaling 52.3% of the total H9 (Arg(+)) cells. At the final passage, the percentage of H9 (Arg (high)) in the total population was 83.7%, equaling 92.4% of the total H9 (Arg(+)) cells. For the H9 (Arg) s.3 subline, the initial percentage of H9 (Arg (high)) was 17.9%, equaling 43.8% of the total H9 (Arg(+)) cells. At the final passage, the percentage of H9 (Arg(high)) in the total population was 89.0%, equaling 95.2% of the total H9 (Arg(+)) cells. Of note, in both sublines, there was an initial delay of competitive advantage, where the percentage of total H9 (Arg(+)) remained similar. For the H9 (Arg) s.1, dominant competitive advantage occurred between CT-4 to CT-6, in three passages. For the H9 (Arg) s.3, competitive advantage occurred between CT-4 to CT-6, in three passages. For the H9 (Arg) s.3, competitive advantage of total H9 (Arg(+)) occurred between CT-8 to CT-13, in six passages. Noteworthy, in the H9 (Arg) s.3 subline, within a short span between passages CT-8 to CT-10, the H9 (Arg(high)) nearly tripled from 24.4% to 72% of the total population.

Next, we determined whether H9 (Arg) cells exhibited increased clonality**.** First, we only used H9 (Arg) cultures that had a high percentage (>80%) of H9 (Arg(+)) cells, as measured by

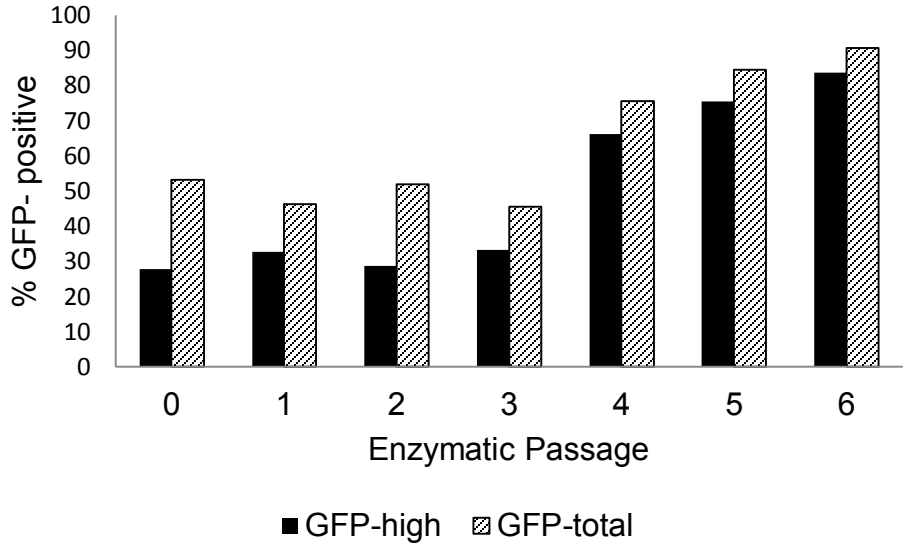

Figure 22. H9 (Arg) s.1 demonstrates competitive advantage under single- cell passaging.

H9 (Arg) lines was maintained on iMEFs under manual passage (CT-0) then switched to single-cell dissociation (CT-1 to CT-6). By flow cytometry, the percentage of GFP positive cells was measured at each passage to assess the proportion of cells overexpressing ARHGDIA. The distribution of GFP signal intensity is bimodal with GFP- high and GFP- low fractions. The H9 (Arg) GFP- high exhibits increased competitive advantage relative to H9 (Arg) GFP- low.

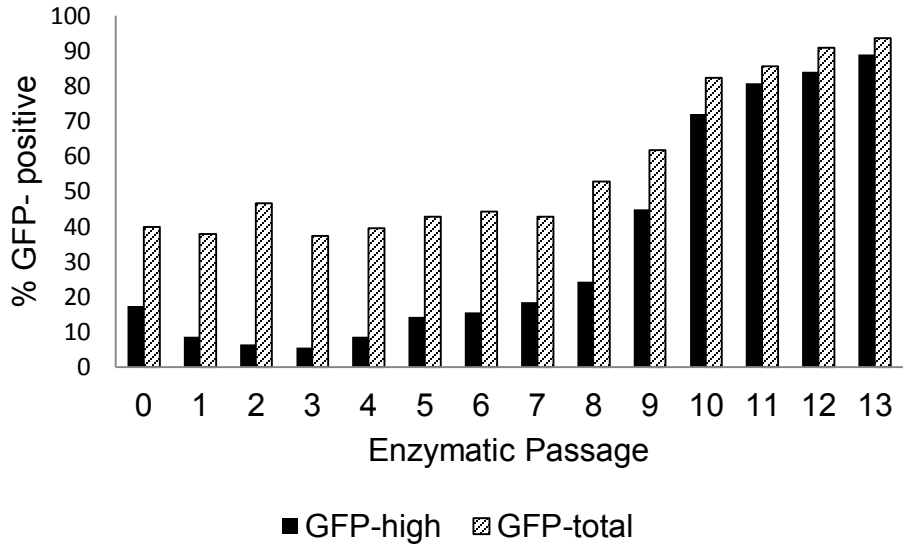

Figure 23. H9 (Arg) s.3 demonstrates competitive advantage under single- cell passaging. H9 (Arg) lines was maintained on iMEFs under manual passage (CT-0) then switched to single-cell dissociation (CT-1 to CT-13). By flow cytometry, the percentage of GFP positive cells was measured at each passage to assess the proportion of cells overexpressing ARHGDIA. The distribution of GFP signal intensity is bimodal with GFP- high and GFP- low fractions. The H9 (Arg) GFP- high exhibits increased competitive advantage relative to H9 (Arg) GFP- low.

GFP- positive expression using flow cytometry. Both sublines, H9 (Arg) s.1 and H9 (Arg) s.3, were used in four independent seedings. Three of the four seedings were plated in triplicate for a total of 10 samples points. The H9 (GFP) controls were plated in triplicate at three different passages for a total of 9 samples and the H9 (WT) was plated in triplicate or duplicate at 3 different passages for a total of 8 samples. H9 (Arg), H9 (GFP), and H9 (WT) were manually passaged until clonal analysis. Clonality was tested on the first enzymatic passage (CT) to control for selective pressure. Each replicate was 40 μm filtered and seeded on iMEFs at 1000 cells per 35 mm petri dish to ensure low density single-cell plating. On day 7, colonies were AP stained to aid visualization and validate pluripotency.

The increased clonality of the H9 (Arg) cells relative to H9 (WT) and H9 (GFP) was striking and statistically significant. Statistical analysis was carried out in the most stringent and conservative manner. Each passage number seeding was considered a biological replicate and the set of plates at that passage seeding were considered technical replicates. The average of the technical replicates was taken for a single biological replicate mean. In this manner, the biological replicate means were used for statistical analysis and hypothesis testing. The number of biological replicates used were H9 (Arg) [n=4], H9 (GFP) [n=3], and H9 (WT) [n=3] respectively. The observed average number of colonies for H9 (Arg), H9 (GFP), and H9 (WT) are 125.66, 31.44, and 42.83, respectively (Figure 24). Therefore, the clonality of H9 (Arg) cells has an increased fold change of 4.0 and 2.93 relative to H9 (GFP) and H9 (WT), respectively. Furthermore, the number of H9 (Arg) colonies was statistically significant to both H9 (WT) and H9 (GFP) with p-values, 0.0023 and 0.0004, respectively. The results from both of the competition and clonality experiments support the conclusion that H9 (Arg) cells have

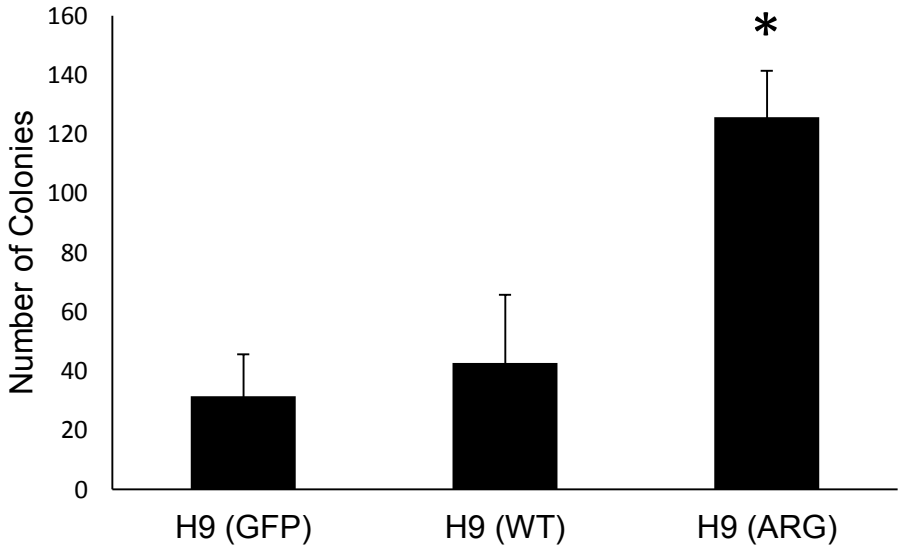

Figure 24. ARHGDIA overexpression increases clonality. H9 control and experimental lines were continually propagated by manual dissection prior to clonal survival analysis. Under initial enzymatic dissociation and 40 μm filtering 1000 single cells were plated per 35mm petri dish. Colonies were AP- stained and counted on Day 7. H9 (Arg) line overexpressing ARHGDIA has significantly increased number of colonies in low density single-cell seeding. * indicates significance ($p < 0.01$) for H9 (Arg) compared to H9 (WT) and H9 (GFP). Abbreviations: ARG- ARHGDIA, WT- wild type, GFP- green fluorescent protein.

competitive advantage by increasing clonality. We did not observe strong promoter silencing in the BG01 (Arg) manually passaged lines, as in the H9 (Arg) manually passaged lines; therefore, we speculated a technical improvement to the co-culture experimental design.

We repeated our competition based assay with BG01 (Arg) cells, while making a few refinements to the approach. First, we controlled for the percentage of the initial BG01 (Arg) seeding population and changed the co-culture to BG01 (Arg) vs BG01 (WT). Similarly, we changed our experimental control to co-culture of BG01 (GFP) vs BG01 (WT). In our BG01 (Arg) vs BG01 (WT) competition assay, we varied substrates, seeding density, and ROCKi exposure. As in the H9 (Arg) competition experiments, we maintained our BG01 (Arg), BG01 (GFP), and BG01 (WT) by manual passaging until time of co-culture experiments, upon which cells were switched to enzymatic passaging. A 40 μm filter was used for plating as single-cells. Percent BG01 (Arg) populations were quantitated by flow cytometry on GFP- positive expression.

The results on competitive advantage of BG01 (Arg) cells in mixed co-cultures with BG01 (WT) are striking. BG01 (Arg) lines exhibited immediate and dominant competitive advantage when co-cultured with BG01 (WT). The co-culture of BG01 (GFP) with BG01 (WT) did not exhibit competitive advantage. The initial co-culture seeding percentage for BG01 (Arg) and BG01 (WT) was estimated to be 30 % for BG01 (Arg) and 70 % for BG01 (WT). The actual initial seeding percentage of BG01 (Arg) varied slightly from this estimate, as 30% was factored by the percentage of BG01 (Arg(+)) cells in the BG01 (Arg) line. The initial seeding percentage for the co-cultures involving BG01 (Arg)- 25k, BG01 (Arg)- 50k, and BG01 (Arg)- ROCKi is

26.97%. For BG01 (Arg)- 100k and BG01 (Arg)- iMEFs, the initial BG01 (Arg) percentages are 18.29 and 25.17%, respectively. Each co-culture experimental condition was carried out in parallel biological triplicates. In their feeder- free cultures, Rosler and colleagues report trisomy 20 as the most frequently observed aberration [193], while Trisomy 17 is prominent in our hPSC cultures propagated on iMEFs. Thus, we wanted to determine whether iMEFs or Matrigel™ influenced competitive advantage of BG01 (Arg) vs BG01 (WT) co-cultures. Both substrates showed strong selection for BG01 (Arg) cells in the mixed populations with BG01 (WT). By enzymatic passage, CT-3, the BG01 (Arg) co-culture, seeded at 100k on iMEFs, had increased to 82.87% of the mixed population. Comparatively, the BG01 (Arg) co-culture, seeded at 100k on Matrigel™, had increased to 79.11% of the mixed population, by enzymatic passage, CT-5. For both enzymatic passages, CT-2 and CT-3, the percent BG01 (Arg) is significantly higher in the iMEFs cultures compared to Matrigel™, $p < 0.01$. These results suggest that iMEFs positively influenced BG01 (Arg) competitive advantage compared to Matrigel™ (Figure 25A).

Next, we wanted to determine whether seeding density influenced competitive advantage. BG01 (Arg) and BG01 (WT) co-cultures were plated on Matrigel™ at seeding densities of 25k, 50k, and 100k cells. Since, low single-cell seeding density could adversely influence survival in WT cells by reduced paracrine signaling [149] or increased cell migration distance [64, 194], it is possible that relative competitive advantage would be greater in low density BG01 (Arg) co-cultures compared to high density BG01 (Arg) co-cultures. BG01 (Arg) competitive advantage was clearly demonstrated within 5 enzymatic passages for each seeding density. The maximal BG01 (Arg) percentages for 25k, 50k, and 100k, are 91.19, 89.52, and 79.11%, respectively, with percentage of BG01 (Arg) cells greatest in the samples seeded at 25k (Figure 25B). The

higher percent of BG01 (Arg) in the 25k samples relative to 50k is significant for CT-4 ($p < 0.05$) and is significant relative to 100k for CT-4 and CT-5 ($p < 0.05$).

Finally, we decided to test the importance of ROCKi given its role in increasing single-cell viability during plating. We hypothesized that ROCKi would reduce the selective advantage of BG01 (Arg) cells relative to BG01 (WT) by increasing the survival of dissociated BG01 (WT) cells. BG01 (Arg) and BG01 (WT) co-cultures were seeded at 100k on Matrigel™ in the presence of ROCKi, Y27632 in the growth medium. Strikingly, when 10μM ROCKi was added during plating and withdrawn on day 2 at medium exchange, we did not observe competitive advantage of BG01 (Arg) cells (Figure 25C). Starting with an initial BG01 (Arg) percentage of 26.97%, by CT-5 the mean percentage of BG01 (Arg) cells was only 29.02%. These results are in stark contrast to the other BG01 (Arg) experiments, without the use of ROCKi, in which competitive advantage was demonstrative. We checked whether BG01 (GFP) subpopulations displayed competitive advantage. Indeed this was not the case; moreover, modest GFP silencing was evident, albeit not to the extent observed with H9s (Figure 25D). BG01 (GFP) vs BG01 (WT) co-cultures started at an estimated 29.7% BG01 (GFP) that by CT-5 had decreased to 15.06% BG01 (GFP). Combined across BG01 (Arg) and H9 (Arg) co-culture and clonality experiments, our results presents compelling evidence that ARHGDIA overexpression confers selective advantage to hPSCs through increased single- cell survival, and this selective advantage can be ameliorated by the addition of ROCKi. This is suggestive that when passaging as single-cell cultures, conditions that increase single- cell survival of genomically normal cells could reduce the selective pressure for clonal genomic variants.

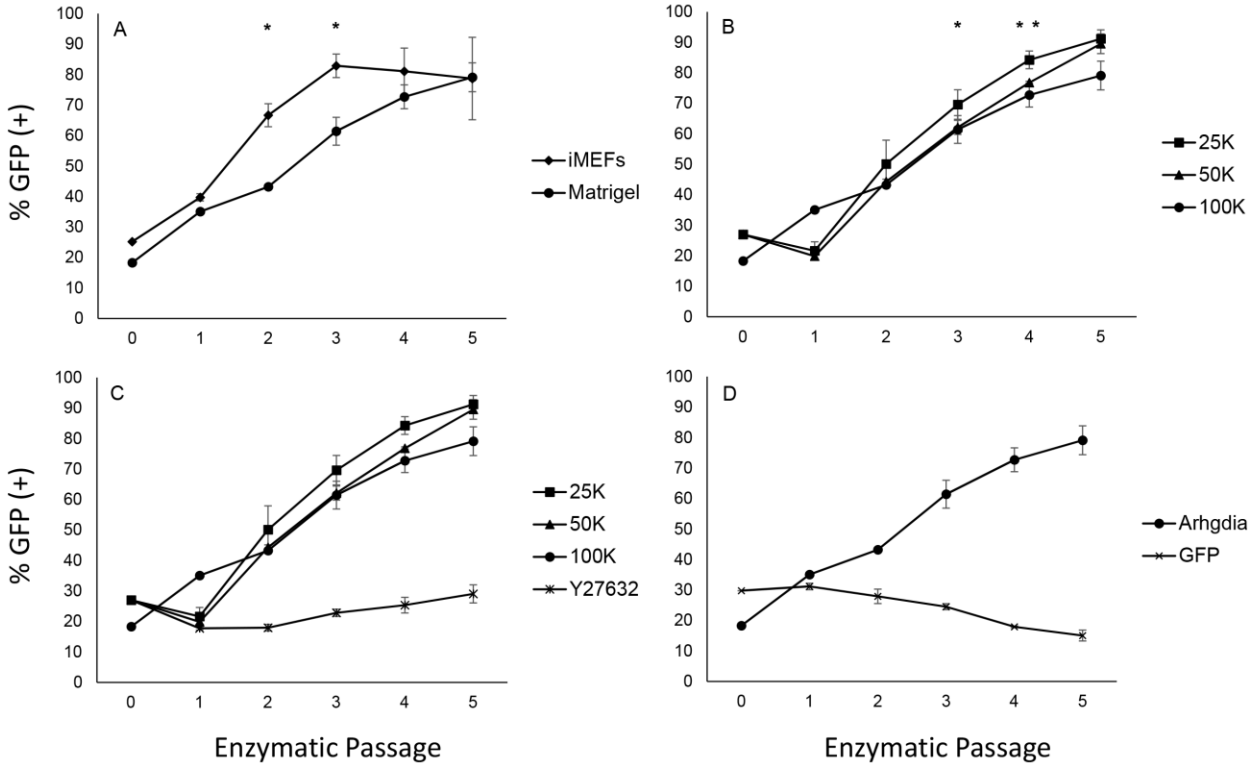

Figure 25. BG01 (Arg) hESCs demonstrate competitive advantage across substrates and seeding densities and selection is inhibited by ROCKi, Y27632. BG01 (Arg) lines co- cultured with BG01 (WT) have competitive advantage across substrates (A) and seeding densities in 35mm petri- dishes (B). ROCKi, ameliorated this seeding density (C) and BG01 (GFP) control did not exhibit competitive advantage (D).

DISCUSSION AND CONCLUSIONS

Trisomy 17 is the most common clonal abnormality observed in our hPSCs lines and was scored in the H9, BG01v, and iPSC lines. In two independent lines, trisomy 17 was common to both trisomy 12 and a gain on X, H9 and iPSC, respectively. Trisomy 17 could increase the presence of additional genomic alterations and further promote genomic instability. Interestingly, trisomy 17 has not been as commonly reported in the literature for iPSCs as in hESCs [89]; however it dominated the iPSC culture relatively early in our enzymatically passaged cultures at CT-31. The structural gain of 15p11.2 in the H1 line has not been reported elsewhere, except for a trisomy 15 [88].Thus, our findings of an amplicon on chromosome 15 may be used to minimize the region of candidate genes on chromosome 15 for further analysis. It is interesting to consider whether trisomy 17 or trisomy 20 is the more dominant variant; since, two recent large- scale studies have focused on the 20q11.21 amplicon [87, 88]. Since trisomy 20 was not previously reported in the BG01(v) line and trisomy 17 was observed first [82], then this could represent an emerging dominant genomic species, alternatively the trisomy 20 cells were only 34% of culture and at that passage had not exhibited the same culture dominance that as trisomy 17 cells comprising 92% of the population. The recurrent abnormality, trisomy 12, was observed in the BG01(v) and H9 lines. NANOG is located on chromosome 12 and increased NANOG expression may confer self- renewal benefit to these populations. Trisomies 12 and 17 are hallmarks of germ cell tumors and the presence of these alterations in hPSCs poses significant clinical concern [95, 195, 196].

Our observations are consistent with the literature that genomic amplifications have a much greater propensity to be clonal than genomic losses which are infrequently observed as populations [88]. Interestingly, when using single- cell based approaches, such as G-banding and FISH, for non- clonal random alterations, monosomies are observed at least or greater than trisomies [103, 106, 148] and chromosomes 17 and 20 are 2 of the 3 least observed aneuploidies in PGS embryos [146].

While initial reports suggested that 20q11.21 amplification was preferential for feeder-free cell culture [193]; after an accumulation of studies, no clear correlation exists between particular recurrent abnormalities and culture conditions or protocols [88]. However, it has been reported that enzymatic passage increases genomic instability more than two-fold [87]. Our results show that trisomy 17 is disproportionately expressed under routine use of iMEFs and CT passaging, indicating the possibility that under single- cell passaging a gain on chromosome 17 is associated with a clonal phenotype. In our studies, we carefully recorded the parental history of the lines and reduced the culture parameters. Loring and colleagues have pointed out the importance of carefully tracking the history and pedigree of PSC lines in the experimental design of hPSC genomic instability studies, in order to tease out potential cell culture condition specific recurrent abnormalities. Thus, our approach may have aided the consistency of observing trisomy 17 under the single- cell passaging protocol [88].

To date, a profile of different hPSC lines characterizing their degree of genomic instability has not been reported; however examples of lines with increased CIN has been suggested [195]. Such a profile could help researchers determine preferential lines and optimal

conditions. However, it remains ambiguous whether mutational load can be decreased, since a high degree of CIN maybe characteristic of the pluripotent state. Our non- clonal g- band analysis on BG01(v) and H9 cell lines suggest that the BG01(v) has greater genomic instability than the H9 line. However, without further analysis, it is not clear whether this increased genomic instability is due to cell line specificity, passage number, or an acquisition of a mutator phenotype from cultured-induced aneuploidy. The BG01(v) line at CT-23 exhibited a complex genomic phenotype with trisomy 12, 17, and X. In the non-clonal analysis of the H9 line, at CT-26 passage, only 5.7% of cells exhibited a random aberration. This is an appreciably lower percentage than the ~30% estimated frequencies for non- clonal aberrations in hPSCs [103, 106]. None of the H9 CT-26 cells expressed more than one genomic abnormality. Therefore, the emergence of trisomy 17 in the H9 line is not associated with a concomitant increase in random alterations and the time to karyotypic abnormality was similar for both H9 and BG01(v) lines. Together this is suggestive that different cell lines may exhibit varying degrees of genomic instability and that selection mechanisms may be the dominate force in the emergence of genomic variants.

Consistent with a prior report [175], we found that the H1 and BG01 lines have an inherently high centrosome error rate. Holubcova and colleagues report centrosome amplification percentages ranging from 12-24% in 12 independent hPSC lines, while not reporting specific percentages for the commonly used H9 cell line. In two of the cell lines (H9 and iPSC) we studied, high centrosome error rates were not observed, suggesting that not all hPSCs suffer from high centrosomal amplification. However, it is worth noting that both the H9 and iPSC lines became abnormal in about the same enzymatic passage span as the BG01 line and

the H1 line took nearly 100 passages to gain a small duplication. The significance of centrosome errors is unclear; however it is interesting to consider the post- mitotic survival of cells with supernumerary centrosome. Post- mitotic survival of cells with supernumerary centrosomes could increase upon extended passaging and may help explain the observation in our BG01(v) line that had a low centrosome error rate but a high rate of random genomic aberrations and clonal species.

Enzymatic passages increases the presence of genomic abnormalities. As one means to explain this observation among labs, we investigated whether enzymatic passage increases mitotic instability. Both the H9 and iPSC lines demonstrated increased centrosomal instability when switched from manual to single- cell passaging. Ding and colleagues have reported that single- cell dissociation in primed PSCs results in E-cadherin instability [45]. WNT signaling members, GSK3β and β- catenin, are essential in pluripotent cells for fidelity in chromatin segregation and the centrosome duplication, respectively [197, 198]. These are attractive candidates for elucidating the mechanism driving single- cell dissociation induced centrosome errors.

Recurrent variations in hPSCs line are well established and highly suggestive of strong selective forces in establishing a variant population. Consistent with Mayshar and colleagues report on gene expression data to predict genomic copy number, our chromosome- specific mean expression levels of active genes demonstrated a dosage correlation with genomic copy number. [89]. Thus, our transcriptional data is highly consistent with the view that a 1.5 fold increase in gene expression is better tolerated by the cellular system than a 50% reduction [146].

Significantly increased genes located on recurrent amplifications are strong candidates for a biological role in positive selection. In our transcriptional analysis, ARHGDIA was the most attractive candidate gene for its location, gene expression, and established role as an inhibitor of RHO signaling and downstream effector ROCK [110].

Our study is the first to functionally demonstrate a gene located on chromosome 17 that confers selective advantage to hPSCs when passaged as single- cells. Analysis on pluripotency, suggests that ARHGDIA overexpression does not adversely affect self- renewal or differentiation, as ARHGDIA transduced cultures were maintained for several months and differentiated into EBs exhibiting all three germ layers. Two independent approaches for ARHGDIA's influence on clonal survival were tested in H9 cell lines. The H9 (Arg(+)) cells demonstrated competitive advantage against H9 (Arg(-)) cells; however on independent runs there was an initial delay in the competitive advantage. Likely this is due to CMV promoter silencing that puts downward pressure on the assay; however an alternate hypothesis is the existence of a epigenetic or post- translation modification that coupled with ARHGDIA overexpression confers selective advantage to a subpopulation of H9 (Arg(+)) cells. Another possibility for this could be a genomic alteration in the H9 (Arg(+)) subpopulation in each of the co- cultures. However, independent runs suggests a companion genomic alteration is unlikely. The H9 clonality assay, did not suffer from the technical issue of promoter silencing, since the cells were GFP- positive at seeding. Indeed single- cell survival was drastically increased in H9 (Arg) cells compared to controls suggesting clonality as the phenotypic advantage.

Our BG01 (Arg) lines exhibited increased stability of ARHGDIA ORF expression. The BG01 (Arg) cells quickly dominated co-cultures in as quickly as three passages in the iMEF sample. Across seeding densities on Matrigel™, the BG01 (Arg) cells with the lowest seeding density of 2.5k/cm^2, exhibited the fastest culture dominance. Human PSCs are known to migrate promoting pro-survival cell- cell contact [194] and for trophic paracrine signaling that may also increase cell- viability [149, 199]. Either of these factors may have reduced the survival of the BG01 (WT) at lower seeding densities with a relative increase in selective advantage of the BG01 (Arg) cells. This poses interesting questions regarding the mechanism in which ARHGDIA overexpression improves single- cell survival, through the possibilities of inhibiting ROCK- associated blebbing, facilitating migration, or in an unidentified cell adhesion manner affecting clonal survival.

Ben- David and colleagues suggest that ROCKi may reduce the rate of genomic adaptation of hPSCs in culture by reducing selective pressure [200]. However, to date there has not been any data to support this hypothesis. Our experiments are the first to provide compelling evidence that ROCK inhibitors can be used to reduce the selection of competitive sub-populations. Current approaches to study selection of genomic variants are plagued by the nature of the biological phenomena in question with culture time to genomic alterations highly variable and easily take months to observe. Therefore culture adaptation studies are wrought with experimental design and statistical issues, when seeking to assess the influence of culture conditions and components. While we do not prove a tight causation for ARHGDIA expression and trisomy 17 selection, these results strongly encourage future studies to eludicate ARHGDIA's role in hPSC culture. Recently, BCL- XL has been shown to mediate the selective

advantage of the 20q11.21 amplicon. Together, ARHGDIA and BCL-XL provide strong candidate genes for engineering genetically defined and biologically relevant hPSC lines that can be used to study culture conditions influencing positive selection of genomic variants. Such genetically defined lines can be used to test small molecules, substrates, 3 dimensional culture systems, and the primed vs naïve pluripotent state on an amenable experimental time- scale. With the widespread culture dominance of trisomy 17, development of the hPSC (Arg) model is a significant advance in the field empowering culture based approaches to reducing the rate of culture adaptation of hPSC genomic variants.

CHAPTER 3

Characterizing Self- Renewal and Differentiation in Human Pluripotent Stem Cells Propagated in Naïve State Culture Conditions

ABSTRACT

Optimized culture conditions that reduce genomic instability during scale-up remains a significant challenge for industry and clinical applications. Traditionally, hPSCs have been cultured in a "primed" pluripotent state in bFGF- supplemented growth medium. In contrast, mouse embryonic stem cells are cultured as "naïve" pluripotent stem cells in LIF- dependent conditions. Here we report the culture of H9 and BG01 lines in growth medium devoid of bFGF and in medium containing LIF plus two inhibitors, MEK inhibitor PD0325901 and p38 inhibitor SB203580. These LIF + 2i lines were manually and enzymatically passaged, as well as cultured on inactivated mouse embryonic fibroblasts and Matrigel™ with iMEF conditioned media. LIF + 2i cultures supported self- renewal for more than a year, irrespective of passage method or substrate. In the BG01 line, after 18 manual passages, self- renewal was aided by switching to single- cell passaging. Histopathological analysis of embryoid bodies generated from the H9 (LIF) lines demonstrate tri-lineage differentiation along each germ- layer. Real- time qPCR analysis supports EB histological analysis confirming expression of germ- layer specific genes; however, the H9 (LIF) s.4 subline cultured on Matrigel™ was the only line to show increased mRNA expression of each germ layer. Finally, to ascertain the influence of LIF + 2i conditions on genomic instability, the percentage of supernumerary centrosomes was quantitated on H9 (LIF) lines maintained on iMEFs and Matrigel™. We observed a statistical increase in supernumerary centrosomes of H9 (LIF) propagated on Matrigel™. Together, our results indicate that hESCs can be stably maintained in LIF-based growth medium while retaining tri-lineage differentiation potential; and that, substrates should be considered when determining the optimal culture conditions for reducing mutation pressure.

INTRODUCTION

Recent advances have contributed to our molecular understanding of mammalian pluripotency, the self-renewal network, and culture conditions that influence pluripotency-associated genomic and epigenetic adaptations. Early work on embryonic stem cells demonstrated conserved and divergent pathways between mESCs and hESCs [18]. While initially perceived to be species- specific differences, recent findings have increased a species-conserved perspective of mammalian pluripotency by identifying distinct metastable stem cell states within the pluripotent compartment [29, 35]. Through the successful derivation of mouse lines from the pre- implantation and post-implantation epiblast [39], representations of "naïve" and "primed" pluripotency have been established [24]. The most distinctive culture associated feature is that naïve pluripotent stem cell lines are LIF- dependent, whereas primed pluripotent stem cell states rely on bFGF for self- renewal [32]. The emerging model is that hPSCs reside in a primed PSC state that is similar to the post- implantation mouse epiblast stem cells (mEpiSCs) [19]. Both naïve and primed pluripotent stem cells express the three essential pluripotency-associated transcription factors, OCT4, SOX2, and NANOG; however, NANOG may have an important role in naïve pluripotency and establishing the ground state of pluripotency [26].
In the well- established conditions for mPSC culture, there are clear technical and biological benefits compared to hPSC cultures. Establishing naïve culture conditions for hPSCs has significant implications for basic research and industry applications for regenerative medicine. In 2008, rodent pluripotent stem cell culture was generalized in conditions that established the ground- state of pluripotency. In this ground- state pluripotency, LIF could be removed and

inhibitors to MEK and GSK3 were sufficient to maintain self- renewal, even in recalcitrant mice strains and rat lines [31, 69, 70]. While there is progress in establishing naïve hPSC lines, culture conditions supporting the ground state of human pluripotency remains an important but significant challenge [20, 37]. Heterogeneity in stem cell culture has plagued the standardization of directed differentiation protocols, with different hPSC lines showing lineage-bias [49]. Additionally, hPSC cultures have been plagued by poor survival at passage, particularly as single-cells during plating [45]. Furthermore, genome- editing approaches in mPSCs are not amenable in hPSCs. Culturing hPSCs in a similar naïve pluripotent states as mPSCs maintains significant advantage for the field by potentially: (a) reducing phenotypic heterogeneity in stem cell culture, (b) increasing viability of clonal stem cells and yields during scale-up, (c) standardizing directed differentiation protocols by reducing lineage- bias and increasing uniform control of aggregate size from single- cell seeding, (d) genetically manipulating clonal cells, and (e) enabling homologous recombination in hPSCs [30, 31, 113]. Developing hPSC culture conditions that promote the ground state of pluripotency may also minimize the components needed for defined culture conditions.

During development, the pluripotent state is transient; whereas, during hPSC culture, pluripotency is forced indefinitely during long-term propagation [27]. Consequently, cell culture introduces significant environmental stressors to hPSCs during propagation inducing continual adaptation of the pluripotent stem cell population. In the presence of LIF, mouse embryonic stem cells are amenable to single- cell passage on gelatin coated petri-dishes [58]. High selective pressure on hPSCs for clonal survival has been suggested to drive the appearance of common chromosomal abnormalities [82, 84]. Indeed, the enzymatic dissociation of hPSCs into single-

cells during passaging increases genomic instability and the appearance of genomic alterations by more than two-fold [87].

In this study, we cultured 4 independent sublines comprised of two different parental hPSC lines, H9 and BG01, for more than one year in LIF + 2i conditions. Along with the cytokine LIF, two inhibitors MEK inhibitor PD0325901 and p38 inhibitor SB203580 were used as part of medium formulations. The MEKi, PD0325901, has been used in mPSC culture to establish the ground state [23]. Human PSCs lines were cultured on iMEFs and Matrigel™ and passaged manually and as single- cells. LIF + 2i cultures supported self- renewal, irrespective of passage method or substrate. In the BG01 line, after 18 manual passages, self- renewal was aided by switching to single- cell passaging. Indefinite self- renewal is shown using standard stem cell characterization assays and pluripotency is demonstrated *in vitro* using EBs for differentiation into each of the three germ layers. EBs from the H9 (LIF) line maintained on Matrigel™ exhibited a consistent increase in germ- layer specific mRNA. Histopathological analysis supported the presence of all germ- layers in each of the EB samples; however the use of ROCKi during the hanging drop step increased EB yield and differentiation.

Work from our laboratory and others has identified supernumerary centrosomes as prominent and variable to culture conditions [175]. Indirect measures on genomic instability, such as centrosome error analysis, have the distinct benefit of being able to assess culture stress at each passage prior to selection bias of genomic variants. After establishing LIF + 2i based culture conditions support self- renewal, we tested two different substrates, iMEFs and Matrigel™, to determine their influence on centrosomal instability. We found H9 (LIF)

propagated on Matrigel™ had an increased percentage of supernumerary centrosomes compared to H9 propagated on iMEFs. Since centrosome amplification is known to cause CIN [167], there is potential for concern when considering its use in LIF-based conditions. Our results show that hESCs can be stably maintained for long-term propagation in LIF-based medium while retaining tri-lineage differentiation potential; and that, substrates should be considered when determining the optimal culture conditions for reducing mutation pressure.

METHODS

Human Pluripotent Stem Cell Culture

HPSCs were maintained on mitomycin C–inactivated mouse embryonic feeder (MEF) layers in DMEM/F-12, 20% knockout serum replacement, 2 mM L-glutamine, 1% nonessential amino acids, 50 U/mL penicillin, 50 microgram per mL streptomycin (all from Gibco/Invitrogen), 0.1 mM beta mercaptoethanol (Sigma), and 4 ng/mL bFGF (Sigma). Cells were enzymatically passaged via sequential dissociation using 1mg/ml type IV collagenase (Gibco) and 0.05% trypsin–ethylene-diamine tetra-acetic acid (trypsin-EDTA, Invitrogen) or manually passaged by fire-pulled pasteur pipette. hPSCs were replated on fresh feeder layers or Matrigel™. Cells grown in Matrigel™ were coated at the lot specific recommended dilution in 35mm plates. Medium was conditioned on iMEFS at 5 x 10^6 cells per T-75 flask for 24 hours up to day 10 from seeding. For growing hPSCs in naive-like conditions, LIF + 2i medium, BG01 and WA09 were cultured in hPSC growth media supplemented with 1-μM mitogen-activated protein kinase/extracellular signal-regulated kinase kinase (MEK) inhibitor PD0325901 (Sigma) and 5-μM p38 (Sigma) inhibitor SB202190 and 1×10^3 human LIF (Invitrogen).

In vitro differentiation of hPSCs and histopathology of hPSC-derived embryoid bodies.

To generate embryoid bodies (EBs), hPSCs were dissociated using 0.05% trypsin and resuspended in growth medium without bFGF. EB formation was facilitated using suspension culture by a hanging drop method, where cells at a density of 5,000 cells per 20 microliters drops were suspended from a Petri dish lid in 50-100 droplets with the addition of 10 micro-molarity ROCKi. After 3 days, the surviving EBs were transferred onto agar plates at in 20 mls of EB

(hPSC, -bfgf) media to facilitate further differentiation with media changes every 2 days for a total differentiation duration of 15-20 days. EBs were prepared for morphological analysis by fixation in 4.0% PFA in 1.5 mL microfuge tubes at 50-100 EBs per tube. EBs were rinsed with PBS to remove PFA, resuspended in 200 lL melted 4% low melting point agarose (Sigma Aldrich) at 42 degrees C, and incubated for 2 h to allow settling. Final pelleting and agarose solidification were performed with brief room temperature centrifugation at 500g. Agarose embedded samples were removed as single plugs and processed by dehydration with increasing ethanol concentration to 100% followed by xylene and paraffination in a Leica TP1020 tissue processor. Hematoxylin and Eosin (H and E) staining was performed on microscope slide mounted 5 lm sections in a Leica Autostainer XL workstation (Leica Microsystems, Richmond, IL). Images were acquired using an Olympus BX51 microscope (Olympus, Center Valley, PA) using the default imaging parameters.

Antibodies and Immunocytochemical Analysis

HPSCs cultured on Matrigel™ or iMEFs in four chambered glass slides or cover slips in 35mm dishes were fixed via paraformaldehyde (PFA, 4%) in PBS or 80% Methanol. Permeabilization for intracellular markers was achieved with 0.2% Triton X-100 in PBS. 3% normal goat serum was used for blocking and to dilute antibodies. Fixed cells were incubated with primary antibodies: OCT4 (Santa Cruz Biotechnology, Santa Cruz, CA), SSEA4 (Millipore, Temecula, CA), Pericentrin (Abcam), Beta-tubulin (Developmental Studies Hybridoma Bank), ARHGDIA (Santa Cruz Biotechnology, Inc.). Goat anti-mouse IgG, anti- rabbit conjugated to Alexa 488 or Alexa 594 (Molecular Probes, Eugene, OR) were used as secondary antibodies. Centrosomes were visualized with percentrin and the spindle apparatus by β-tubulin. Cells were

counterstained with DAPI (4'-6-diamidino-2-phenylindole). At 40x magnification, centrosomes were counted per mitotic cell and the polarity recorded. Fluorescent images were acquired using a Cool- Snap EZ camera (Photometrics, Tucson, AZ) mounted on a Nikon Eclipse TE 2000-S inverted microscope (Nikon, Melville, NY) with NIS Elements BR software.

RNA isolation, real time reverse transcription quantitative polymerase chain reaction and gene expression analysis

RNA was isolated from hPSCs propagated at various passages under different conditions and from EBs after 15 days in suspension using DNA/RNA All Prep (Qiagen) and quantified using BioMate3 UV-VIS Spectrophotometer (Thermo Scientific, Waltham, MA) or Nanodrop 2000. cDNA was synthesized from 1 mg of RNA using cDNA High Capacity reverse transcription kit (Applied Biosystems, Foster City, CA). Transcriptional expression on genes listed in Table 6 were analyzed using quantitative real time RT-PCR (QPCR). QPCR was performed on a Bio-Rad CFX96 Touch Real-Time PCR Detection System. Comparative gene expression analysis (three replicates) was conducted using the ΔCT or $\Delta\Delta$CT method depending on the analysis and samples. GAPDH was used for normalization in all analyses. Relative gene expression for hPSC experimental samples was assessed against hPSC controls and reported as fold change and the student's T- test used for statistical significance testing.

Alkaline Phosphatase Assay

Staining for alkaline phosphatase was performed as per manufacturer instructions (Vector Laboratories, Burlingame, CA). Briefly, the hPSCs were rinsed in with deionized water to remove traces of growth medium. The final solution was prepared by adding in order 2 drops of

each constituent to 200mM Tris HCl buffer, pH 8.5. The hPSCs were incubated in the final mixture for 45 min in the dark and images were acquired using a Nikon DS-Fi1 camera mounted on a Nikon TS100 Microscope (Nikon, Melville, NY).

RESULTS

hESCs cultured in LIF + 2i proliferate and maintain stem cell colony morphology

After long- term propagation in LIF + 2i containing hESC medium, we performed the standard pluripotent stem cell characterization assays widely accepted to demonstrate the hPSC state. We cultured two independent parental lines, H9 (LIF) and BG01 (LIF), for greater than 30 passages. Three independent sublines lines of H9 (LIF) were passaged in parallel, H9 (LIF) s.2, H9 (LIF) s.3, and H9 (LIF) s.4. The H9 (LIF) s.2 and H9 (LIF) s.3 were maintained on iMEFs and the H9 (LIF) s.4 was propagated on Matrigel™. Prior to switching to LIF + 2i conditions, the H9 and BG01 lines were maintained by manual passaging on iMEFs. For the H9 (LIF) lines, the cultures were concomitantly switched to LIF + 2i conditions and passaged by enzymatic single- cell dissociation methodologies. The H9 (LIF) sublines were initially seeded at high density at 20-25k/cm^2. In contrast to hESCs maintained in bFGF containing medium, the H9 (LIF) sublines on initial enzymatic passage, CT-1, had high viability and formed robust colonies with strong boundaries and cobblestone morphology (data not shown). For the next few passages, viability of the iMEF sublines decreased and the H9 (LIF) s.1 subline was discarded due to poor viability. After this initial cytokine adaptation, the H9 (LIF) s.2 and H9 (LIF) s.3 proliferated very well and was continuously propagated for over a year. Interestingly, two morphologically distinct colony types emerged, one type was compact and mounded and the other was flatter and spread out (Figure 26B). On Matrigel™, the viability of H9 (LIF) s.4 remained consistently high but heterogeneity in colony formation increased between, p4 and p6, as a significant number of single cells peripheral to the colony emerged. Often these single cells are considered signs of differentiation and these single cells were similar to the human

pluripotent stem cell derived fibroblasts (hPDFs) reported by Bhatias's group [191]**.** However, the presence of robust stem cell colonies was very prominent during these passages. Starting on p7 of H9 (LIF) s.4 on Matrigel™ culture, the seeding density was reduced to 7.5k/cm^2. The cultures responded very well with little signs of differentiation; and, in general, the cultures were homogenous for robust colonies with strong boundaries and cobblestone morphology (Figure 26C).

The BG01 (LIF) line was manually propagated on iMEFs for the first 18 LIF + 2i passages and then was switched to enzymatic single- cell passaging and maintained on iMEFs. By morphological analysis, manual passaging of BG01 (LIF) demonstrated a high degree of differentiation Figure 39A. For the initial five LIF + 2i passages, greater than 50% of colonies differentiated; however, manual selection of morphologically superior colonies supported continued propagation. Significant differentiation in the BG01 (LIF) manually passaged cultures persisted until greater than 15 passages Figure 39B. At passage 18, the plates were switched to enzymatic passaging. During the initial enzymatic passaging the cells had good viability, formed robust colonies with strong borders and cobblestone morphology. The colonies were mostly monolayer at BG01 (LIF), p20 and CT-2. Around BG01 (LIF), p23 and CT-5, the emergence of compact and mounded colonies became more prominent. By morphological analysis, the BG01 (LIF) handled single-cell passaging better than manual passaging. Morphologically, both the H9 (LIF) and BG01 (LIF) handled the initial enzymatic transition well with good viability and strong colony formation.

It is widely recognized that differentiating hPSCs lose expression of the alkaline phosphatase (AP) marker. We found the AP stain to be a sensitive method to screen for undifferentiated hPSCs in LIF + 2i conditions. In the H9 (LIF) s.2, H9 (LIF) s.3, and H9 (LIF) s.4 lines the colonies were AP-positive for greater than or equal to 30 passages in LIF + 2i medium. Similarly, the BG01 (LIF) line was AP positive at passage 30 in LIF + 2i medium (Figure 26, D-E).

hPSCs propagated in LIF + 2i medium are able to self-renew and maintain undifferentiated state

Empirical data increasingly supports a complex model of pluripotency consisting of heterogeneous metastable states, with the transcription factors OCT4, SOX2, and NANOG common to both naïve and primed mammalian pluripotency. Using immunocytochemical analysis, we assessed pluripotency in the H9 (LIF) and BG01 (LIF) lines, at multiple passages extending greater than or equal to 30 passages in LIF + 2i conditions. At each passage assessed, the sublines of the H9 (LIF) and BG01 (LIF) lines were OCT4 and SSEA4 positive (Figure 27 and 28). In the hPSC sublines (H9 (LIF) s.2 and H9 (LIF) s.3) propagated on iMEFs, we noticed that the single- cells peripheral to the colony maintained OCT4 expression, while in compact colonies, cells in the mounded center lost OCT4 expression. In the BG01 (LIF) line, p17, manually maintained on iMEFs, differential OCT4 expression was observed Figure 40. Thus, OCT4 appears to be a sensitive marker for hPSC cultures in LIF + 2i conditions. Using real- time PCR, we quantitatively assessed pluripotent stem cell gene expression on the transcription factors OCT4 and NANOG. Transcriptional activation of OCT4 is a key factor for inducing pluripotency from differentiated cells and its expression is essential to hPSC self-renewal.

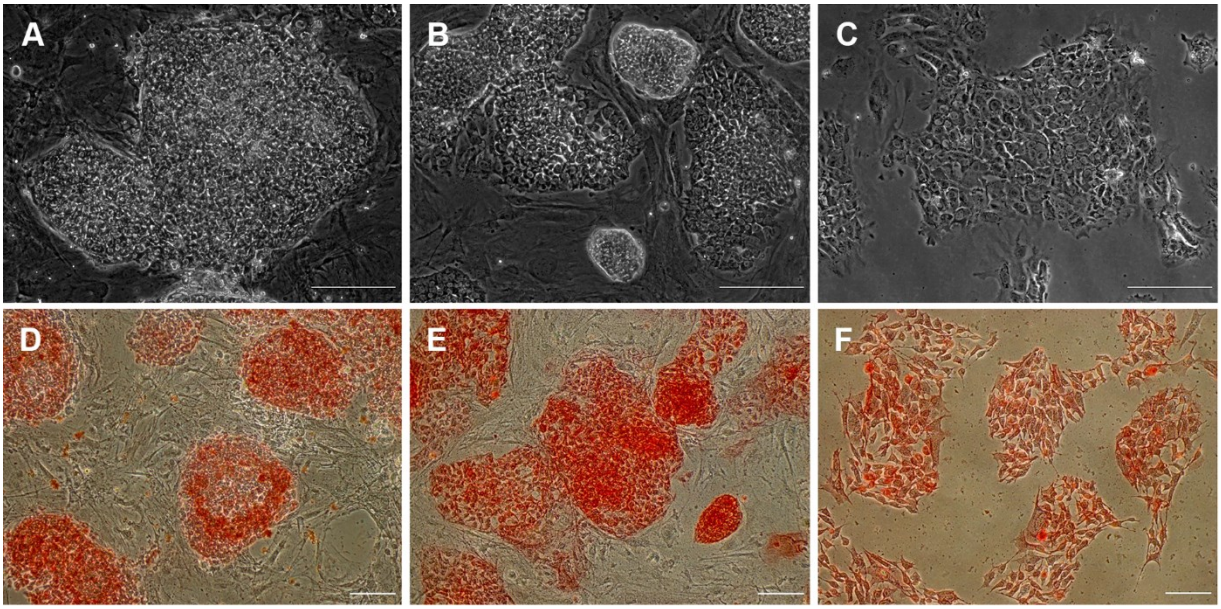

Figure 26. LIF based medium supports strong colony formation and alkaline phosphatase positive staining of hESCs on iMEFs and Matrigel™. Each line is positive for strong colony borders, cobblestone morphology, high nuclear to cytoplasmic ratio, and AP staining. BG01 (LIF) cultured on iMEFs (A, D). H9 (LIF) cultured on iMEFs (B, E). H9 (LIF) cultured on Matrigel™ with conditioned medium (C, F). Each line propagated for greater than 30 passages. Scale bars= 100µm.

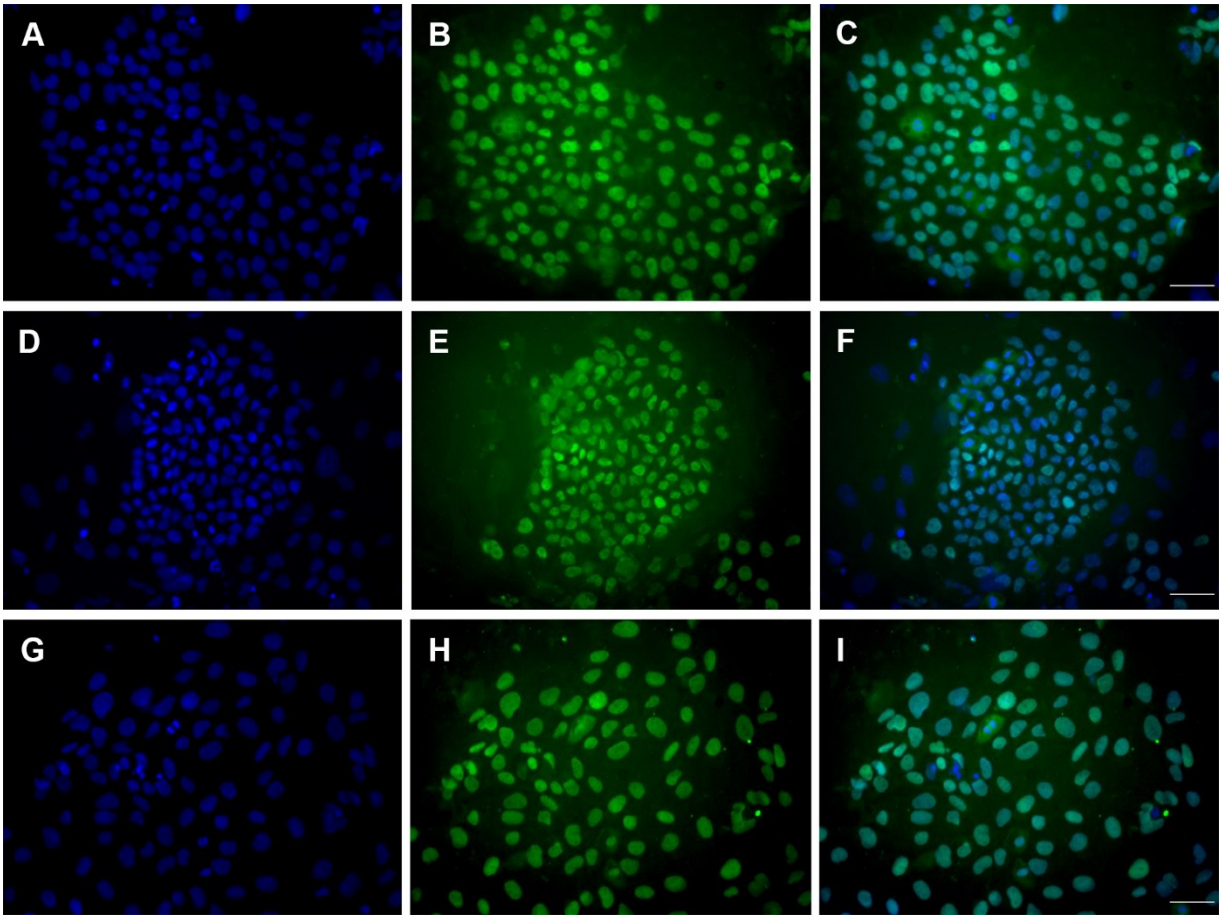

Figure 27. Positive OCT4 expression in hPSCs propagated in LIF+2i containing medium. Positive nuclear expression of the OCT4 transcription factor in lines BG01 (LIF) on iMEFs (A-C), H9 (LIF) on iMEFs (D-F), and H9 (LIF) on Matrigel™ (G-I). Each of the hPSC lines were propagated greater than 30 passages. DAPI- blue (A, D, G), OCT4- green (B, E, H), and DAPI/OCT4 nucleus overlay (C, F, I). Scale bar= 50 μm.

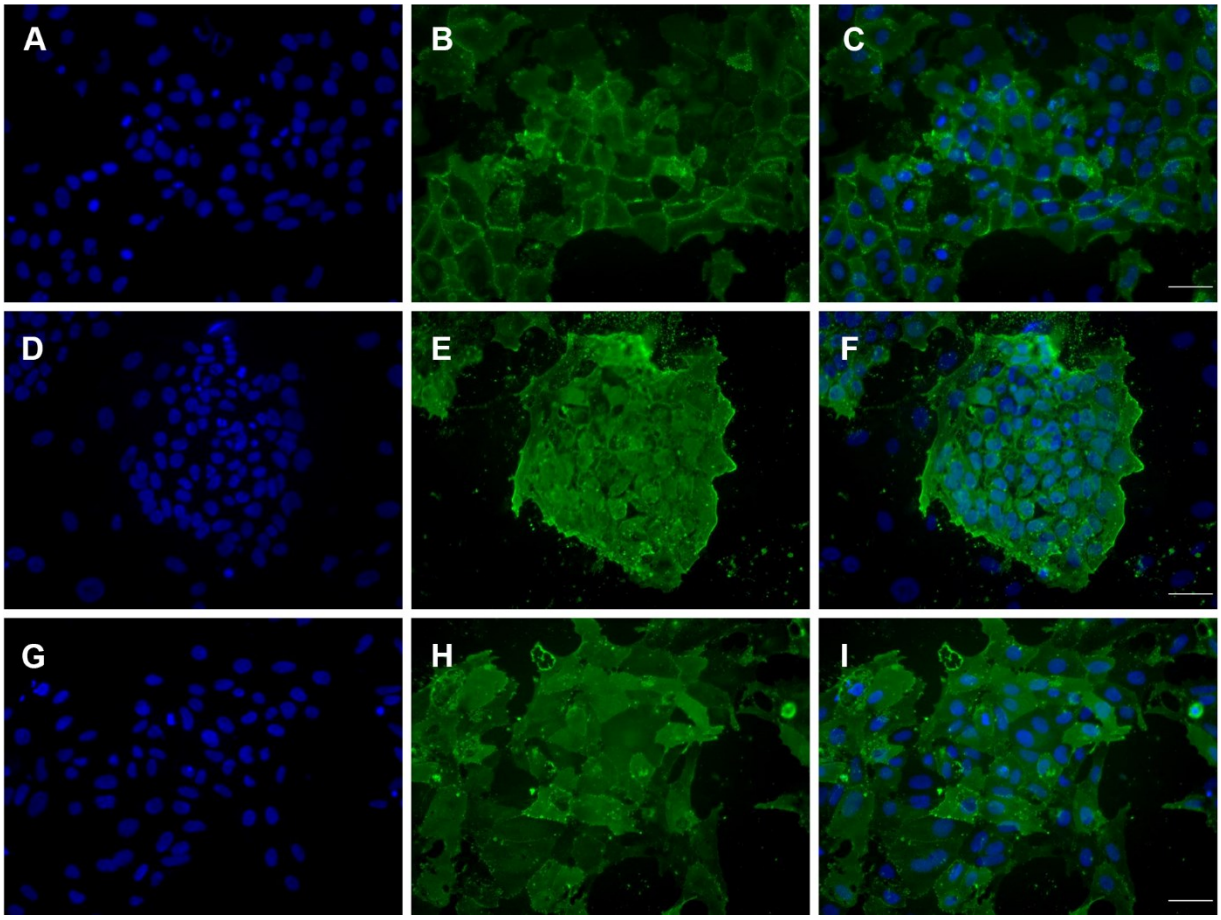

Figure 28. Positive SSEA4 expression in hPSCs propagated in LIF+2i containing medium. Positive cell- surface expression of the SSEA4 in lines BG01 (LIF) on iMEFs (A-C), H9 (LIF) on iMEFs (D-F), and H9 (LIF) on Matrigel™ (G-I). Each of the hPSC lines were propagated greater than 30 passages. DAPI- blue (A, D, G), OCT4- green (B, E, H), and DAPI/OCT4 nucleus overlay (C, F, I). Scale bar= 50 μm.

NANOG is a pluripotent specific marker that is critical in formation of epiblast from the ICM and is biallelically expressed in the ground- state [22]. To determine the maintenance of the self-renewal program, we compared H9 (LIF) sublines and BG01 (LIF) to H9 and BG01 lines cultured in bFGF medium and also to human dermal fibroblast (hDFs). H9 (LIF) RNA was isolated from samples that were cultured for greater than 20 passages and the BG01 (LIF) RNA samples, more than 30 passages.

Each of the H9 (LIF) and BG01 (LIF) lines were transcriptionally positive for OCT4 and NANOG. The fold change of NANOG in the hPSC (LIF + 2i) lines relative to hDFs ranged between 3k-5k fold increase. For OCT4, the samples grown on iMEFs, H9 (LIF) s.2, H9 (LIF) s.3, and BG01 (LIF) the fold change relative to hDFs ranged between 23-26 fold increase. The H9 (LIF) s.4 grown on Matrigel™ had a 6.1 fold change for OCT4 relative to hDFs (Figure 29 and Figure 30). For iMEF cultures, the hPSC (LIF + 2i) samples were greater than or equal to the respective hPSC (bFGF) samples for OCT4 and NANOG expression. Relative to the hPSC (bFGF) samples, OCT4 fold change increases for H9 (LIF) s.2, H9 (LIF) s.3, and BG01 (LIF) are 2.7, 2.9, and 1.8, respectively. Likewise, relative to the hPSC (bFGF) samples, NANOG fold change increases for H9 (LIF) s.2, H9 (LIF) s.3, and BG01 (LIF) are 1.0, 1.5, and 1.4, respectively. The H9 (LIF) s.4 line was positive for OCT4 and NANOG expression; however, OCT4 and NANOG expression decreased to 72% and 91% in the H9 (LIF) s.4 line relative to H9 (bFGF) samples (Figure 31 and Figure 32).

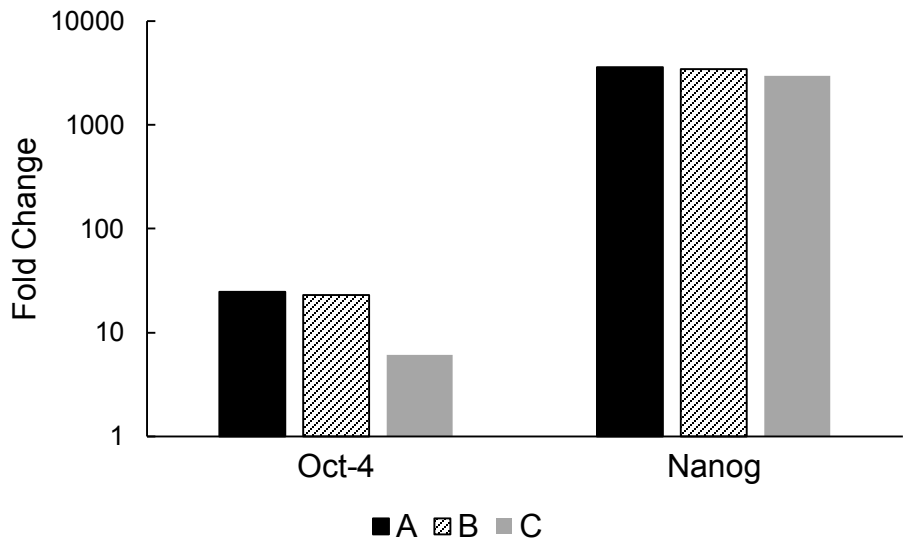

Figure 29: H9 (LIF) samples maintain high OCT4 and NANOG expression relative to human dermal fibroblasts. Three independent sublines of H9s were cultured in LIF + 2i containing medium: H9 (LIF) s.2 (A), H9 (LIF) s.3 (B), and H9 (LIF) s.4 (C). The fold change values are determined via the $\Delta\Delta C_T$ method using GAPDH as the reference gene. Fold change was calculated relative to hDFs. A, B, C have drastically increased NANOG expression relative to hDFs and significantly increased OCT4 expression relative to hDFs.

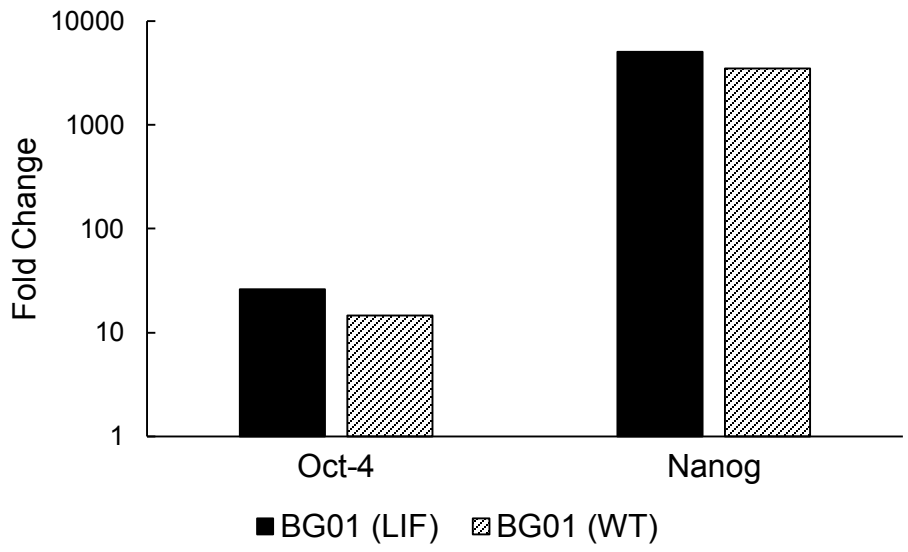

Figure 30: BG01 (LIF) samples maintain high OCT4 and NANOG expression relative to human dermal fibroblasts. BG01 (LIF) and BG01 (bFGF) were compared to hDFs. The fold change values are determined via the ΔC_T method using GAPDH as the reference gene. Fold change was calculated relative to hDFs. Both BG01 (LIF) and BG01 (bFGF) have similar increased OCT4 and NANOG expression relative to hDFs. BG01 (LIF) and BG01 (WT) were evaluated in triplicate, n=3, and the resultant geometric mean for each was used for determining the fold change.

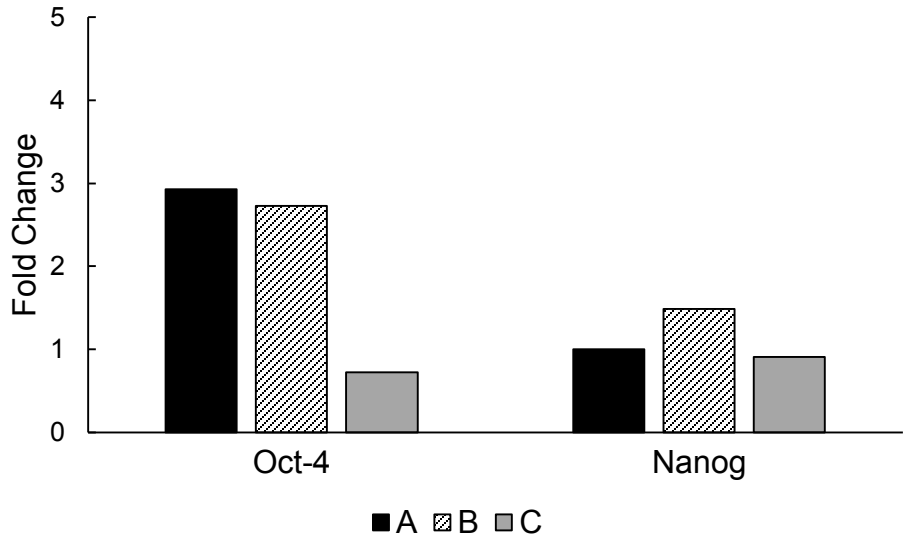

Figure 31: H9 (LIF) expresses OCT4 and NANOG at higher levels than H9 (bFGF). Three independent sublines of H9s were cultured in LIF + 2i containing medium: H9 (LIF) s.2 (A), H9 (LIF) s.3 (B), and H9 (LIF) s.4 (C). Fold change values are determined via the $\Delta\Delta C_T$ method using GAPDH as the reference gene. A and B have increased OCT4 expression relative to H9s propagated in bFGF containing hESC media. H9 (LIF) s.4 has comparable expression of OCT4 and NANOG as H9s propagated in bFGF containing hESC medium.

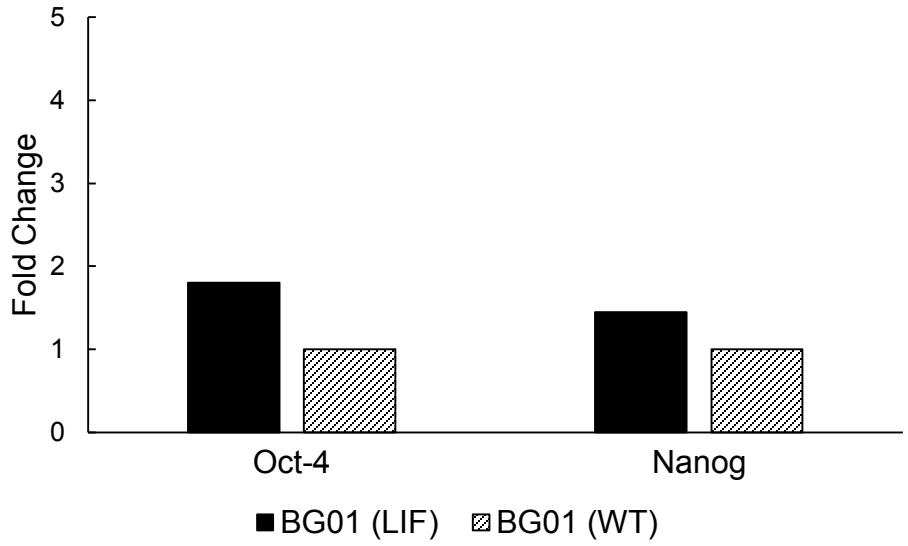

Figure 32: BG01 (LIF) expresses OCT4 and NANOG at higher levels than BG01 (bFGF). BG01 (LIF) was compared to BG01 samples propagated in bFGF containing hESC medium. The fold change values are determined via the ΔC_T method using GAPDH as the reference gene. BG01 (LIF) has increased OCT4 and NANOG expression relative to BG01s propagated in bFGF containing hESC medium. BG01 (LIF) and BG01 (WT) were evaluated in triplicate samples, n=3, and the resultant geometric mean for each line was used for determining the fold change.

hESC cultured in LIF + 2i conditions maintain in vitro differentiation capabilities.

Pluripotency is defined by self-renewal and the capacity to differentiate into each of the three germ layers, ectoderm, endoderm, and mesoderm. Having validated self-renewal, we sought to determine whether each of the three H9 (LIF) sublines propagated for at least 20 passages would demonstrate tri-lineage differentiation. EBs were formed via the hanging drop method from single- cells seeded at 5000 cells per drop. Interestingly, EB formation was aided by exposure to 10μM ROCK inhibitor (ROCKi) during the initial hanging drop step. On the H9 (LIF) s.4 subline maintained on Matrigel™, two consecutive attempts to form EBs without ROCKi exposure were unsuccessful in generating EBs. In the presence of ROCKi, more than twice the number of EB aggregates formed on the sublines, H9 (LIF) s.2 and H9 (LIF) s.3, compared to the same sublines without ROCKi exposure. A noticeable difference in EB morphology was observed between samples grown on iMEFs vs Matrigel™. EBs from H9 (LIF) s.4 were dense tight aggregates, with increased size-uniformity and spherical symmetry. However, the H9 (LIF) s.2 and H9 (LIF) s.3 EBs had cystic pockets, were lobular and non-uniform in size Figure 41.

For histopathological analysis, we analyzed 5 independent EB samples across two serial passages. Each samples consisted of 30-100 EB aggregates. The first sample set consisted only of H9 (LIF) s.2 and H9 (LIF) s.3 without ROCKi treatment. The subsequent sample set consisted of H9 (LIF) s.2, H9 (LIF) s.3, and H9 (LIF) s.4 exposed to ROCKi during the initial hanging drop step. All samples demonstrated differentiation and most of the samples exhibited each of the three germ layers. Endoderm was the least expressed germ layer and this could be attributed to insufficient duration in suspension culture of only 15 days. ROCKi exposure seems to have

influenced differentiation, as both samples without ROCKi treatment were less differentiated than the three samples with ROCKi treatment. ROCKi (-) samples exhibited the presence of neural rosettes, primitive connective mesenchyme, and cyst- like structures suggestive of endoderm. ROCKi (+) samples exhibited neural ectoderm, primitive mesenchyme, some muscle, and lined vascular formation indicative of endoderm (Figure 33).

Next we performed real- time qPCR analysis on the EBs that were generated from each of the three H9 (LIF) sublines. For analysis, we paired the expression data of OCT4 and NANOG between the H9 (LIF) sublines and their corresponding EB sample, EB s.2, EB s.3, EB s.4. Indeed, we observed significant down regulation of OCT4 and NANOG in each of the EBs samples, relative to their H9 (LIF) counterpart. The OCT4 fold change decrease is -205.3, -76.6, -10.3 for EB s.2, EB s.3, and EB s.4, respectively. The NANOG fold change decrease is -18.6, -6.2, and -6.2 for EB s.2, EB s.3, and EB s.4, respectively (Figure 34). Down- regulation of these pluripotency specific transcription factors suggests that our H9 (LIF) cultures maintained indefinite self- renewal, and upon prolonged propagation retained the capacity to differentiate. Figure 35 presents the results of our germ layer marker gene expression in our EB samples. Our germ- layer panel of 6 genes consisted of Nestin and SOX1 for ectoderm, IGF2 and brachyury (T) for mesoderm, and AFP and GATA-4 for endoderm. A difference was observed in the mRNA profile between the EBs generated from iMEF maintained cultures and the Matrigel™ maintained line. The fold change expression pattern in the iMEF maintained samples is consistent. Independently, EB s.2 and EB s.3 samples show up- regulation and down- regulation of the same germ- layer associated genes. In the EB s.2 and EB s.3 samples, AFP was drastically increased and GATA-4 was marginally increased. In the EB s.4 sample, 5 of the 6

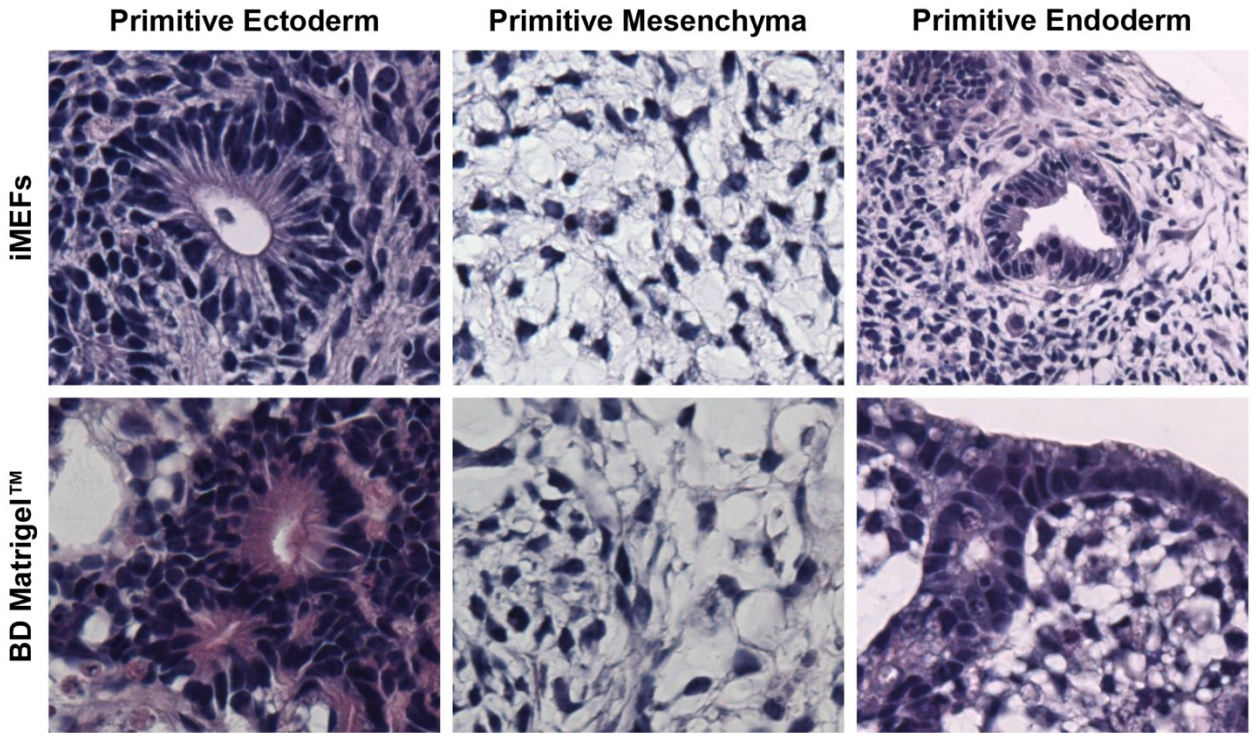

Figure 33. Histopathological evidence of germ- layer specification in embryoid bodies generated from hPSCs propagated in LIF + 2i conditions. Hematoxylin and eosin-stained histologic sections of EBs from H9s propagated in LIF + 2i containing hESC medium. Neural rosettes indicate primitive ectoderm (left). Primitive mesenchyma is present with connective tissue like structures (middle). Vascular and interior- lining like structures are observed that are suggestive of primitive endoderm (right). Magnification is 40x.

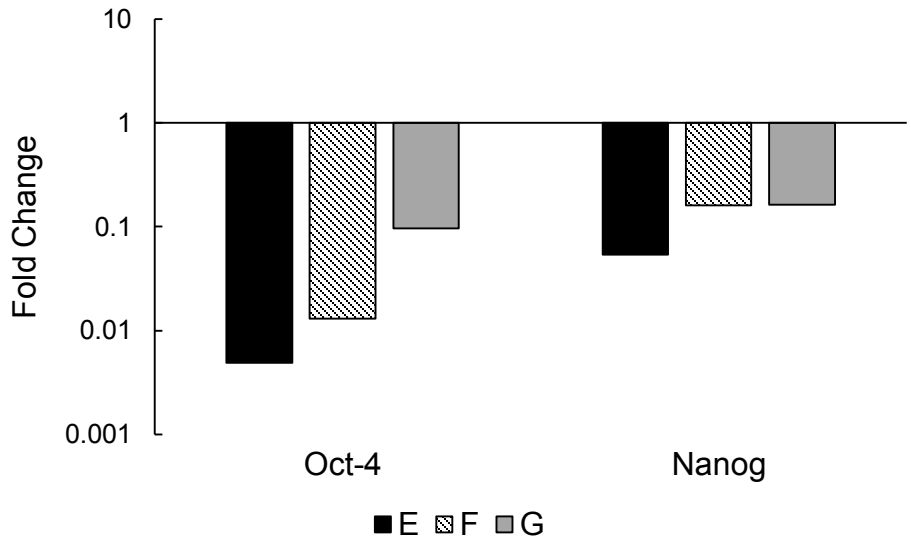

Figure 34: Embryoid bodies lose OCT4 and NANOG expression. Embryoid bodies were generated from each of the H9 (LIF) sublines. EB expression of OCT4 and NANOG relative to H9 (LIF) samples were markedly decreased. Fold change values are determined via the Livak $\Delta\Delta C_T$ method using GAPDH as the reference gene. Abbreviations: E- EB s.2 relative to H9 (LIF) s.2, F- EB s.3 relative to H9 (LIF) s.3, G- EB s.4 relative to H9 (LIF) s.4.

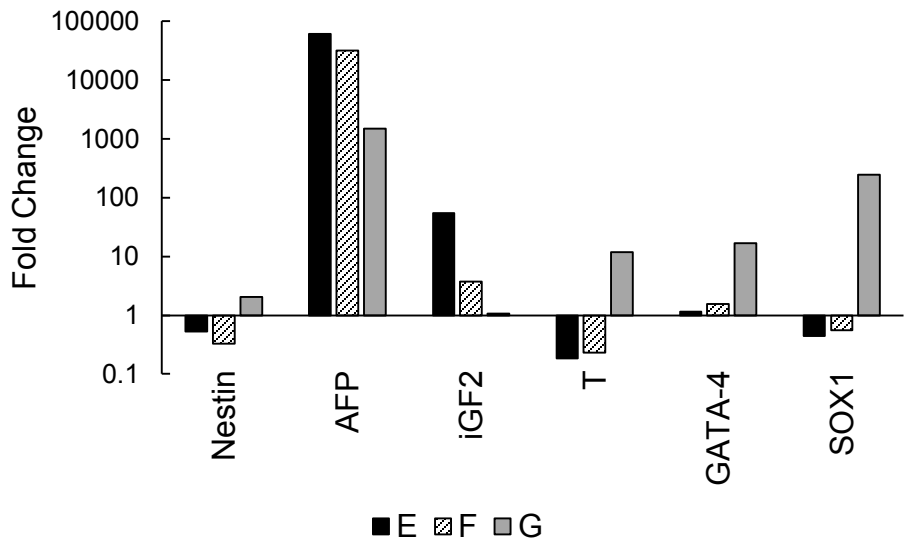

Figure 35: Embryoid bodies express germ- layer specific markers. Embryoid bodies were generated from each of the H9 (LIF) sublines. EB s.4 has an increase in 5 of 6 germ- layer associated genes. The EB s.2 and EB s.3 samples show a demonstrative increase in AFP expression and a marginal increase in GATA-4 expression. Fold change values are determined via the Livak $\Delta\Delta C_T$ method using GAPDH as the reference gene. Abbreviations: E- EB s.2 relative to H9 (LIF) s.2, F- EB s.3 relative to H9 (LIF) s.3, G- EB s.4 relative to H9 (LIF) s.4.

germ- layer genes demonstrated an increase in expression. IGF2 was at the limits of positive detection with a CT value of 38.32. Therefore, IGF2 could be viewed as absent in both H9 (LIF) s.4 and EB s.4 samples. The expression of endodermal lineage marker AFP is remarkable. In all three EB cultures, AFP transcript levels is strikingly increased. Taken together, this data suggest LIF + 2i conditions support pluripotency and that hPSC (LIF) lines self- renew indefinitely and maintain tri-lineage differentiation capacity.

Human PSCs grown in LIF + 2i culture exhibit substrate dependent centrosome stability

Compared to genotyping, indirect measures on genomic instability, such as centrosome error analysis, have the distinct benefit of being able to assess culture stress at each passage prior to selection bias of genomic variants. In contrast, techniques such as karyotyping can require months before a genomic aberration can be detected. Prior data from our lab and others has identified the prominence of supernumerary centrosomes in hESC culture suggesting that centrosomes should be monitored when testing new culture conditions [175]. We initially established that the H9 line, propagated in bFGF conditions, has a relatively low centrosome error rate of approximately 4%. Therefore, the H9 line was chosen for the centrosome error analysis on LIF + 2i conditions between iMEFs and Matrigel™. The H9 (LIF) s.2 and H9 (LIF) s.3 sublines maintained on iMEFs were compared to the H9 (LIF) s.4 line propagated on BD Matrigel™. Each subline was assessed in triplicate across two passages. The H9 (LIF) s.4 subline had been in LIF + 2i containing media for 15 and 25 passages and the total passage count was passages 65 and 75. The H9 (LIF) sublines maintained on iMEFs had an average centrosome error rate of 3.51% (+/- 1.17). However the H9 (LIF) s.4 line maintained on BD Matrigel™ has

an average percentage centrosome errors of 10.76% (+/- 1.84), with the centrosome error increase found to be statistically significant ($p < 0.01$) (Figure 36).

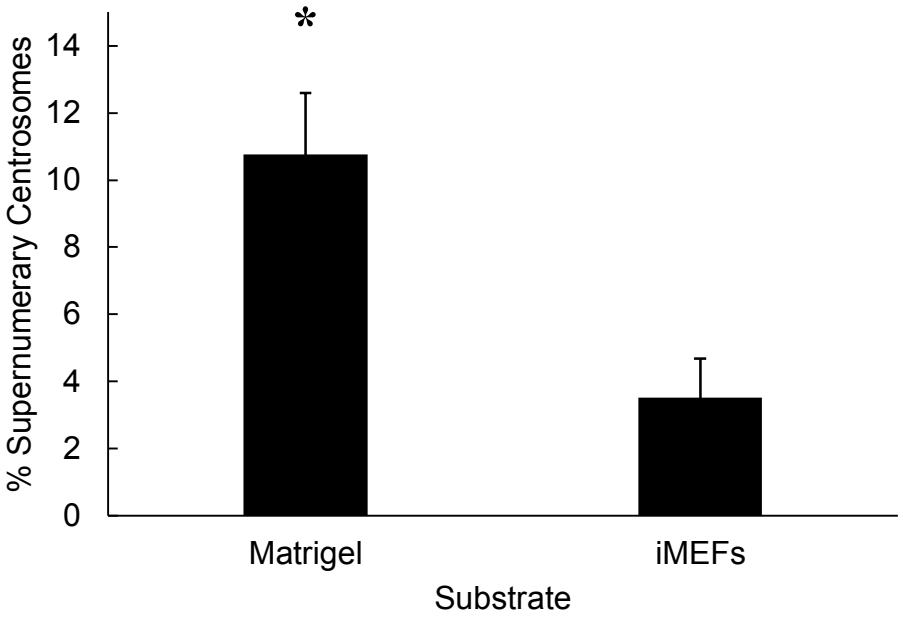

Figure 36. Increased supernumerary centrosomes in H9 (LIF) propagated on Matrigel™. H9 (LIF) samples maintained on BD Matrigel™ demonstrate a significantly increased number of supernumerary centrosomes compared to lines maintained on iMEFs. (*) indicates p-value < 0.01.

DISCUSSION AND CONCLUSIONS

In this study, we were able to demonstrate the long- term self- renewal of hPSCs in a low complexity LIF + 2i medium, devoid of bFGF. Use of MEKi is notable, since it has been used to culture ground state naïve mPSCs. This LIF + 2i formulation contained p38i, instead of GSK3β, as suggested by Xu and colleagues, and merited further characterization of self- renewal and differentiation in these LIF-response hPSC cukture conditions [112]. The hPSC (LIF) cultures were maintained for greater than 30 passages and were positive for all markers associated with self- renewal. Notably in our hPSC (LIF) lines, maintained on iMEFs, OCT4 and NANOG had increased expression relative to hPSC (bFGF) samples. In hPSCs, NANOG is a target of SMAD 2/3 induced by bFGF, therefore the sustained and high expression of NANOG in our lines in the absence of bFGF is strongly supportive of a distinct self- renewal program supported by LIF + 2i. The presence of LIF- responsive hPSC is highly indicative that a ground state for hPSCs exists [24, 25]. It will be interesting to explore the distribution of NANOG positive- cells in order to determine if the LIF+2i culture condition increases homogeneity of NANOG- high expressors and influences the allelic expression of NANOG, as has been reported for the ground state of mPSCs [22, 26].

LIF + 2i medium formulations supported survival and proliferation of hPSCs. The initial single- cell passaging in LIF conditions was more robust than in bFGF conditions, which is consistent with prior reports that culture converted naïve hPSCs have increased clonal yields [20]. However, in subsequent transitory passages, yields decreased and then cultures were stably and robustly maintained. This is possibly due to significant differentiation of the H9 cells upon

LIF + 2i exposure, where a subpopulation of convertible hPSCs were able to emerge and be established as stable robust self- renewing LIF+ 2i dependent hPSCs. Since these cells are likely clonal, then these converted cells are more likely to pass on the LIF+2i responsive phenotype to their progeny. In contrast to the single- cell culture, differentiation was persistent in the BG01 (LIF) manually passaged lines. However, upon transition to enzymatic dissociation, BG01 (LIF) culture homogeneity significantly improved, minimal morphological differentiation was observed, and the BG01 LIF + 2i gained stable robust gene expression. The benefit of single- cell dissociation for LIF + 2i hPSCs is unclear at this time. However, in single- cell culture the selection process is on clonal cells, a phenotype more suited for naïve pluripotency. Additionally, since E-cadherin is turned over during single- cell dissociation and E-cadherin and WNT signaling are tightly coupled, single- cell dissociation may perturb GSK3β and β- catenin signaling. Given that GSK3i is used to establish the ground state of mPSCs, then there exists the possibility of pro- survival WNT signaling upon dissociation of hPSCs (LIF + 2i) passaged as single- cells. Histopathological analysis of EBs confirmed the expression of each of the three germ layers. However it is noticeable that the addition of ROCKi improved EB yields and increased the level of differentiation. Additionally, EBs generated from hPSCs propagated on Matrigel™ were denser and more symmetrical, thus in generating EBs, BD Matrigel™ seems preferable to iMEFs.

Although the real time PCR analysis yielded mixed results across different genes, consistent patterns existed indicating that the results contain information of biological relevance. Perhaps the dominant factor in lack of robust differentiation in the short EB culture time of 15 days could be a factor, given that EBs are often cultured for 20 days or more. Another

consideration is to choose a better primer selection for genes more indicative of the naïve pluripotent state. AFP is an extraembryonic endoderm marker expressed in the cells supporting the epiblast cells and is typically not robustly in differentiated hPSCs that should have definitive endoderm. In our studies, we observed strong up-regulation of AFP and since AFP is a marker of early development at the pre-implantation stage, this is promising and suggests the need to screen additional genes for their expression in EBs obtained from hPSCs propagated in LIF + 2i conditions. Another interpretation of the EB QPCR data is that the hPSCs propagated under LIF +2i conditions maintained robust stem cell self- renewal but had difficulty in readily differentiating in the timeframe provided. A similar result was observed by Buecker and colleagues, where their HLR5 hPSC (LIF) line maintained self- renewal but lost differentiation capacity [30].

Notably, the LIF + 2i conditions that were used in this study did not utilize the same inhibitors published for the murine ground state culture conditions [29]. Instead of using GSK3βi, we used p38i as recommended by Xu and colleagues. Recently, Ware and colleagues demonstrated that naive hPSC lines can be derived in LIF + 2i conditions (GSK3-β) and suggest using a reverse toggling with HDAC inhibitors first, followed by FGF+ 2i. However, in our LIF + 2i (p38i) cocktail this "toggling" did not seem necessary. Hanna and colleagues, recently published the use of 2i/LIF, p38i, JNKi together with FGF2 and TGF-Beta1 to culture human iPSCs in a converted naïve pluripotent state [20]. Their group's similar use of p38i is notable; however, their formulation is complex and strikingly combines the use of LIF and bFGF.

In conclusion, the LIF + 2i medium used in this study is a simple formulation that was found to be successful in maintaining self- renewing hPSCs. Gene expression analysis indicate that the EBs from the H9 (LIF) s.4 line were differentiating with an observable upregulation in five of the six genes, indicating tri-lineage differentiation potential. Studies on use of this culture condition for ascertaining core difference between hPSCs in their naïve and primed state is now feasible.

CHAPTER 4

Conclusions and Future Directions

Numerous studies have shown that RHO signaling pathway has a critical role for PSCs in survival and essential roles in cellular proliferation, differentiation, and migration [109, 194, 201]. Data from our laboratory is consistent with the requirement of RHO signaling for maintenance of cell-cell contact in cohesive hPSC colonies through ROCK and pMLC activation of myosin II [188]. We have observed that small molecule inhibition of ROCK, by Y27632, demonstrates reversible inhibition of cell-cell contact by F-actin staining, (Figure 42), that does not appear to adversely influence self- renewal. ROCKi inhibitors are routinely used by labs for the culture of hPSCs to increase survival, particularly during single- cell plating. However, the consequences of ROCKi exposure in hPSC culture is unknown, and undesirable side- affects are suspected, such as an increase in genomically abnormal hPSCs; as, ROCKi may have anti-apoptotic side- effects that would allow the persistence of variant hPSCs, since apoptosis in hPSCs is an integral mechanism in preserving genetic integrity [153, 202]. Additionally, RHO-ROCK signaling has essential roles in mitosis during centrosome separation and cytokinesis [203-205]. Thus, concerns for routine use of ROCKi in hPSC cultures seems warranted. Therefore, alternative approaches to using ROCKi for increasing the viability of hPSCs during propagation and scale- up is a significant and unmet challenge in the field.

Recently, the molecular pathway responsible for the pluripotent state dependency of dissociation-induced apoptosis was elucidated [76]. Ohgushi and colleagues demonstrate that RHO signaling activation upon loss of e-cadherin based cell-cell contact is different between naïve and primed PSCs. Upon loss of e-cadherin-dependent intercellular contact, primed PSCs are characterized by a high amount of active RHOA and low amount of active RAC1. Thus, primed PSCs activate ROCK induced blebbing and cell death upon dissociation. Conversely,

naïve PSCs are characterized by low active RHOA and high active RAC1 state and do not exhibit the same pathway induced cell death. Further demonstrated, by this group, is the dependency of ROCK activation on the chromosome 17 located gene, active BCR-related gene (ABR). However, expression of ABR is positively correlated with ROCK activation and inversely with RAC1 activation; therefore, a trisomy 17 overexpression is not consistent with ABR as a functional candidate gene for selective advantage. They propose an upstream epiblast state linked regulator that is an effector of both RHOA and RAC1 activation upon loss of E-cadherin based cell- cell contact [76]. Xu and colleagues show RHO signaling is regulated by E-cadherin based cell- cell contact and that naïve and primed PSCs have differential e-cadherin turnover kinetics upon dissociation. MPSCs (???) have decreased intracellular cycling times and cell surface re-expression of E-cadherin upon dissociation, conferring robust clonality to naïve PSCs. Additionally, TZV, a ROCK inhibitor, was shown to increase stability of E-cadherin expression upon dissociation induced turnover, suggesting an E-cadherin based mechanism to this small molecule rather than by ROCK inhibition alone [45].

ARHGDIA is a RHO- GDP dissociation inhibitor that inhibits activation of members of the RAS superfamily of G- proteins by preventing the exchange of GDP for GTP, thereby fixing the inactive GDP bound state. ARHGDIA binds RHOA with high affinity and a long half- life [206], as well as RAC1. Differential phosphorylation states for ARHGDIA and protein expression levels have been proposed as mechanisms in regulation of RHO signaling [207]. ARHGDIA's capacity to act on both RHOA and RAC1 is intriguing when considering a molecular state associated with dissociation induced apoptosis. It has been shown that p21-activated kinase (PAK1) phosphorylates ARHGDIA at serine 101 and serine 174 and in this

particular state, ARHGDIA p101/174, tightly binds RHOA, stabilizing RHO- GDP inactive state and dissociates from RAC1, allowing RAC1- GTP active state [208]. Also, Elfenbein and colleagues have shown in HeLa cells that bFGF affects RHO signaling through phosphorylation of ARHGDIA at serine 96 [209]. Therefore, we hypothesize that differential action of the cytokines LIF and bFGF could influence the phosphorylation of ARHGDIA; thereby, affecting naïve vs primed pluripotency via RHO signaling through differential regulation of the active RHOA and RAC1 states. In future studies, we propose using mass spectrometry to profile the phosphorylation states of ARHGDIA in hPSC culture, and in particular between our established LIF-dependent hPSC and bFGF-dependent hPSC lines.

In our work, we observed the sufficiency of ARHGDIA overexpression to increase single- cell survival and confer selective advantage in co-cultures with normal hPSCs. Our preliminary data suggests that ARHGDIA overexpression is sufficient to reduce RHOA- GTP levels (Figure 42). In trypsin dissociated H9 hPSCs, we observed reduced RHOA- GTP levels in H9 (Arg) hPSCs relative to H9 (GFP) hPSCs. Initial samples were used to determine maximal levels of RHOA- GTP in time series from 0- 30 minutes post- dissociation and plating. Building on technical establishment of this assay in our laboratory, future studies will monitor both RHOA- GTP and RAC1- GTP levels in dissociated hPSCs across ARHGDIA expression levels and cytokine support.

The known biological roles for ARHGDIA are in the context of its action on RHO GTPases; as such, ARHGDIA is a potential potent effector of cell- ECM adhesion, cell- cell adhesion, and differentiation [207]. Indeed, we observed a pronounced morphological affect in

our H9 hPSC line upon ARHGDIA overexpression. True hPSC clonal survival vs hPSC migration promoted cell- cell contact have been established as independent mechanisms leading to increased hPSC survival under single- cell plating [64]. ROCKi, Y27632, significantly increases migration of hPSCs and could help explain its pro-survival affects for single- cells [194]. The LN- 521 substrate has been demonstrated to promote single- cell survival through migration; however, LN- 521 is insufficient to increase clonal survival. Recently, a LN-521/E-cadherin defined matrix was demonstrated to support clonal propagation of hPSCs in absence of migration [64]. In contrast to Y27632's null effect on E-cadherin, the small molecule, TZV, increases stability of E-cadherin expression upon dissociation, suggesting an independent mechanism involving E-cadherin based hPSC clonal survival. Active RAC1 has been shown to positively influence E-cadherin cell adhesion strength in complex with IQGAP1 and β– catenin [210]. When staining for F-actin, ARHGDIA overexpression did not induce the same morphological influence as cells exposed to Y27632 (Figure 42A). The low seeding density of 100 cells/cm^2 on iMEFs is suggestive that ARHGDIA overexpression impacted clonality rather than by migration induced cell- cell contact. Further studies will look at the mechanisms by which ARHGDIA overexpression confers selective advantage. In particular, the level of active ROCK and phosphorylated MLC will be quantitated across ARHGDIA expression levels and phosphorylation states. Initial results suggest, that upon dissociation, RHOA activation in ARHGDIA overexpressing lines is less compared to control lines (Figure 43). The impact of ARHGDIA expression on actin myosin contractile induced blebbing and on migration will also be determined. Preliminary data from our laboratory demonstrates that turnover of E-cadherin after trypsin digestion is linear (Figure 44) and that a positive correlation between ARHGDIA expression and E-cadherin may exist (Figure 45 and Figure 46). A similar analysis, with TZV as

a control, will be performed to determine whether increased ARHGDIA expression stabilizes E-cadherin expression reducing the turnover time after dissociation.

Reducing selective pressure for phenotypic advantage has been suggested as one approach to reducing the rate of culture- induced genomic adaptation [200]. Anecdotal cases are now emerging suggesting the impact of approaches improving clonality on reducing genomic alterations in hPSC culture**.** Ware and colleagues compared their naïve- converted hPSC line against a primed hPSC line. The naïve H1 hPSC line passaged by trypsin as single cells had a normal karyotype at passage 93, while the companion primed H1 hPSC line had acquired trisomy 12 and 17 [37]. Culture time to genomic alterations is highly variable and can easily take months to observe, posing significant challenges to rigorous analysis of culture conditions influencing selection of hPSC genomic variants. With the functional validation of ARHGDIA conferring selective advantage and the development of our defined genetically engineered hPSC lines, H9 (Arg) and BG01 (Arg), culture conditions can now be varied to assess influence of selection forces.

The consequence of pluripotent state and dissociation induced apoptosis on scale- up is significant. In one week, mPSCs with higher clonal survival and reduced cell cycle time [46], can be expanded at two orders of magnitude greater than hPSCs, at 1000- fold for mPSCs compared to 10 fold for hPSCs [43]. Additionally, with enzymatic passaging inducing a 2 fold increase in genomic instability, improved culture for genomically stable propagation and scale-up is a pressing concern for research labs and industry when billions of cells are needed per application [176]. The ground state of pluripotency is an attractive candidate for culture

conditions improving stable propagation of genomically normal hPSCs and has several distinct benefits compared to culture conditions developed for primed hPSCs. The ground state is comprised of normal hPSCs that are clonal and have faster cell cycle times than primed hPSCs, thereby implying that variants hPSCs will have a much steeper climb to gaining selective advantage. Establishing the ground state in hPSCs may also have a significant biological advantage for stable propagation by providing the most pristine pluripotent cells devoid of selection, lineage bias, and as a pre- genomic self- correction *in vivo* analog. However with the essential role of WNT signaling, GSK3β and β-catenin, in maintaining the integrity of centrosomes and chromosome segregation during mitosis, the debate between mutation and selection is likely to remain unresolved, even as hPSC culture moves towards ground state establishment for generation of genomically stable hPSCs for use in future regenerative biomedical therapies.

Bibliography

1. Thomson, J.A., et al., *Embryonic stem cell lines derived from human blastocysts.* Science, 1998. **282**(5391): p. 1145-7.
2. Tannenbaum, S.E., et al., *Derivation of xeno-free and GMP-grade human embryonic stem cells--platforms for future clinical applications.* PloS one, 2012. **7**(6): p. e35325.
3. Ausubel, L.J., P.M. Lopez, and L.A. Couture, *GMP scale-up and banking of pluripotent stem cells for cellular therapy applications.* Methods in molecular biology, 2011. **767**: p. 147-59.
4. Okano, H. and S. Yamanaka, *iPS cell technologies: significance and applications to CNS regeneration and disease.* Molecular brain, 2014. **7**(1): p. 22.
5. Kuijk, E.W., et al., *The different shades of mammalian pluripotent stem cells.* Human reproduction update, 2011. **17**(2): p. 254-71.
6. Thomson, J.A., *Embryonic Stem Cell Lines Derived from Human Blastocysts.* Science, 1998. **282**(5391): p. 1145-1147.
7. Shamblott, M.J., et al., *Derivation of pluripotent stem cells from cultured human primordial germ cells.* Proceedings of the National Academy of Sciences of the United States of America, 1998. **95**(23): p. 13726-31.
8. Andrews, P.W., et al., *Pluripotent embryonal carcinoma clones derived from the human teratocarcinoma cell line Tera-2. Differentiation in vivo and in vitro.* Laboratory investigation; a journal of technical methods and pathology, 1984. **50**(2): p. 147-62.
9. Takahashi, K., et al., *Induction of pluripotent stem cells from adult human fibroblasts by defined factors.* Cell, 2007. **131**(5): p. 861-72.
10. Tachibana, M., et al., *Human embryonic stem cells derived by somatic cell nuclear transfer.* Cell, 2013. **153**(6): p. 1228-38.
11. Andrews, P.W., et al., *Cell-surface antigens of a clonal human embryonal carcinoma cell line: morphological and antigenic differentiation in culture.* International journal of cancer. Journal international du cancer, 1982. **29**(5): p. 523-31.
12. Sheridan, S.D., V. Surampudi, and R.R. Rao, *Analysis of embryoid bodies derived from human induced pluripotent stem cells as a means to assess pluripotency.* Stem cells international, 2012. **2012**: p. 738910.
13. Brennand, K., et al., *Phenotypic differences in hiPSC NPCs derived from patients with schizophrenia.* Molecular psychiatry, 2014.
14. O'Connor, M.D., et al., *Alkaline phosphatase-positive colony formation is a sensitive, specific, and quantitative indicator of undifferentiated human embryonic stem cells.* Stem cells, 2008. **26**(5): p. 1109-16.
15. O'Connor, M.D., M.D. Kardel, and C.J. Eaves, *Functional assays for human embryonic stem cell pluripotency.* Methods in molecular biology, 2011. **690**: p. 67-80.
16. Buta, C., et al., *Reconsidering pluripotency tests: do we still need teratoma assays?* Stem cell research, 2013. **11**(1): p. 552-62.
17. Razak, S.R., et al., *Profiling of microRNA in human and mouse ES and iPS cells reveals overlapping but distinct microRNA expression patterns.* PloS one, 2013. **8**(9): p. e73532.
18. Rao, M., *Conserved and divergent paths that regulate self-renewal in mouse and human embryonic stem cells.* Developmental biology, 2004. **275**(2): p. 269-86.
19. Bernemann, C., et al., *Distinct developmental ground states of epiblast stem cell lines determine different pluripotency features.* Stem cells, 2011. **29**(10): p. 1496-503.

20. Gafni, O., et al., *Derivation of novel human ground state naive pluripotent stem cells.* Nature, 2013. **504**(7479): p. 282-6.
21. Jouneau, A., et al., *Naive and primed murine pluripotent stem cells have distinct miRNA expression profiles.* RNA, 2012. **18**(2): p. 253-64.
22. Miyanari, Y. and M.E. Torres-Padilla, *Control of ground-state pluripotency by allelic regulation of Nanog.* Nature, 2012. **483**(7390): p. 470-3.
23. Nichols, J., et al., *Suppression of Erk signalling promotes ground state pluripotency in the mouse embryo.* Development, 2009. **136**(19): p. 3215-22.
24. Nichols, J. and A. Smith, *Naive and primed pluripotent states.* Cell stem cell, 2009. **4**(6): p. 487-92.
25. Nichols, J. and A. Smith, *Pluripotency in the embryo and in culture.* Cold Spring Harbor perspectives in biology, 2012. **4**(8): p. a008128.
26. Silva, J., et al., *Nanog is the gateway to the pluripotent ground state.* Cell, 2009. **138**(4): p. 722-37.
27. Silva, J. and A. Smith, *Capturing pluripotency.* Cell, 2008. **132**(4): p. 532-6.
28. Wray, J., T. Kalkan, and A.G. Smith, *The ground state of pluripotency.* Biochemical Society transactions, 2010. **38**(4): p. 1027-32.
29. Ying, Q.L., et al., *The ground state of embryonic stem cell self-renewal.* Nature, 2008. **453**(7194): p. 519-23.
30. Buecker, C. and N. Geijsen, *Different flavors of pluripotency, molecular mechanisms, and practical implications.* Cell stem cell, 2010. **7**(5): p. 559-64.
31. De Los Angeles, A., et al., *Accessing naive human pluripotency.* Current opinion in genetics & development, 2012. **22**(3): p. 272-82.
32. Gu, Q., et al., *Rapid conversion of human ESCs into mouse ESC-like pluripotent state by optimizing culture conditions.* Protein & cell, 2012. **3**(1): p. 71-9.
33. Hassani, S.N., et al., *Signaling roadmap modulating naive and primed pluripotency.* Stem cells and development, 2014. **23**(3): p. 193-208.
34. Gardner, R.L. and R.S. Beddington, *Multi-lineage 'stem' cells in the mammalian embryo.* Journal of cell science. Supplement, 1988. **10**: p. 11-27.
35. Bhatia, S., et al., *Demarcation of stable subpopulations within the pluripotent hESC compartment.* PloS one, 2013. **8**(2): p. e57276.
36. Hanna, J., et al., *Human embryonic stem cells with biological and epigenetic characteristics similar to those of mouse ESCs.* Proceedings of the National Academy of Sciences of the United States of America, 2010. **107**(20): p. 9222-7.
37. Ware, C.B., et al., *Derivation of naive human embryonic stem cells.* Proceedings of the National Academy of Sciences of the United States of America, 2014. **111**(12): p. 4484-9.
38. Brons, I.G., et al., *Derivation of pluripotent epiblast stem cells from mammalian embryos.* Nature, 2007. **448**(7150): p. 191-5.
39. Tesar, P.J., et al., *New cell lines from mouse epiblast share defining features with human embryonic stem cells.* Nature, 2007. **448**(7150): p. 196-9.
40. Nichols, J. and A. Smith, *The origin and identity of embryonic stem cells.* Development, 2011. **138**(1): p. 3-8.
41. Greber, B., et al., *Conserved and divergent roles of FGF signaling in mouse epiblast stem cells and human embryonic stem cells.* Cell stem cell, 2010. **6**(3): p. 215-26.
42. Niwa, H., *Mechanisms of Stem Cell Self-Renewal.* 2014: p. 81-94.

43. Hasegawa, K., et al., *A method for the selection of human embryonic stem cell sublines with high replating efficiency after single-cell dissociation.* Stem cells, 2006. **24**(12): p. 2649-60.
44. Becker, K.A., et al., *Self-renewal of human embryonic stem cells is supported by a shortened G1 cell cycle phase.* Journal of cellular physiology, 2006. **209**(3): p. 883-93.
45. Xu, Y., et al., *Revealing a core signaling regulatory mechanism for pluripotent stem cell survival and self-renewal by small molecules.* Proceedings of the National Academy of Sciences of the United States of America, 2010. **107**(18): p. 8129-34.
46. Coronado, D., et al., *A short G1 phase is an intrinsic determinant of naive embryonic stem cell pluripotency.* Stem cell research, 2013. **10**(1): p. 118-31.
47. Mehta, A., et al., *Intrinsic properties and external factors determine the differentiation bias of human embryonic stem cell lines.* Cell biology international, 2010. **34**(10): p. 1021-31.
48. Tavakoli, T., et al., *Self-renewal and differentiation capabilities are variable between human embryonic stem cell lines I3, I6 and BG01V.* BMC Cell Biol, 2009. **10**: p. 44.
49. Cahan, P. and G.Q. Daley, *Origins and implications of pluripotent stem cell variability and heterogeneity.* Nature reviews. Molecular cell biology, 2013. **14**(6): p. 357-68.
50. Honda, A., et al., *Naive-like conversion overcomes the limited differentiation capacity of induced pluripotent stem cells.* The Journal of biological chemistry, 2013. **288**(36): p. 26157-66.
51. Buecker, C., et al., *A murine ESC-like state facilitates transgenesis and homologous recombination in human pluripotent stem cells.* Cell stem cell, 2010. **6**(6): p. 535-46.
52. Kitajima, H. and H. Niwa, *Clonal expansion of human pluripotent stem cells on gelatin-coated surface.* Biochemical and biophysical research communications, 2010. **396**(4): p. 933-8.
53. Chambers, I., et al., *Functional expression cloning of Nanog, a pluripotency sustaining factor in embryonic stem cells.* Cell, 2003. **113**(5): p. 643-55.
54. Niwa, H., et al., *A parallel circuit of LIF signalling pathways maintains pluripotency of mouse ES cells.* Nature, 2009. **460**(7251): p. 118-22.
55. Mitsui, K., et al., *The homeoprotein Nanog is required for maintenance of pluripotency in mouse epiblast and ES cells.* Cell, 2003. **113**(5): p. 631-42.
56. Hambiliki, F., et al., *Co-localization of NANOG and OCT4 in human pre-implantation embryos and in human embryonic stem cells.* Journal of assisted reproduction and genetics, 2012. **29**(10): p. 1021-8.
57. Blair, K., J. Wray, and A. Smith, *The liberation of embryonic stem cells.* PLoS genetics, 2011. **7**(4): p. e1002019.
58. Tamm, C., S. Pijuan Galito, and C. Anneren, *A comparative study of protocols for mouse embryonic stem cell culturing.* PloS one, 2013. **8**(12): p. e81156.
59. Evans, M.J. and M.H. Kaufman, *Establishment in culture of pluripotential cells from mouse embryos.* Nature, 1981. **292**(5819): p. 154-6.
60. Smith, A.G., et al., *Inhibition of pluripotential embryonic stem cell differentiation by purified polypeptides.* Nature, 1988. **336**(6200): p. 688-90.
61. Ying, Q.L., et al., *BMP induction of Id proteins suppresses differentiation and sustains embryonic stem cell self-renewal in collaboration with STAT3.* Cell, 2003. **115**(3): p. 281-92.

62. Ying, Q.L. and A.G. Smith, *Defined conditions for neural commitment and differentiation.* Methods in enzymology, 2003. **365**: p. 327-41.
63. Lei, Y. and D.V. Schaffer, *A fully defined and scalable 3D culture system for human pluripotent stem cell expansion and differentiation.* Proceedings of the National Academy of Sciences of the United States of America, 2013. **110**(52): p. E5039-48.
64. Rodin, S., et al., *Clonal culturing of human embryonic stem cells on laminin-521/E-cadherin matrix in defined and xeno-free environment.* Nature communications, 2014. **5**: p. 3195.
65. Silva, J., et al., *Promotion of reprogramming to ground state pluripotency by signal inhibition.* PLoS biology, 2008. **6**(10): p. e253.
66. Anton, R., H.A. Kestler, and M. Kuhl, *Beta-catenin signaling contributes to stemness and regulates early differentiation in murine embryonic stem cells.* FEBS letters, 2007. **581**(27): p. 5247-54.
67. Gardner, R.L. and F.A. Brook, *Reflections on the biology of embryonic stem (ES) cells.* The International journal of developmental biology, 1997. **41**(2): p. 235-43.
68. Anderson, P.D., et al., *Genetic factors on mouse chromosome 18 affecting susceptibility to testicular germ cell tumors and permissiveness to embryonic stem cell derivation.* Cancer research, 2009. **69**(23): p. 9112-7.
69. Buehr, M., et al., *Capture of authentic embryonic stem cells from rat blastocysts.* Cell, 2008. **135**(7): p. 1287-98.
70. Li, P., et al., *Germline competent embryonic stem cells derived from rat blastocysts.* Cell, 2008. **135**(7): p. 1299-310.
71. Kristensen, D.M., M. Kalisz, and J.H. Nielsen, *Cytokine signalling in embryonic stem cells.* APMIS : acta pathologica, microbiologica, et immunologica Scandinavica, 2005. **113**(11-12): p. 756-72.
72. Nichols, J., et al., *Physiological rationale for responsiveness of mouse embryonic stem cells to gp130 cytokines.* Development, 2001. **128**(12): p. 2333-9.
73. Kawase, E., et al., *Strain difference in establishment of mouse embryonic stem (ES) cell lines.* The International journal of developmental biology, 1994. **38**(2): p. 385-90.
74. Ptak, G.E., J.A. Modlinski, and P. Loi, *Embryonic diapause in humans: time to consider?* Reproductive biology and endocrinology : RB&E, 2013. **11**: p. 92.
75. Ptak, G.E., et al., *Embryonic diapause is conserved across mammals.* PloS one, 2012. **7**(3): p. e33027.
76. Ohgushi, M., et al., *Molecular pathway and cell state responsible for dissociation-induced apoptosis in human pluripotent stem cells.* Cell stem cell, 2010. **7**(2): p. 225-39.
77. Lomax, G.P. and A.O. Trounson, *Correcting misperceptions about cryopreserved embryos and stem cell research.* Nature biotechnology, 2013. **31**(4): p. 288-90.
78. Lomax, G.P. and S.R. Peckman, *Stem cell policy exceptionalism: proceed with caution.* Stem cell reviews, 2012. **8**(2): p. 299-304.
79. Abraham, S., et al., *Propagation of human embryonic and induced pluripotent stem cells in an indirect co-culture system.* Biochemical and biophysical research communications, 2010. **393**(2): p. 211-6.
80. Unger, C., et al., *Good manufacturing practice and clinical-grade human embryonic stem cell lines.* Human molecular genetics, 2008. **17**(R1): p. R48-53.

81. Draper, J.S., et al., *Culture and characterization of human embryonic stem cells.* Stem cells and development, 2004. **13**(4): p. 325-36.
82. Mitalipova, M.M., et al., *Preserving the genetic integrity of human embryonic stem cells.* Nature biotechnology, 2005. **23**(1): p. 19-20.
83. Maitra, A., et al., *Genomic alterations in cultured human embryonic stem cells.* Nature genetics, 2005. **37**(10): p. 1099-103.
84. Draper, J.S., et al., *Recurrent gain of chromosomes 17q and 12 in cultured human embryonic stem cells.* Nature biotechnology, 2004. **22**(1): p. 53-4.
85. Nguyen, H.T., M. Geens, and C. Spits, *Genetic and epigenetic instability in human pluripotent stem cells.* Human reproduction update, 2013. **19**(2): p. 187-205.
86. Sun, Y., et al., *Identification of proteins related to epigenetic regulation in the malignant transformation of aberrant karyotypic human embryonic stem cells by quantitative proteomics.* PloS one, 2014. **9**(1): p. e85823.
87. Amps, K., et al., *Screening ethnically diverse human embryonic stem cells identifies a chromosome 20 minimal amplicon conferring growth advantage.* Nature biotechnology, 2011. **29**(12): p. 1132-44.
88. Laurent, L.C., et al., *Dynamic changes in the copy number of pluripotency and cell proliferation genes in human ESCs and iPSCs during reprogramming and time in culture.* Cell stem cell, 2011. **8**(1): p. 106-18.
89. Mayshar, Y., et al., *Identification and classification of chromosomal aberrations in human induced pluripotent stem cells.* Cell stem cell, 2010. **7**(4): p. 521-31.
90. Narva, E., et al., *High-resolution DNA analysis of human embryonic stem cell lines reveals culture-induced copy number changes and loss of heterozygosity.* Nature biotechnology, 2010. **28**(4): p. 371-7.
91. Werbowetski-Ogilvie, T.E., et al., *Characterization of human embryonic stem cells with features of neoplastic progression.* Nature biotechnology, 2009. **27**(1): p. 91-7.
92. Baker, D.E., et al., *Adaptation to culture of human embryonic stem cells and oncogenesis in vivo.* Nature biotechnology, 2007. **25**(2): p. 207-15.
93. Fazeli, A., et al., *Altered patterns of differentiation in karyotypically abnormal human embryonic stem cells.* The International journal of developmental biology, 2011. **55**(2): p. 175-80.
94. Andrews, P.W., et al., *Embryonic stem (ES) cells and embryonal carcinoma (EC) cells: opposite sides of the same coin.* Biochemical Society transactions, 2005. **33**(Pt 6): p. 1526-30.
95. Harrison, N.J., D. Baker, and P.W. Andrews, *Culture adaptation of embryonic stem cells echoes germ cell malignancy.* International journal of andrology, 2007. **30**(4): p. 275-81; discussion 281.
96. Gokhale, P.J. and P.W. Andrews, *The development of pluripotent stem cells.* Current opinion in genetics & development, 2012. **22**(5): p. 403-8.
97. Hemberger, M., W. Dean, and W. Reik, *Epigenetic dynamics of stem cells and cell lineage commitment: digging Waddington's canal.* Nature reviews. Molecular cell biology, 2009. **10**(8): p. 526-37.
98. Peterson, S.E. and J.F. Loring, *Genomic instability in pluripotent stem cells: implications for clinical applications.* The Journal of biological chemistry, 2013.

99. Corrales, N.L., et al., *Copy number variations (CNVs) in human pluripotent cell-derived neuroprogenitors.* Gene, 2012. **506**(2): p. 377-9.
100. Devalle, S., et al., *Implications of aneuploidy for stem cell biology and brain therapeutics.* Frontiers in cellular neuroscience, 2012. **6**: p. 36.
101. Brennand, K.J. and F.H. Gage, *Concise review: the promise of human induced pluripotent stem cell-based studies of schizophrenia.* Stem cells, 2011. **29**(12): p. 1915-22.
102. Knoepfler, P.S., *Deconstructing stem cell tumorigenicity: a roadmap to safe regenerative medicine.* Stem cells, 2009. **27**(5): p. 1050-6.
103. Peterson, S.E., et al., *Normal human pluripotent stem cell lines exhibit pervasive mosaic aneuploidy.* PloS one, 2011. **6**(8): p. e23018.
104. Fragouli, E. and D. Wells, *Aneuploidy in the human blastocyst.* Cytogenetic and genome research, 2011. **133**(2-4): p. 149-59.
105. Vanneste, E., et al., *Chromosome instability is common in human cleavage-stage embryos.* Nature medicine, 2009. **15**(5): p. 577-83.
106. Biancotti, J.C., et al., *The in vitro survival of human monosomies and trisomies as embryonic stem cells.* Stem cell research, 2012. **9**(3): p. 218-24.
107. Sverdlov, E.D. and K. Mineev, *Mutation rate in stem cells: an underestimated barrier on the way to therapy.* Trends in molecular medicine, 2013. **19**(5): p. 273-80.
108. Lefort, N., et al., *Human embryonic stem cells reveal recurrent genomic instability at 20q11.21.* Nature biotechnology, 2008. **26**(12): p. 1364-6.
109. Watanabe, K., et al., *A ROCK inhibitor permits survival of dissociated human embryonic stem cells.* Nature biotechnology, 2007. **25**(6): p. 681-6.
110. Chen, G., et al., *Actin-myosin contractility is responsible for the reduced viability of dissociated human embryonic stem cells.* Cell stem cell, 2010. **7**(2): p. 240-8.
111. Baharvand, H., et al., *An efficient and easy-to-use cryopreservation protocol for human ES and iPS cells.* Nature protocols, 2010. **5**(3): p. 588-94.
112. Xu, Y., et al., *Revealing a core signaling regulatory mechanism for pluripotent stem cell survival and self-renewal by small molecules.* Proc Natl Acad Sci U S A. **107**(18): p. 8129-34.
113. Chen, K.G., et al., *Human pluripotent stem cell culture: considerations for maintenance, expansion, and therapeutics.* Cell stem cell, 2014. **14**(1): p. 13-26.
114. Chen, H.F., et al., *Derivation, characterization and differentiation of human embryonic stem cells: comparing serum-containing versus serum-free media and evidence of germ cell differentiation.* Human reproduction, 2007. **22**(2): p. 567-77.
115. Chen, G., et al., *Chemically defined conditions for human iPSC derivation and culture.* Nature methods, 2011. **8**(5): p. 424-9.
116. Abraham, S., et al., *Stable propagation of human embryonic and induced pluripotent stem cells on decellularized human substrates.* Biotechnology progress, 2010. **26**(4): p. 1126-34.
117. Falconer, E. and P.M. Lansdorp, *Strand-seq: a unifying tool for studies of chromosome segregation.* Seminars in cell & developmental biology, 2013. **24**(8-9): p. 643-52.
118. Falconer, E., et al., *DNA template strand sequencing of single-cells maps genomic rearrangements at high resolution.* Nature methods, 2012. **9**(11): p. 1107-12.

119. Harper, J.C. and J.D. Delhanty, *Detection of chromosomal abnormalities in human preimplantation embryos using FISH.* Journal of assisted reproduction and genetics, 1996. **13**(2): p. 137-9.
120. Delhanty, J.D., et al., *Multicolour FISH detects frequent chromosomal mosaicism and chaotic division in normal preimplantation embryos from fertile patients.* Human genetics, 1997. **99**(6): p. 755-60.
121. Zhao, Y., et al., *In vitro fertilization: four decades of reflections and promises.* Biochimica et biophysica acta, 2011. **1810**(9): p. 843-52.
122. Barbash-Hazan, S., et al., *Preimplantation aneuploid embryos undergo self-correction in correlation with their developmental potential.* Fertility and sterility, 2009. **92**(3): p. 890-6.
123. Mertzanidou, A., et al., *Microarray analysis reveals abnormal chromosomal complements in over 70% of 14 normally developing human embryos.* Human reproduction, 2013. **28**(1): p. 256-64.
124. Fragouli, E., et al., *The origin and impact of embryonic aneuploidy.* Human genetics, 2013. **132**(9): p. 1001-13.
125. Zhang, C., et al., *A single cell level based method for copy number variation analysis by low coverage massively parallel sequencing.* PloS one, 2013. **8**(1): p. e54236.
126. Yin, X., et al., *Massively parallel sequencing for chromosomal abnormality testing in trophectoderm cells of human blastocysts.* Biology of reproduction, 2013. **88**(3): p. 69.
127. Mantzouratou, A. and J.D. Delhanty, *Aneuploidy in the human cleavage stage embryo.* Cytogenetic and genome research, 2011. **133**(2-4): p. 141-8.
128. Voet, T., E. Vanneste, and J.R. Vermeesch, *The human cleavage stage embryo is a cradle of chromosomal rearrangements.* Cytogenetic and genome research, 2011. **133**(2-4): p. 160-8.
129. Wells, D. and J.D. Delhanty, *Comprehensive chromosomal analysis of human preimplantation embryos using whole genome amplification and single cell comparative genomic hybridization.* Molecular human reproduction, 2000. **6**(11): p. 1055-62.
130. Dekel-Naftali, M., et al., *Chromosomal integrity of human preimplantation embryos at different days post fertilization.* Journal of assisted reproduction and genetics, 2013. **30**(5): p. 633-48.
131. Bazrgar, M., et al., *Self-correction of chromosomal abnormalities in human preimplantation embryos and embryonic stem cells.* Stem cells and development, 2013. **22**(17): p. 2449-56.
132. Ambartsumyan, G. and A.T. Clark, *Aneuploidy and early human embryo development.* Human molecular genetics, 2008. **17**(R1): p. R10-5.
133. Boheler, K.R., *Stem cell pluripotency: a cellular trait that depends on transcription factors, chromatin state and a checkpoint deficient cell cycle.* Journal of cellular physiology, 2009. **221**(1): p. 10-7.
134. Mantel, C., et al., *Checkpoint-apoptosis uncoupling in human and mouse embryonic stem cells: a source of karyotpic instability.* Blood, 2007. **109**(10): p. 4518-27.
135. Damelin, M., et al., *Decatenation checkpoint deficiency in stem and progenitor cells.* Cancer cell, 2005. **8**(6): p. 479-84.
136. Voullaire, L., et al., *Chromosome analysis of blastomeres from human embryos by using comparative genomic hybridization.* Human genetics, 2000. **106**(2): p. 210-7.

137. Munne, S., et al., *Differences in chromosome susceptibility to aneuploidy and survival to first trimester.* Reproductive biomedicine online, 2004. **8**(1): p. 81-90.
138. Munne, S., et al., *Self-correction of chromosomally abnormal embryos in culture and implications for stem cell production.* Fertility and sterility, 2005. **84**(5): p. 1328-34.
139. Wells, D., et al., *Expression of genes regulating chromosome segregation, the cell cycle and apoptosis during human preimplantation development.* Human reproduction, 2005. **20**(5): p. 1339-48.
140. Abyzov, A., et al., *Somatic copy number mosaicism in human skin revealed by induced pluripotent stem cells.* Nature, 2012. **492**(7429): p. 438-42.
141. Zucchelli, M., et al., *In vivo differentiated human embryonic stem cells can acquire chromosomal aberrations more frequently than in vitro during the same period.* Stem cells and development, 2012. **21**(18): p. 3363-71.
142. Westra, J.W., et al., *Aneuploid mosaicism in the developing and adult cerebellar cortex.* The Journal of comparative neurology, 2008. **507**(6): p. 1944-51.
143. Yang, A.H., et al., *Chromosome segregation defects contribute to aneuploidy in normal neural progenitor cells.* The Journal of neuroscience : the official journal of the Society for Neuroscience, 2003. **23**(32): p. 10454-62.
144. Rehen, S.K., et al., *Constitutional aneuploidy in the normal human brain.* The Journal of neuroscience : the official journal of the Society for Neuroscience, 2005. **25**(9): p. 2176-80.
145. Bushman, D.M. and J. Chun, *The genomically mosaic brain: aneuploidy and more in neural diversity and disease.* Seminars in cell & developmental biology, 2013. **24**(4): p. 357-69.
146. Narwani, K., et al., *Human embryonic stem cells from aneuploid blastocysts identified by pre-implantation genetic screening.* In vitro cellular & developmental biology. Animal, 2010. **46**(3-4): p. 309-16.
147. Lavon, N., et al., *Derivation of euploid human embryonic stem cells from aneuploid embryos.* Stem cells, 2008. **26**(7): p. 1874-82.
148. Dekel-Naftali, M., et al., *Screening of human pluripotent stem cells using CGH and FISH reveals low-grade mosaic aneuploidy and a recurrent amplification of chromosome 1q.* European journal of human genetics : EJHG, 2012. **20**(12): p. 1248-55.
149. Bai, H., et al., *Bcl-xL enhances single-cell survival and expansion of human embryonic stem cells without affecting self-renewal.* Stem cell research, 2012. **8**(1): p. 26-37.
150. Avery, S., et al., *BCL-XL Mediates the Strong Selective Advantage of a 20q11.21 Amplification Commonly Found in Human Embryonic Stem Cell Cultures.* Stem cell reports, 2013. **1**(5): p. 379-86.
151. Nguyen, H.T., et al., *Gain of 20q11.21 in human embryonic stem cells improves cell survival by increased expression of Bcl-xL.* Molecular human reproduction, 2014. **20**(2): p. 168-77.
152. Trautmann, K., et al., *Chromosomal instability in microsatellite-unstable and stable colon cancer.* Clinical cancer research : an official journal of the American Association for Cancer Research, 2006. **12**(21): p. 6379-85.
153. Cervantes, R.B., et al., *Embryonic stem cells and somatic cells differ in mutation frequency and type.* Proceedings of the National Academy of Sciences of the United States of America, 2002. **99**(6): p. 3586-90.

154. Tichy, E.D., et al., *Mismatch and base excision repair proficiency in murine embryonic stem cells.* DNA repair, 2011. **10**(4): p. 445-51.
155. Adams, B.R., et al., *ATM-independent, high-fidelity nonhomologous end joining predominates in human embryonic stem cells.* Aging, 2010. **2**(9): p. 582-96.
156. Adams, B.R., et al., *Dynamic dependence on ATR and ATM for double-strand break repair in human embryonic stem cells and neural descendants.* PloS one, 2010. **5**(4): p. e10001.
157. Maynard, S., et al., *Human embryonic stem cells have enhanced repair of multiple forms of DNA damage.* Stem cells, 2008. **26**(9): p. 2266-74.
158. Gisselsson, D., *Chromosome instability in cancer: how, when, and why?* Advances in cancer research, 2003. **87**: p. 1-29.
159. Alexandrov, L.B. and M.R. Stratton, *Mutational signatures: the patterns of somatic mutations hidden in cancer genomes.* Current opinion in genetics & development, 2014. **24C**: p. 52-60.
160. Heng, H.H., et al., *Clonal and non-clonal chromosome aberrations and genome variation and aberration.* Genome, 2006. **49**(3): p. 195-204.
161. Fenech, M., *Cytokinesis-block micronucleus assay evolves into a "cytome" assay of chromosomal instability, mitotic dysfunction and cell death.* Mutation research, 2006. **600**(1-2): p. 58-66.
162. Klein, A., et al., *Different mechanisms of mitotic instability in cancer cell lines.* International journal of oncology, 2006. **29**(6): p. 1389-96.
163. Shimizu, N., et al., *Selective entrapment of extrachromosomally amplified DNA by nuclear budding and micronucleation during S phase.* The Journal of cell biology, 1998. **140**(6): p. 1307-20.
164. Utani, K., A. Okamoto, and N. Shimizu, *Generation of micronuclei during interphase by coupling between cytoplasmic membrane blebbing and nuclear budding.* PloS one, 2011. **6**(11): p. e27233.
165. Fenech, M., et al., *Molecular mechanisms of micronucleus, nucleoplasmic bridge and nuclear bud formation in mammalian and human cells.* Mutagenesis, 2011. **26**(1): p. 125-32.
166. Selvarajah, S., et al., *The breakage-fusion-bridge (BFB) cycle as a mechanism for generating genetic heterogeneity in osteosarcoma.* Chromosoma, 2006. **115**(6): p. 459-67.
167. Ganem, N.J., S.A. Godinho, and D. Pellman, *A mechanism linking extra centrosomes to chromosomal instability.* Nature, 2009. **460**(7252): p. 278-82.
168. Imreh, M.P., et al., *In vitro culture conditions favoring selection of chromosomal abnormalities in human ES cells.* Journal of cellular biochemistry, 2006. **99**(2): p. 508-16.
169. Xu, F., et al., *Embryonic stem cell bioprinting for uniform and controlled size embryoid body formation.* Biomicrofluidics, 2011. **5**(2): p. 22207.
170. Antonchuk, J., *Formation of embryoid bodies from human pluripotent stem cells using AggreWell plates.* Methods in molecular biology, 2013. **946**: p. 523-33.
171. Mohr, J.C., et al., *The microwell control of embryoid body size in order to regulate cardiac differentiation of human embryonic stem cells.* Biomaterials, 2010. **31**(7): p. 1885-93.
172. Ng, E.S., et al., *Forced aggregation of defined numbers of human embryonic stem cells into embryoid bodies fosters robust, reproducible hematopoietic differentiation.* Blood, 2005. **106**(5): p. 1601-3.

173. Rocha, C.R., et al., *The role of DNA repair in the pluripotency and differentiation of human stem cells.* Mutation research, 2013. **752**(1): p. 25-35.
174. Hong, Y. and P.J. Stambrook, *Restoration of an absent G1 arrest and protection from apoptosis in embryonic stem cells after ionizing radiation.* Proceedings of the National Academy of Sciences of the United States of America, 2004. **101**(40): p. 14443-8.
175. Holubcova, Z., et al., *Human embryonic stem cells suffer from centrosomal amplification.* Stem cells, 2011. **29**(1): p. 46-56.
176. Abbasalizadeh, S., et al., *Bioprocess development for mass production of size-controlled human pluripotent stem cell aggregates in stirred suspension bioreactor.* Tissue engineering. Part C, Methods, 2012. **18**(11): p. 831-51.
177. Muller, F.J., et al., *Regulatory networks define phenotypic classes of human stem cell lines.* Nature, 2008. **455**(7211): p. 401-5.
178. Aguilera, A. and B. Gomez-Gonzalez, *Genome instability: a mechanistic view of its causes and consequences.* Nat Rev Genet, 2008. **9**(3): p. 204-17.
179. Heng, H.H., et al., *Cancer progression by non-clonal chromosome aberrations.* J Cell Biochem, 2006. **98**(6): p. 1424-35.
180. Caisander, G., et al., *Chromosomal integrity maintained in five human embryonic stem cell lines after prolonged in vitro culture.* Chromosome research : an international journal on the molecular, supramolecular and evolutionary aspects of chromosome biology, 2006. **14**(2): p. 131-7.
181. Prosser, S.L., K.R. Straatman, and A.M. Fry, *Molecular dissection of the centrosome overduplication pathway in S-phase-arrested cells.* Molecular and cellular biology, 2009. **29**(7): p. 1760-73.
182. Brinkley, B.R., *Managing the centrosome numbers game: from chaos to stability in cancer cell division.* Trends in cell biology, 2001. **11**(1): p. 18-21.
183. Josephson, R., et al., *Qualification of embryonal carcinoma 2102Ep as a reference for human embryonic stem cell research.* Stem cells, 2007. **25**(2): p. 437-46.
184. Ashburner, M., et al., *Gene ontology: tool for the unification of biology. The Gene Ontology Consortium.* Nat Genet, 2000. **25**(1): p. 25-9.
185. Ben-Porath, I., et al., *An embryonic stem cell-like gene expression signature in poorly differentiated aggressive human tumors.* Nat Genet, 2008. **40**(5): p. 499-507.
186. Kaiser, J., *National Institutes of Health. NCI gears up for cancer genome project.* Science, 2005. **307**(5713): p. 1182.
187. Ben-David, U. and N. Benvenisty, *High prevalence of evolutionarily conserved and species-specific genomic aberrations in mouse pluripotent stem cells.* Stem cells, 2012. **30**(4): p. 612-22.
188. Harb, N., T.K. Archer, and N. Sato, *The Rho-Rock-Myosin signaling axis determines cell-cell integrity of self-renewing pluripotent stem cells.* PloS one, 2008. **3**(8): p. e3001.
189. DerMardirossian, C. and G.M. Bokoch, *GDIs: central regulatory molecules in Rho GTPase activation.* Trends in cell biology, 2005. **15**(7): p. 356-63.
190. Harding, M.A. and D. Theodorescu, *RhoGDI signaling provides targets for cancer therapy.* European journal of cancer, 2010. **46**(7): p. 1252-9.
191. Bendall, S.C., et al., *IGF and FGF cooperatively establish the regulatory stem cell niche of pluripotent human cells in vitro.* Nature, 2007. **448**(7157): p. 1015-21.

192. Soncin, F., et al., *Abrogation of E-cadherin-mediated cell-cell contact in mouse embryonic stem cells results in reversible LIF-independent self-renewal.* Stem cells, 2009. **27**(9): p. 2069-80.
193. Rosler, E.S., et al., *Long-term culture of human embryonic stem cells in feeder-free conditions.* Developmental dynamics : an official publication of the American Association of Anatomists, 2004. **229**(2): p. 259-74.
194. Li, L., et al., *Individual cell movement, asymmetric colony expansion, rho-associated kinase, and E-cadherin impact the clonogenicity of human embryonic stem cells.* Biophysical journal, 2010. **98**(11): p. 2442-51.
195. Hovatta, O., et al., *A teratocarcinoma-like human embryonic stem cell (hESC) line and four hESC lines reveal potentially oncogenic genomic changes.* PloS one, 2010. **5**(4): p. e10263.
196. Almstrup, K., et al., *Embryonic stem cell-like features of testicular carcinoma in situ revealed by genome-wide gene expression profiling.* Cancer research, 2004. **64**(14): p. 4736-43.
197. Acevedo, N., et al., *Glycogen synthase kinase-3 regulation of chromatin segregation and cytokinesis in mouse preimplantation embryos.* Molecular reproduction and development, 2007. **74**(2): p. 178-88.
198. Raggioli, A., et al., *Beta-catenin is vital for the integrity of mouse embryonic stem cells.* PloS one, 2014. **9**(1): p. e86691.
199. Przybyla, L. and J. Voldman, *Probing embryonic stem cell autocrine and paracrine signaling using microfluidics.* Annual review of analytical chemistry, 2012. **5**: p. 293-315.
200. Ben-David, U., N. Benvenisty, and Y. Mayshar, *Genetic instability in human induced pluripotent stem cells: classification of causes and possible safeguards.* Cell cycle, 2010. **9**(23): p. 4603-4.
201. Linseman, D.A. and F.A. Loucks, *Diverse roles of Rho family GTPases in neuronal development, survival, and death.* Frontiers in bioscience : a journal and virtual library, 2008. **13**: p. 657-76.
202. Hong, Y., et al., *Protecting genomic integrity in somatic cells and embryonic stem cells.* Mutat Res, 2007. **614**(1-2): p. 48-55.
203. Narumiya, S. and S. Yasuda, *Rho GTPases in animal cell mitosis.* Current opinion in cell biology, 2006. **18**(2): p. 199-205.
204. Heng, Y.W., et al., *TPPP acts downstream of RhoA-ROCK-LIMK2 to regulate astral microtubule organization and spindle orientation.* Journal of cell science, 2012. **125**(Pt 6): p. 1579-90.
205. Duan, X., et al., *Rho-GTPase effector ROCK phosphorylates cofilin in actin-meditated cytokinesis during mouse oocyte meiosis.* Biology of reproduction, 2014. **90**(2): p. 37.
206. Tnimov, Z., et al., *Quantitative analysis of prenylated RhoA interaction with its chaperone, RhoGDI.* The Journal of biological chemistry, 2012. **287**(32): p. 26549-62.
207. Garcia-Mata, R., E. Boulter, and K. Burridge, *The 'invisible hand': regulation of RHO GTPases by RHOGDIs.* Nature reviews. Molecular cell biology, 2011. **12**(8): p. 493-504.
208. DerMardirossian, C., A. Schnelzer, and G.M. Bokoch, *Phosphorylation of RhoGDI by Pak1 mediates dissociation of Rac GTPase.* Molecular cell, 2004. **15**(1): p. 117-27.

209. Elfenbein, A., et al., *Suppression of RhoG activity is mediated by a syndecan 4-synectin-RhoGDI1 complex and is reversed by PKCalpha in a Rac1 activation pathway.* The Journal of cell biology, 2009. **186**(1): p. 75-83.
210. Kaibuchi, K., et al., *Regulation of cadherin-mediated cell-cell adhesion by the Rho family GTPases.* Current opinion in cell biology, 1999. **11**(5): p. 591-6.

APPENDIX

Table 6 Primer Sequences for Self Renewal, Differentiation, and RHO signaling

Gene	Primers: 5' to 3'	Annotation
AFP F	CTTTGGGCTGCTCGCTATGA	Germ Layer
AFP R	GCATGTTGATTTAACAAGCTGCT	Germ Layer
Arhgdia- FP	GGATGAGCACTCGGTCAACTA	Rho Signaling
Arhgdia - RP	GGCCTCCTTGTACTTTCGCAG	Rho Signaling
GATA4 F	GTGTCCCAGACGTTCTCAGTC	Germ Layer
GATA4 R	GGGAGACGCATAGCCTTGT	Germ Layer
IGF2 F	TCCTCCCTGGACAATCAGAC	Germ Layer
IGF2 R	AGAAGCACCAGCATCGACTT	Germ Layer
Nanog F	TTTGTGGGCCTGAAGAAAACT	Pluripotency
Nanog R	AGGGCTGTCCTGAATAAGCAG	Pluripotency
Nestin F	CTGCTACCCTTGAGACACCTG	Germ Layer
Nestin R	GGGCTCTGATCTCTGCATCTAC	Germ Layer
OCT4 F	GGGAGATTGATAACTGGTGTGTT	Pluripotency
OCT4 R	GTGTATATCCCAGGGTGATCCTC	Pluripotency
SOX1 F	ATGCACCGCTACGACATGG	Germ Layer
SOX1 R	CTCATGTAGCCCTGCGAGTTG	Germ Layer
SOX2 FP	TACAGCATGTCCTACTCGCAG	Pluripotency
SOX2 RP	GAGGAAGAGGTAACCACAGGG	Pluripotency
T Brachyury F	TGCTTCCCTGAGACCCAGTT	Germ Layer
T Brachyury R	GATCACTTCTTTCCTTTGCATCAAG	Germ Layer

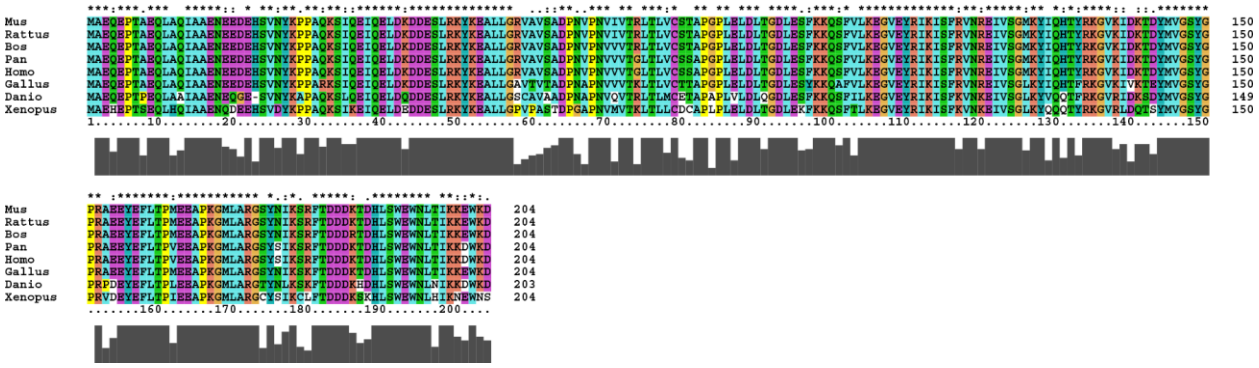

Figure 37. ARHGDIA is a highly conserved protein across vertebrates. Multiple sequence alignment was performed using Clustal X 2.1.

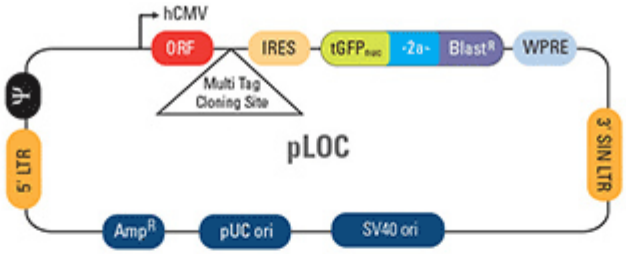

Vector Element	Utility
hCMV	Human cytomegalovirus promoter drives strong transgene expression
ORF	Full-length human ORFs from the ORFeome Collaboration Collection
Multi Tag Cloning Site	Convenient cloning site for the addition of a purification or tracking tag
IRES	Internal ribosomal entry site allows expression of TurboGFP and puromycin resistance genes in a single transcript
$tGFP_{nuc}$	TurboGFP reporter expressed in the cell nucleus to facilitate visual tracking of transduction and expression
$Blast^R$	Blasticidin resistance permits antibiotic-selective pressure and propagation of stable integrants
2a	2a self-cleaving peptide allows simultaneous expression of $tGFP_{nuc}$ and blasticidin resistance proteins from a single transcript
5' LTR	5' long terminal repeat
3' SIN LTR	3' self-inactivating long terminal repeat for increased lentivirus safety
Ψ	Psi packaging sequence allows viral genome packaging using lentiviral packaging systems
WPRE	Woodchuck hepatitis posttranscriptional regulatory element enhances transgene expression in the target cells

Figure 38. Precision LentiORF lentiviral expression vector. Precision LentiORFs are human cDNA open reading frames (ORFs) cloned into a lentiviral expression vector and used for overexpressing human genes and proteins in mammalian cells. The experiment in this study expressed ARHGDIA. Sourced from GE Healthcare.

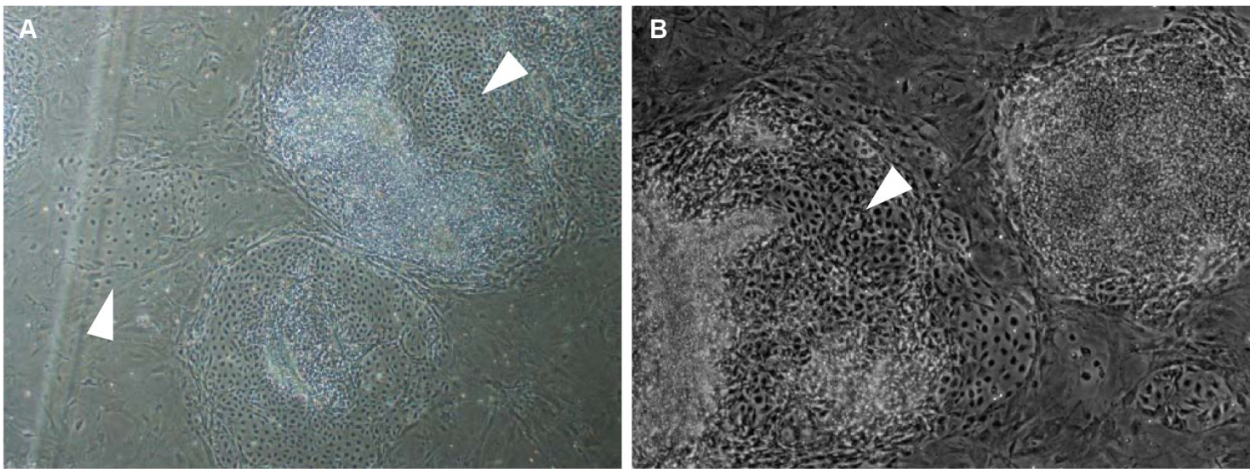

Figure 39. Heterogeneous metastable states of hPSCs cultured in LIF + 2i medium exhibit differentiation and self- renewal. Within a colony some cells self- renew and some differentiate (white arrow) suggesting the coexistence of cells that are LIF- responsive and indicative of naïve PSCs and some cells that are prone to differentiation. BG01 (LIF) at p+1 (A) and BG01 (LIF) at p+15 (B). Magnification is 4x.

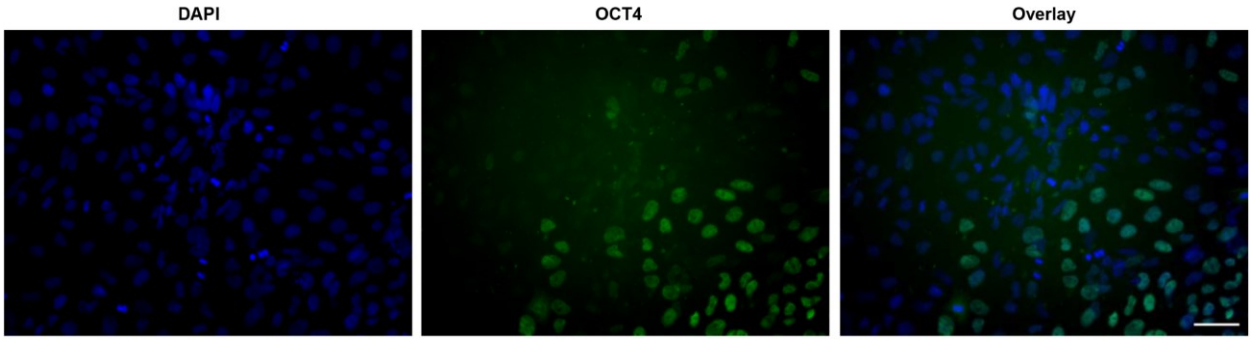

Figure 40. Heterogeneous OCT4 expression in BG01 (LIF) manually passaged cultures. Within a colony, cells exhibit differential likelihood of self- renewal. OCT4 is known to persist in initial stages of differentiation, however this suggest that OCT4 is a sensitive marker and that hPSC (LIF) are prone to down regulation of OCT4. BG01 (LIF) at p+17. Scale bar = 50 μm.

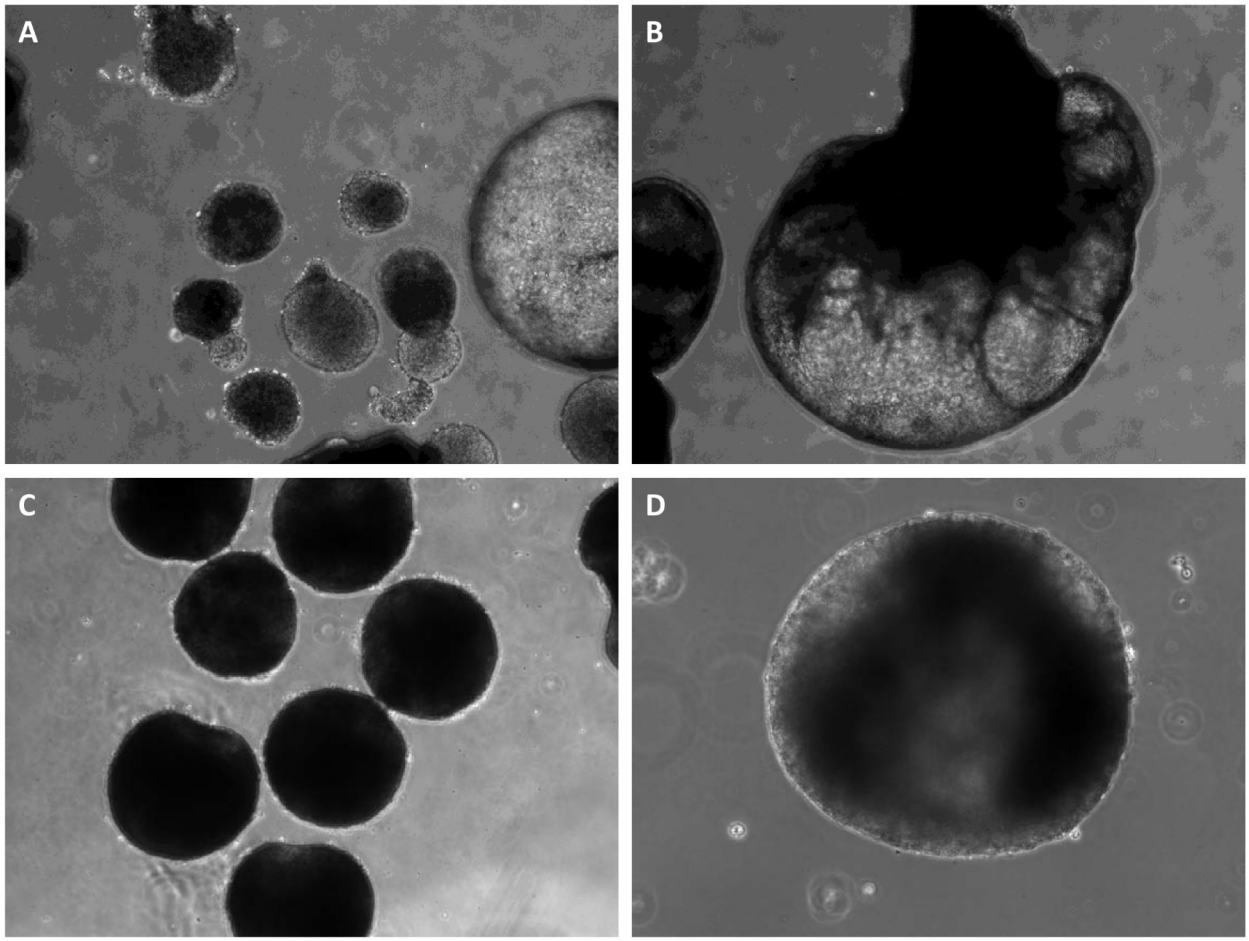

Figure 41. Embryoid bodies generated from H9 hPSCs propagated on Matrigel™ and iMEFs in LIF +2i medium. H9 (LIF + 2i) lines grown on iMEFs exhibit irregular shape and poor density (A&B). H9 (LIF + 2i) grown on Matrigel™ are dense and symmetrical (C & D). 10 mM ROCKi used at the initial hanging drop step. Magnification 4x = A, C; 10x= B, D.

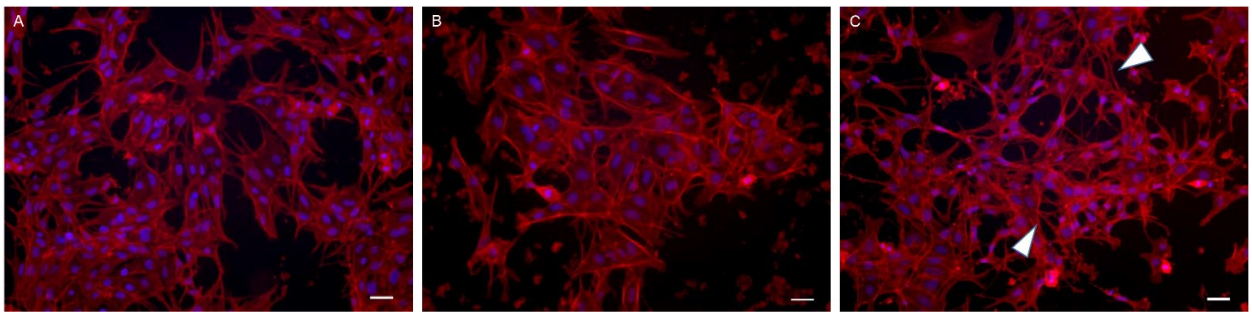

Figure 42. ROCKi, Y27632, inhibits cell- cell contact within hPSC colonies. Phalloidin is stained to visualize F- actin. BG01 (Arg) with 0 μM ROCKi (A), BG01 (WT) with 0 μM ROCKi (B), and BG01 (WT) with 10 μM ROCKi for 24 hours (C). In the ROCKi exposed sample the cytoskeleton is retracted and there is loss of cell- cell contact (white arrows). Scale bar= 50 μm

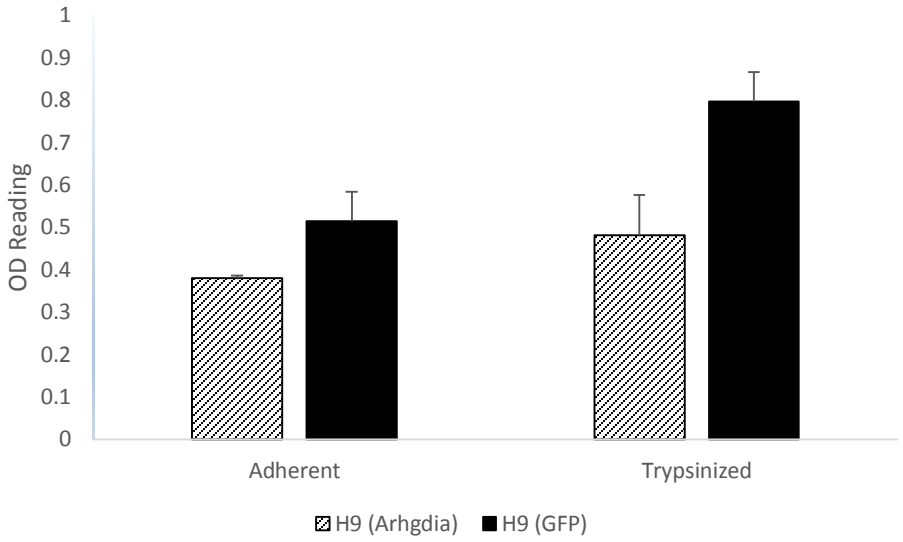

Figure 43. RHOA activation is inhibited in hPSCs overexpressing ARHGDIA. H9 (Arg) is compared to matched controls H9 (GFP). Basal (adherent) expression is less in the H9 (Arg) line. 15 minutes post- trypsinization and plating RHOA is activated in the H9 (GFP) sample; however to a lesser extent is RHOA activated upon trypsinization in the H9 (Arg) line. Upon trypsinization total active RHOA is less in the H9 (Arg) line. RHOA activation was determined using the G- Lisa kit from Cytoskelton, Inc. for the antibody RHOA- GTP.

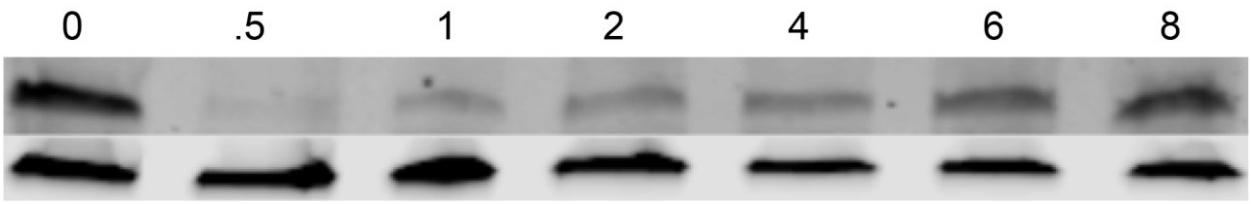

Figure 44. E-cadherin turnover is linear after single- cell dissociation by trypsin. E-cadherin (upper band) and B-tubulin (lower band). H9 hPSC line was dissociated using 0.05% trypsin. Full length E-cadherin is cleaved after dissociation and is linearly increased to near basal levels by 8 hours.

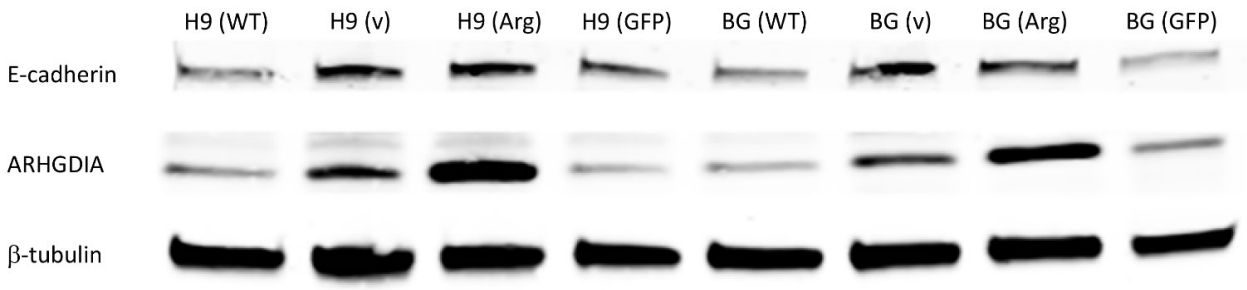

Figure 45. E- cadherin expression is correlated with Arhgdia expression levels. The H9(v), H9 (Arg), BG01(v), and BG01 (Arg) have increased protein expression of ARHGDIA and E-cadherin as determined by Western Analysis. H9(v) has trisomy 17 and BG01(v) has trisomy 17 and complex karyotype. All other samples are euploid.

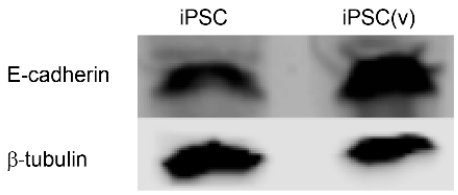

Figure 46. IPSC(v) overexpresses E-cadherin. iPSC(v) with trisomy 17 and X has increased E-cadherin protein expression relative to euploid iPSC, as determined by Western Analysis.

Vitae

Marion (Joe) Riggs went to high school in Tampa, FL at Temple Heights Christian School. He went on the earn an undergraduate degree in Mathematics at the University of South Florida, where he subsequently obtained a Master's degree in Bioinformatics before pursuing his doctoral studies at VCU in the Integrative Life Sciences Program. In 2003, Joe founded the Student Society for Stem Cell Research (SSSCR), which helps students learn how to become involved in stem cell research at the bench and as an advocate. In 2006, he was recipient of the Stem Cell Action National Advocacy Award for his work with SSSCR. From 2006-2010 he served on the Junior Investigator Committee of the International Society for Stem Cell Research. He has been an invited speaker at the World Stem Cell Summit for the years 2005 and 2012. He is a devoted and proud father of a beautiful 6 year old daughter, Elyce, who was born in 2008. Joe would like to be known for his love of others, appreciation for service to mankind, and his determined spirit.